REGULATION OF BREAST CANCER BIOMARKERS BY INTRINSIC AND EXTRINSIC FACTORS

by

© Nikitha K. Pallegar

Under the supervision

of

Dr. Sherri Christian

Thesis submitted to the school of graduate studies in partial fulfillment of requirements for the degree of Doctor of Philosophy, Biochemistry,

Memorial University of Newfoundland,

2018

St. Johns, NL, Canada

Abstract

Cancer metastases are accountable for almost 90% of all human cancer-related deaths including breast cancer (BC). BC is the most common cancer among Canadian women, with one in four women diagnosed per year. BC is a heterogenous disease and is broadly classified into Luminal A (estrogen/progesterone receptor $(ER/PR)^{+}$), Luminal B (ER/PR^{+} and human epidermal growth receptor 2^{+} ($HER2^{+}$)), $HER2^{+}$, and triple negative breast cancer (TNBC, $ER^{-}/PR^{-}/HER2^{-}$). BC heterogeneity and progression are primarily dependent on intrinsic factors such as genetic or epigenetic changes to genes that regulate cell growth and proliferation. In addition, extrinsic factors such as, the extracellular matrix and adipocytes in the surrounding microenvironment contribute to cancer progression and initiation of metastasis. Therefore, the main aim of this thesis was to analyze the contribution of some of the intrinsic and extrinsic factors that regulate BC progression. One known intrinsic factor is CD24; a glycosylphosphatidylinositol-anchored surface glycoprotein that can regulate proliferation and apoptosis of various cell types. Breast cancer stem cells (BCSCs), which can initiate tumor formation, maintain tumor heterogeneity, have high invasive properties, and favor metastasis, have low CD24 expression. Moreover, drug treatment of TNBC tumors can cause a switch from $CD24^{+}$ to $CD24^{-}$ and *vice versa* exhibiting differential drug resistance in these patients. In order to better understand the role of CD24, I first analyzed the CD24 gene, and found that the sequence of the mature peptide, but not the genomic structure is conserved over 200 million years. Next, I studied the regulation of CD24 expression by the oncogenic Ras pathway and found that Ras is essential for suppression of CD24 surface expression.

Extrinsic factors, such as adipocytes, can also contribute to BC progression and metastasis. To study this, I developed a 3-dimensional co-culture system to mimic the *in vivo* interactions between BC cells and adipocytes. I found that adipocytes promote a mesenchymal-to-epithelial-like transition in BC cells suggesting that secondary tumour formation might be promoted by adipocytes. Overall, these data will aid in understanding the intrinsic and extrinsic factors that should be considered in the future development of combination drug treatments to successfully cure BC.

Acknowledgements

Thanks, are best when concrete. First and foremost, I am very grateful to Dr. Sherri Christian for being an excellent supervisor who has given me the opportunity, constant support and guidance through ups and downs of research and kept me motivated. I have learnt a lot through the level of detail she has while writing or while designing an experiment. I would like to express my deep gratitude for her encouragement and enthusiasm which allowed me to become an independent and better researcher.

I am thankful to my committee members, Dr. Kensuke Hirasawa and Dr. Robert Brown for their invaluable and constructive inputs on my research.

I am grateful to Dr. Alicia Viloria-Petit (University of Guelph) for her guidance and training, especially through my latest research on developing 3D co-culture system to study the role of adipocytes on breast cancer progression. Also thankful to her lab mates for making my stay comfortable while training in her lab at Guelph.

Additional thanks to Dr. Andrew Lang and Dr. Marta Canuti for their guidance in phylogenetic analysis.

I am grateful to Craig Ayre, for being a moral support through stressful times of the research. As a friend and colleague, I also thank him for his time in discussions that lead to problem solving or new ideas in my research. I would also like to thank Nicole Smith, for her technical support in various experiments in lab.

Assistance provided by Mathepan Mahendralingam (University of Guelph) through development of 3D co-culture system is greatly appreciated. I am particularly thankful for the assistance given by Chantae Garland in confocal image analysis. I also wish to acknowledge the help provided by Eman Elbakry for helping with abbreviations. I appreciate all the help provided by the past and present lab members.

I am grateful to the Biochemistry staff and faculty for providing the support through my research.

I am thankful to my funding agencies, school of graduate studies, Memorial university of Newfoundland. I am particularly grateful to Beatrice Hunter Cancer Research Institute and the Terry Fox Strategic Health Research Training Program in Cancer Research at CIHR for supporting through my training and research.

Finally, I would like to thank my family and friends for making my graduate life easier.

Table of Contents

List of Tables

List of Figures

Figure 6.1: Schematic illustration of the tumor microenvironment showing the interaction between the tumor cells and the surrounding ECM and non-cancerous cells at secondary site.

List of Abbreviations

3D - 3 dimensional

ADAM - a disintegrin and metalloproteinase

ALDH - aldehyde dehydrogenase

AR - androgen receptor

AT - adipose tissue

ATGL - adipose triglyceride lipase

ATP - adenosine triphosphate

ATX - Autotaxin

BAT - brown adipose tissue

BC - breast cancer

BCA - bicinchoninic acid

BCSCs - breast cancer stem cell

bHLH - basic helix loop helix

BL1 - basal-like 1

BL2 - basal-like 2

BLIA - basal-like immune activated

BLIS - basal-like immunosuppressed

BMI - body mass index

BODIPY - boron-dipyrromethene

BSA - bovine serum albumin

CAA - cancer associated adipocyte

CD24 - cluster of differentiation 24

CD24L – cluster of differentiation 24-like

CD44v – cluster of differentiation 44 variant

Cdc42 - cell division cycle 42

CM - conditioned medium

COX2 - cyclooxygenase-2

CSCs - cancer stem cell

CTCs - circulating tumor cell

DAG - diacylglycerol

DAPI - 4',6-diamidino-2-phenylindole

DCIS - ductal carcinoma *in situ*

DMEM - Dulbecco's Modified Eagle Medium

DMSO - dimethyl sulphoxide

E2 - Estradiol

E-box - enhancer-box

EGF - epidermal growth factor

EGFR - epidermal growth factor receptor

EMT - epithelial to mesenchymal transition

EMT-TFs - epithelial to mesenchymal transition-transcription factor

EPHA2 - ephrin type A receptor 2

ER - endoplasmic reticulum

ER - estrogen receptor

ERK - extracellular signal regulated kinase

FABP - fatty acid binding protein

FACS - fluorescent activated cell sorting

FBS - fetal bovine serum

FFPE-IF/IHC - formalin fixed paraffin embeding - immunofluorescence or immunohistochemistry

FOXC1 - forkhead box C1

FOXC2 - forkhead box C2

FOXO3 - forkhead box O3

FOXP1 - forkhead box P1

GAP - GTPase activating protein

GDP - guanine diphosphate

GEO - gene expression omnibus

GPI - glycosyl phosphatidylinositol

Grb2 - Growth factor receptor bound protein

GTP - Guanine triphosphate

HER2 - human epidermal growth factor receptor

HGF - hepatocyte growth factor

HIF - hypoxia inducible factor

HSD - Honest Significant Difference

HSL - hormone sensitive lipase

HT - Hydroxytamoxifen

IDC - invasive ductal carcinoma

IF - immunofluorescence

IGF - insulin-like growth factor

IM - immunomodulatory

IntDen - Integrated density

IL-6 - interleukin-6

ILC - invasive lobular carcinoma

JAK/STAT - janus kinase/signal transducers and activators of transcription

LAR - luminal/androgen receptor

LD - lipid droplet

LBX1 - ladybird homebox 1

LCIS - lobular carcinoma *in situ*

M - mesenchymal

MAPK - mitogen activated protein kinase ERK

MEBM - mammary epithelial basal medium

MEK kinase - mitogen-activated protein kinase kinase 1

MET - mesenchymal to epithelial transition

MME - membrane metalloendopeptidases

MMPs - matrix metalloproteinase

MMP2 - matrix metalloproteinase 2

MSL - mesenchymal stem-like

MT1-MMP - membrane type 1-matrix metalloproteinase

MT2-MMP - membrane type 2-matrix metalloproteinase

MT4-MMP - membrane type 4-matrix metalloproteinase

mTOR - mechanistic target of rapamycin

NDRG-2 - N- myc downstream regulated gene 2

NFAT5 - nuclear factor of activated T-cells 5

NFkB - nuclear factor kappa B

NK - natural killer

NSCLC - non-small cell lung cancer cell

P-Akt - phosphorylated Akt

PAK - p21-activated kinase

PARP1 - poly-ADP ribose polymerase 1

PBS - phosphate-buffered saline

PCL - polycaprotactone

PDGF - platelet-derived growth factor

PDK1 - phosphoinositide-dependent kinase 1

PDK2 - phosphoinositide-dependent kinase 2

P-ERK - phosphorylated ERK

PI3K - phosphatidylinositol-3-kinase

PIK3C - phosphatidylinositol-4,5-bisphosphate 3-kinase, catalytic subunit

PIK3R - phosphatidylinositol-4,5-bisphosphate 3-kinase, regulatory subunit

PIP_3 - phosphotidylinositol-3,4,5-trisphosphate

PLC-γ - phospholipase C- γ

PLD - phospholipase D

PKC - protein kinase C

PR - progesterone receptor

RALGDS - Ral guanine nucleotide dissociation stimulator

RAR - retinoic acid receptor

RPMI - Roswell Park Memorial Institute

RT - room temperature

RTK - receptor tyrosine kinases

RT-qPCR - quantitative reverse transcriptase-polymerase chain reaction

SAT - subcutaneous adipose tissue

SOS - son of sevenless

SOX - SRY related HMG box

SP-1 - specificity protein 1

STAT3 - signal transducer and activator of transcription 3

SVF - stromal vascular fraction

TAM - tumor associated macrophage

TBST - tris-buffered saline and tween

TCF-4 - T-cell factor 4

TGFβ - transforming growth factor β

tGLI1 - truncated glioma associated oncogene homolog 1

TME - tumor microenvironment

TNBC - triple negative breast cancer

TNF-α - tumor necrosis factor-α

TP63 - tumor protein 63

TSS - transcription start site

TWIST - twist family basic helix loop helix transcription factor

UTR - untranslated region

VAT - visceral adipose tissue

VEGF - vascular endothelial growth factor

WAT - white adipose tissue

WHO - World Health Organization

Wnt - wingless/integrated

YB-1 - Y-box binding protein 1

ZEB 1 - zinc finger E-box binding homebox 1

ZEB 2 - zinc finger E-box binding homebox 2

ZO1 - zonula occludens 1

List of Appendices

Chapter 1. Introduction

1.1 Breast cancer and its subtypes

Breast cancer (BC) is the most common cancer in women; with one in four cancer diagnoses being BC. According to Canadian cancer statistics 2017, in an average woman's lifetime, one in nine women develop BC and one in 30 women die because of BC. Consequently, BC is the second leading cause of death from cancer in Canadian women. Five-year survival rates for BC diagnosed at early stages are 80-90%, falling to 24% when diagnosed at more advanced stages. Advanced screening, diagnosis and research have decreased deaths from BC by 44% through the period of 1989 to 2014 [1, 2].

BC is a heterogenous disease. Classification of BC into various types over the decades is based on histology, phenotype, and molecular profiling.

Histologically, BC subtypes are characterized based on the location of tumor such as in ducts and lobes of the breast (Fig 1.1A). Moreover, these subtypes are broadly categorized into pre-invasive and invasive carcinomas based on their ability to invade the basement membrane. The growth of pre-invasive cancer is restricted to the ducts and lobes of breast tissue. Pre-invasive cancer is a benign condition but poses a risk of developing into invasive cancer. Pre-invasive cancers are sub-divided into ductal carcinoma *in situ* (DCIS) and lobular carcinoma *in situ* (LCIS). Heterogeneity in DCIS can lead to invasive cancer when untreated in comparison to LCIS. Invasive cancers have the ability to penetrate through the basement membrane. They are further classified as invasive ductal carcinoma (IDC) constituting 76% of BC and, invasive lobular carcinoma

A

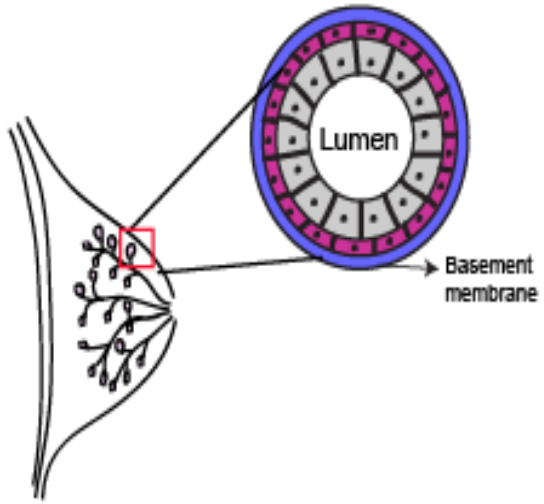
Lumen
Basement membrane

B

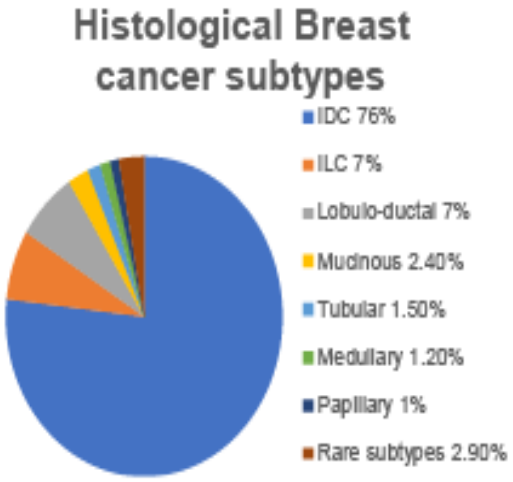
Histological Breast cancer subtypes
IDC 76%
ILC 7%
Lobulo-ductal 7%
Mucinous 2.40%
Tubular 1.50%
Medullary 1.20%
Papillary 1%
Rare subtypes 2.90%

C

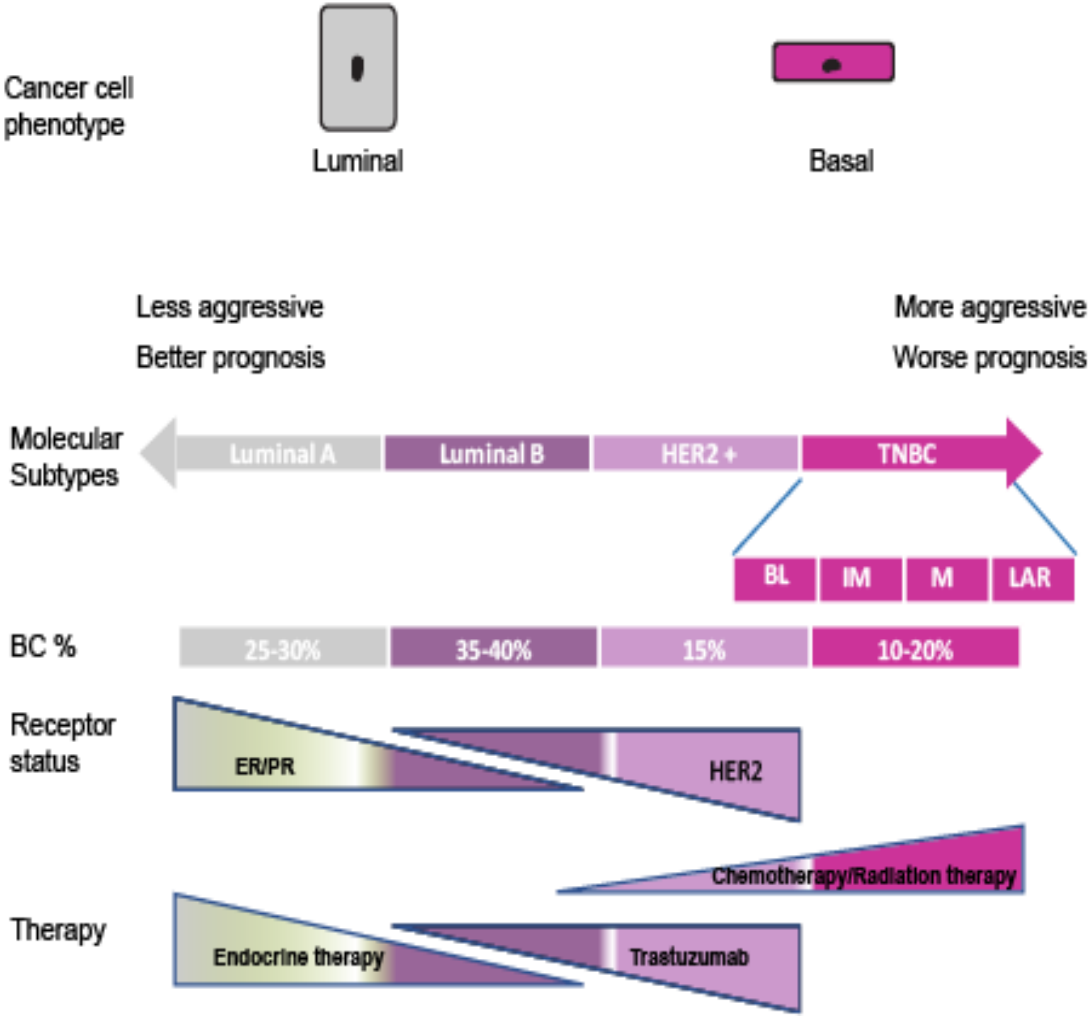
Cancer cell phenotype
Luminal
Basal
Less aggressive
Better prognosis
More aggressive
Worse prognosis
Molecular Subtypes
Luminal A
Luminal B
HER2 +
TNBC
BL
IM
M
LAR
BC %
25-30%
35-40%
15%
10-20%
Receptor status
ER/PR
HER2
Chemotherapy/Radiation therapy
Therapy
Endocrine therapy
Trastuzumab

Figure 1.1: Schematic representation of breast cancer subtypes:

(A) Breast tissue consists of 10-20 lobes which are connected by ducts. Each lobe consists of lobules that secrete milk. Lobes and ducts are formed by luminal epithelial cells and surrounds the lumen which are further lined by basal/myoepithelial cells surrounded by basement membrane. The phenotype of the cell also designates the type of cancer as luminal or basal. (B) Pie chart showing the incidence of different types of histological invasive breast cancer subtypes. IDC: Invasive ductal carcinoma, ILC: Invasive lobular carcinoma. (C) BC subtypes are classified as Luminal A, Luminal B, HER2 positive and TNBC which are further classified as basal like (BL), immunomodulatory (IM), mesenchymal (M), luminal androgen receptor (LAR) based on molecular profiling. Receptor status that shows ER/PR are highly expressed in luminal A cancers compared to luminal B cancers. HER2 is expressed in both HER2 positive and Luminal B cancers. ER/PR or HER2 are absent in TNBC subtype. Chemotherapy is more effective in TNBC than any other subtype. Herceptin or trastuzumab targeted therapy is available for HER2 positive and Luminal B subtypes and endocrine therapy for ER/PR positive subtypes. Aggressiveness, prognosis and occurrence is indicated as BC%. Adapted from [3].

(ILC) with a lower incidence constituting 7% of BC (Fig 1.1B). Other invasive BC include medullary, tubular, papillary, and mucinous carcinomas (Fig 1.1B) [4–8].

The anatomy of ducts and lobes within the breast consists of a lumen surrounded by luminal or epithelial cells followed by a layer of basal or myoepithelial cells which are intact with surrounding basement membrane (Fig 1.1A). Cancers originating from luminal or basal cell phenotype are defined as luminal or basal cancers. Molecular profiling of basal or luminal cancer cells can drive therapeutic decisions (Table 1.1).

Molecular subtypes are broadly classified based on the expression of the estrogen receptor (ER), progesterone receptor (PR), human epidermal growth factor receptor (HER2 or c-erbB2), or the Ki67 proliferation marker. BC molecular subtypes are ER/PR positive cancers (luminal), HER2 positive cancers (basoluminal) and triple negative breast cancers (TNBC) (basal) [9, 10]. Luminal cancers constitute up to 70% of breast cancers and are further divided into Luminal A (40%) and Luminal B (30%) cancers. Luminal tumors have the lowest rate of recurrence and highest rate of disease-free survival with smaller tumors, and benefit from endocrine therapies [5, 11]. Luminal A cancers constitute only ER/PR-positive cancers whereas Luminal B cancers include both ER/PR-positive and HER2 overexpression. Patients with Luminal B cancer have worse disease prognosis than those with Luminal A cancers [12]. HER2-positive cancers occur in luminal or basal cell phenotypes and constitute 15% of breast cancers. Patients with HER2-positive tumors are generally younger than patients with ER/PR-positive tumors and benefit from targeted therapy with trastuzumab [10] (Fig 1.1C). TNBC are

Table 1.1 Breast cancer subtypes

Breast cancer subtype	**Frequency of BC subtype**	**ER/PR status**	**HER2 status**	**Ki67 status**	**Therapy available**
Luminal A	25-30%	+	-	-	Hormonal treatment
Lumina B	35-40%	+	+/-	+	Chemotherapy, anti- HER2 and hormonal treatment
HER2 positive	15%	-	+		Chemotherapy, and anti-HER2
Basal - triple negative breast cancer	10-15%	-	-		Chemotherapy
Normal-like	10%	+	-	-	Chemotherapy

+ overexpression, +/- moderate expression and –absence of the marker.

characterized by the presence of ER, PR or HER2 expression in less than 1% of the tumors and constitute about 15-20% of invasive breast cancers. However, the definition of negative has been debatable in the past, as it is considered ER/PR positive only when the expression is seen in >10% of the tumor [13]. TNBC tend to occur in younger women and has the poorest prognosis [13]. TNBC tumors tend to be larger, more aggressive, and more molecularly heterogeneous. TNBC tumors are characterized by high genetic instability, complex patterns of copy number alterations and structural rearrangements [14]. TNBC patients tend to have a high risk of metastasis and death within 5 years of diagnosis [15]. There are no targeted therapies available for TNBC treatment, and the treatment available is chemotherapy or radiotherapy (Fig 1.1C). TNBC patients respond to chemotherapy better than patients with other BC subtypes, but only 80% of patients show complete response [16].

1.2 Triple negative breast cancer

TNBC show diversity in histologic patterns and subtypes which contributes to poor prognoses. In 2007 TNBC were defined as basal-like cancers and categorized into five subtypes using first generation gene sequencing [17]. Since then, refinement of TNBC subtypes has been constantly updated. Lehman *et al.* [18] performed gene expression analysis of 21 BC data sets and identified 6 BC subtypes, basal-like 1 (BL1), basal-like 2 (BL2), immunomodulatory (IM), luminal/androgen receptor (LAR), mesenchymal (M), and mesenchymal stem-like (MSL). Furthermore, they refined 6 subtypes to 4 subtypes to reduce complexity of varying histology among tumor specimens [19]. Based upon these subtypes, several studies re-categorized TNBC

subtypes using different high throughput techniques such as genomics DNA copy number arrays, DNA methylation, exome sequencing, messenger RNA arrays, microRNA sequencing, and reverse phase protein arrays [13, 20–23]. However, here I will focus on the 5 subtypes, initially identified by Lehman *et al.* [18, 19], that include BL1, BL2, IM, LAR, and mesenchymal/mesenchymal stem-like (M) (Fig 1C).

BL1 and BL2 TNBCs originate from basal/myoepithelial cells and constitute 75-80% of TNBC. The remaining 25% of TNBC include a mixture of other BC subtypes, mostly HER2 positive which do not exhibit features like basal subtype. Histologically, BL1 is largely seen in ductal carcinomas and BL2 in medullary carcinomas. BL1 has an increased activation of DNA damage response and cell cycle pathways promoting cell proliferation while BL2 has an enriched growth factor signaling and basal/myoepithelial markers. (Table 1.2). Currently, chemotherapies such as anthracyclines, alkylating agents and taxanes are the only option for both early and advanced-TNBC, however, there are several targeted therapeutics based on the molecular classification in clinical studies indicating importance of molecular characterization of tumor and its treatment. For instance, phase II where 25-100 people are treated with new drug tested in phase I and phase III studies where several hundreds of patients are treated, targeting DNA damage response pathways with platinum salt and poly-ADP ribose polymerase 1 (PARP1) inhibitors respectively, showed significantly greater incidence of complete remission of pathology [24].

IM TNBC has increased expression of the genes related to T-cell, B-cell and natural killer cell function. Histologically, immune signaling pathways in the IM subtype

Table1.2: Molecular characteristics of TNBC subtypes.

TNBC subtype	Gene expression (Transcript level)	Functions of the pathways	Intrinsic subtype
BL1	↑ Ki67	↑ Cell cycle division and regulation	Basal, HER2
BL2	↑ EGFR, MET, EPHA2, TP63 and MME	↑ Growth factor signaling, glycolysis and gluconeogenesis	Basal
IM	↑ NFkB, TNF and JAK/STAT	↑ Immune cell processes	Basal
M	↑ TGFβ signaling genes and EMT- associated genes	↑ Cell motility	Basal, Normal-like
MSL	↓ Claudin 3, 4, and 7 ↑ TGFβ signaling genes and EMT-assoiated genes	↑ Cell motility and cellular differentiation, growth pathways, angiogenesis, immune signaling, and stem cell associated genes. ↓Proliferation and cell cycle regulation	Basal, Normal-like, Luminal B
LAR	↑ Androgen receptor targets and co-activators	↑Steroid synthesis and androgen/oestrogen metabolism	Luminal A

[a]Abbreviations: EGFR – epidermal growth factor receptor, EPHA2 - ephrin type A receptor 2, TP63 - tumor protein 63, MME - membrane metalloendopeptidases, NFkB – nuclear factor kappa B, TNF - tumor necrosis factor, JAK/STAT - janus kinase/signal transducers and activators of transcription, TGFβ - transforming growth factor β.
Information in this table is sourced from [19, 21, 23]

overlap with signaling pathways found activated in medullary BC. The classification scheme of Burstein *et al.* [23] combined basal-like with immunomodulatory pathways to identify basal-like immunosuppressed (BLIS) and basal-like immune activated (BLIA) subtypes. The BLIS subtype had a worse prognosis than the BLIA subtype. Despite its high-grade histology, the IM subtype is known to show better prognosis with the best overall and relapse-free survival rates in comparison to other TNBC subtypes. In a phase I trial, patients treated with immune checkpoint regulators such as PD-L1 showed an 18.5% response rate.

The LAR subtype falls under the 25% non-basal-like TNBC subtypes where in ER negative tumors, activation of hormone regulated pathways including estrogen/androgen metabolism is observed. Despite the classification as ER negative tumors, gene expression profiling of LAR shows molecular evidence of ER activation due to 1-2% of tumors expressing ER protein. . Histologically, LAR is reported to be lobular carcinomas.. LAR tumors also express androgen receptor (AR) targets and co-activators. In a phase II trial, AR positive TNBC patients had a 12% complete response when AR was targeted with enzalumatide, indicating AR blockage as one therapeutic strategy for this subtype [25].

Mesenchymal and mesenchymal stem-like (MSL) subtypes are enriched with genes related to epithelial-to-mesenchymal transition (EMT) pathways. Specifically, MSL subtype show low levels of proliferation genes, which is accompanied by increase in gene expression associated with stem cells. Moreover, both M and MSL subtypes show a decrease in claudin 2, 3 and 7 which indicates EMT promotion. MSL also show

an upregulation of phosphatidylinositol-3-kinase (PI3K) signaling, contributing to cell proliferation. Histologically, this subtype is seen in metaplastic carcinomas. In addition, MSL are highly invasive and metastatic in nature in comparison to other subtypes and are chemoresistant. Therefore, blockage of PI3K pathway or the EMT pathway genes might be potential targets for this subtype (Table 1.2).

1.3 Breast cancer metastasis

Cancer metastases account for 90% of all human cancer-related deaths, including BC [26]. The metastatic cascade is a very complex and poorly understood process. It includes a series of steps that starts with tumor progression, tumor invasion, matrix remodelling, intravasation, extravasation, and ends with colonization of the tumor cells at distant sites (Fig 1.2). During metastasis, cancer cells undergo dissemination from the primary tumor and can achieve migration via an EMT, followed by a colonization of tumor at secondary site via mesenchymal to epithelial transition (MET) The most common secondary sites of metastasis in BC are bone, lung, liver, and brain, with bone and lung being especially common in TNBC [27]. The sites of BC metastasis can be categorized as non-visceral, which include bone, locoregional lymph nodes, brain, lungs, and visceral, defined as affecting organs in the viscera. The metastatic pattern among TNBC subtypes is different. For instance, TNBC patients with the LAR subtype display an increase in lymph node metastasis, and M subtype has higher tendency to metastasize in lungs in comparison to other subtypes.

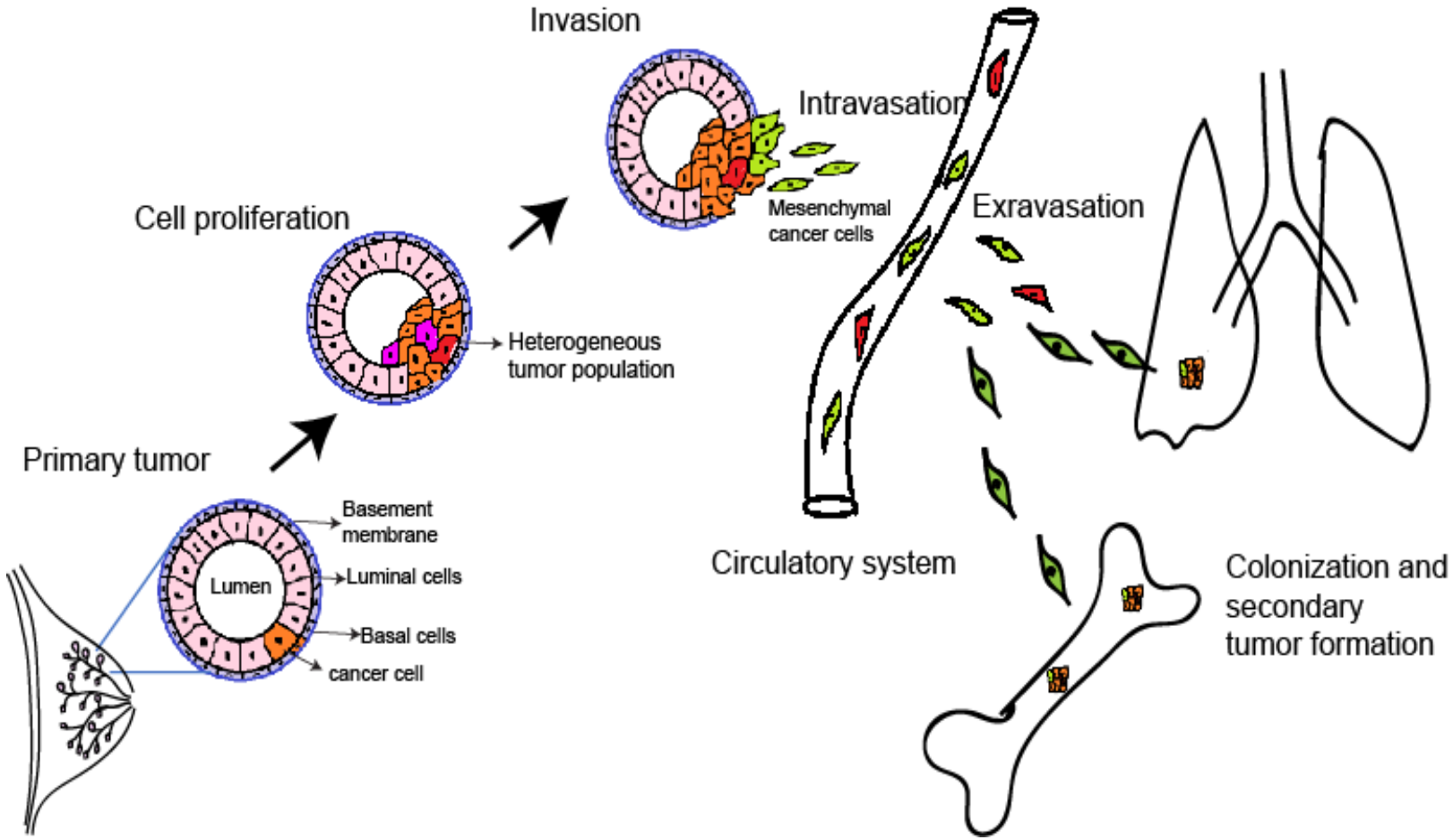
Invasion
Intravasation
Mesenchymal
cancer cells
Cell proliferation
Exravasation
Heterogeneous
tumor population
Primary tumor
Basement
membrane
Lumen
Luminal cells
Basal cells
cancer cell
Circulatory system
Colonization and
secondary
tumor formation

Figure 1.2: Stages of BC initiation, progression and metastasis.

Increased genetic and epigenetic instability leads to tumorigenesis and increase in cell proliferation (orange). Accumulation of mutations leads to heterogeneous tumor population including cancer stem cells (red), cancer cells with different mutation (dark purple) burden. Consequently, epithelial cells change to mesenchymal cells (green) to invade the basement membrane and remodel the extracellular matrix. Mesenchymal tumor cells intravasate into the circulatory system, migrate to distant sites. Extravasate into tissue parenchyma, colonize and form tumors at secondary sites such as lung or bone. Source for information [28].

1.3.1 Epithelial to mesenchymal transition

Genetic or epigenetic instability in BC cells at the primary site leads to increased proliferation and decreased apoptosis that enhance the tumor progression and accumulates tumor burden. Moreover, increased epigenetic or genetic alterations in BC cells allow them to undergo invasion, intravasation, survival and extravasation.EMT is a process whereby epithelial cells acquire mesenchymal cell-like properties with increased motility and decreased cell adhesion. This process has been divided as type I EMT, type II EMT and type III EMT. When re-arrangement or migration of cells occurs during embryonic development and organ formation, it is defined as type I EMT. If this change occurs during tissue regeneration or wound healing, it is defined as type II EMT. Here, I will discuss about type III EMT where acquisition of mesenchymal properties by epithelial tumor cells occurs [29].

1.3.1.1 Epithelial cells

Normal epithelial cells are characterized by polarization of their plasma membrane with the presence of distinct surface domains that supports the structure, function and composition of the cells and interactions with the basement membrane and adjacent cells. The basement membrane is a specialized extracellular matrix (ECM) that separates the epithelial cells from connective tissue, keeps the epithelial cells together, and maintains the integrity of the tissue. The major components of basement membranes are laminins and type IV collagen. The composition of basement membrane varies across the tissues based on the physiologic or pathophysiologic state of tissue. The permeability,

cell-cell adhesion strength, cell-microenvironment interaction, and transportation of some metabolites is regulated by the cell type junctions including adherens junctions, tight junctions, gap junctions, desmosomes, and hemidesmosomes. [16, 26, 30–39]. Adherens junctions, and desmosomes are cadherin-containing anchoring junctions that bind to adjacent cells giving strength and rigidity to the epithelia.

Among the classical cadherins, E-cadherin is the most widely expressed in epithelial cells and considered an important marker for the epithelial phenotype [40, 41]. E-cadherin plays an essential role in cell-cell interactions and in epithelial integrity of the cell. The tight junction proteins occludins and claudins stop diffusion of proteins and some lipids in the plasma membrane. Moreover, tight junctions have a role in cell-cell interactions and epithelial cell polarity. Hemidesmosomes are integrin-containing junctions and gap junctions are connexon-containing junctions that participate in cell-cell and cell-matrix adhesions, respectively. Epithelial cells undergo trans-differentiation, a natural process of cells, where they transform into a different cell type in order to migrate during wound healing, tissue generation, or metastasis. When the trans-differentiation is triggered in epithelial cells to transform into mesenchymal cells, epithelial cells acquire mesenchymal properties such as increased expression of vimentin, N-cadherin, fibronectin, smooth muscle actin and matrix metalloproteinases (MMPs) (Fig 1.3).

1.3.1.2 Invasion

Genetic or epigenetic instability within a tumor cell, accompanied by external inflammatory tumor-associated stroma, induces EMT. Particularly, initiation of EMT is

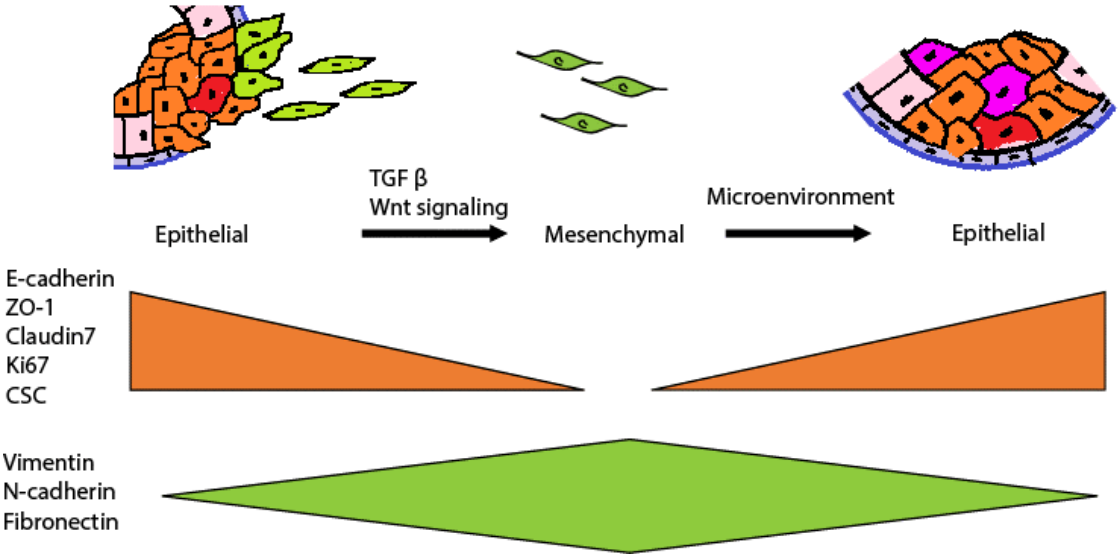

Figure 1.3: Epithelial to mesenchymal transition and mesenchymal to epithelial transition:

Transition of stable, polar epithelial cancer cells (orange) to migratory, non-polar mesenchymal cancer cells (green) is known as EMT. Illustration shows the changes in the biomarkers where epithelial markers (E-cadherin, ZO-1, claudin-7) are suppressed during mesenchymal status and regain their expression during MET. In contrast, mesenchymal biomarkers (vimentin, N-cadherin and fibronectin) are suppressed during epithelial status and expressed during mesenchymal status. Activation of TGFβ signaling, wingless/integrated (Wnt) signaling by external factors enhance mesenchymal phenotype, however activation of MET is still elusive. Cancer stem cells (CSCs) shown in red are increased during EMT and decreased during MET. Other colours such as dark purple in tumor represent the heterogenous tumor population.

regulated by intrinsic factors such as activation of signaling pathways, transcription factors, microRNAs, or epigenetic modulation influenced by extrinsic factors such as tumor-stroma interactions [42]. Stromal cells such as adipocytes can induce the expression of mesenchymal markers and promote invasiveness of BC cells, suggesting a pro-EMT regulation [43]. Also, adipocytes from visceral white adipose tissue (WAT) have enhanced effects on the EMT of BC cells compared to those from subcutaneous WAT [44]. The stromal secretions such as growth factors, including transforming growth factor (TGFβ), epidermal growth factor (EGF), platelet-derived growth factor (PDGF) and hepatocyte growth factor (HGF), can also induce EMT as well as inducing other functions of cancer cells such as proliferation, protection from apoptosis, and angiogenesis [45, 46]. The signaling pathways that are associated with induction of EMT are the TGFβ, wingless/integrated (Wnt)/β-catenin, and Notch pathways [42]. These pathways activate the master regulators of EMT: the EMT-transcription factors (EMT-TFs) Snail, Slug, zinc finger E-box binding homebox 1 (ZEB 1), ZEB2, goosecoid, forkhead box C1 (FOXC1), FOXC2 and twist family basic helix loop helix (bHLH) transcription factor (TWIST). EMT-TFs transcriptionally downregulate the expression of adherens junction and integrin proteins, which allows transformed cells to lose polarity and dissociate from adjacent cells and the basal membrane [37, 47]. The E-cadherin promoter is repressed by Snail, Slug and ZEB2 directly and by TWIST1, FOXC2, and ZEB1 indirectly, which disrupts cell polarity and maintains the mesenchymal phenotype to promote EMT [47, 48]. TWIST1 can transform normal mammary epithelial cell into

mesenchymal like cells that have increased expression of vimentin, N-cadherin and fibronectin [49] (Fig 1.3).

Once EMT is initiated, cells lose polarity and become mobile whereupon they can invade the basement membrane and degrade the extracellular matrix. Snail1 and Snail2 expression in BC cells increase membrane type1-matrix metalloproteinase (MT1-MMP), MT2-MMP, MT4-MMP and MMP2 expression which further leads to the degradation ofbasement membrane and allows subsequent tumor metastasis [50]. EMT-TFs induce the formation of specialized structures called invadopodia, that invade local ECM. TWIST1 and TGFβ enhance invadopodia formation, which actively promotes degradation of the matrix [51].Moreover, MMPs and other chemokines released from epithelial cells and inflammatory cells disrupt the basement membrane and promote focal degradation of extracellular matrix proteins such as collagen and laminins [29].

1.3.1.3 Intravasation

Cancer cells undergo intravasation to invade into the lymphatic and blood circulatory systems. EMT markers, matrix remodeling proteins and angiogenic factors have an essential role in intravasation of cancer cells. In pancreatic cancer, increases in ZEB1 expression enhances the migration through the endothelial barrier followed by metastatic colonization [52]. Activation of membrane bound proteins, MT1-MMP and MT2-MMP but not MMP, allow cancer cells to come in contact with endothelial cells and then intravasate into the vasculature [50]. To disrupt the vascular integrity during both intravasation and extravasation, cancer cells express vascular endothelial growth factor (VEGF), MMPs, and a disintegrin and metalloproteinase (ADAM) [53].

Once the cancer cells disseminate, they intravasate into the circulatory system as single cells or clusters in a mesenchymal state. Circulating tumor cells (CTCs) retain mesenchymal properties via activation of the TGFβ pathway [54]. Moreover, in a mouse mammary tumor model, increases in the protein expression of the EMT marker TWIST1 was found during early stages of tumor formation, and cells remain in a mesenchymal state until they reach the bone marrow [55].

1.3.1.4 Survival and extravasation

The circulatory system provides a hostile situation for CTCs, with constant clearance by natural killer (NK) cells and physical strain from the circulation [56]. CTCs survive the immune insult followed by the attachment to the wall of blood vessel to finally prepare for extravasation from the circulation. CTCs, once in circulation, rapidly interact with platelets via tissue factor present on cancer cells. Platelets provide physical protection by coating the CTCs and also by inhibiting lysis by blocking NK cells via TGFβ and PDGF [56]. Removal of TGFβ in platelets impairs the extravasation of CTCs and thus reduces metastasis [57]. In addition, platelets can change intracellular signaling within cancer cells to contribute to successful metastasis [57]. Moreover, neutrophils in circulation can also provide physical protection to CTCs from NK cells and further aid in extravasation [56]. Expression of TWIST1 or Snail1 in mammary epithelial cells promotes survival by triggering microtenacle formation, a microtubule based membrane protrusion that allows attachment of CTCs to leukocytes, platelets and endothelium to aid in extravasation [51]. Furthermore, β1 integrin signaling not only maintains EMT phenotype but also triggers protrusion formation in CTCs that mediate extravasation [58].

Macrophages at the site of CTC attachment also play a role in invadopodia formation, disruption of endothelium, and extravasation. Cancer cells that metastasize to the lung show high expression of VEGF that facilitates disruption of the endothelium. Increase in MMPs such as MMP2, MMP1 and cyclooxygenase-2 (COX2) also promote extravasation and metastasis [53, 59]. Collectively, all the factors discussed above work together to aid and contribute in survival and extravasation of CTCs.

1.3.2 Mesenchymal to epithelial transition

The reverse process of EMT is known as MET, where the mesenchymal CTCs survive the circulation, extravasate into the distant tissue parenchyma and dedifferentiate into an epithelial phenotype to form a secondary tumor (Fig 1.2). The mechanisms involved in organ specific extravasation of CTCs are still elusive. According to previous studies, many factors such as the circulatory system, microenvironment, adaptability to the tissue parenchyma, and tumor initiating ability have an impact on colonization of CTC's at a specific site. In some cancers, like colorectal cancer, metastasis in the liver is explained by the draining of blood in the portal vein into the liver from the colon [60]. When CTCs enter the microenvironment of the tissue parenchyma at a secondary site, they encounter ECM and stromal cells including fibroblasts, adipocytes, and inflammatory cells. In prostate and breast cancer, E-cadherin is re-expressed or upregulated when co-cultured with hepatocytes, which indicates MET of cancer cells at a secondary site [61, 62]. Aokage *et al.* showed that non-small cell lung cancer cells (NSCLC) express low E-cadherin while migrating through lymphatic vessels. Moreover,

when NSCLC encounter lung parenchyma, they re-express E-cadherin, to undergo micrometastasis [63]. Co-culture of adipose tissue-derived stem cells upregulates E-cadherin expression, and downregulates vimentin and N-cadherin expression in liver cancer cells [64]. However, how these factors are involved in macro- or micro-metastases induction is unclear.

During EMT, cell division is repressed by Snail1 and ZEB2 via inhibition of cyclin D activity, which slows down the cell proliferation and promotes differentiation [51]. Regaining epithelial properties is essential for cancer cells to proliferate and colonize at distant organs [65]. Several pathways such as the Ras- extracellular signal regulated kinases (ERK), PI3K-Akt, and Wnt signaling pathways in BC cells induce an epithelial phenotype [60, 66]. TFs such as Snail and TWIST that promote EMT are also repressed during metastasis which further assists in suppressing the mesenchymal phenotype. In various studies, it was proven that mesenchymal cells acquire epithelial properties after metastasis which was recognized by expression of E-cadherin [60, 62, 67]. Forced expression of E-cadherin can, in fact, induce MET in prostate cancer cells [68]. Moreover, cancer cells use E-cadherin to connect with local normal epithelial cells and establish the tumor formation at a secondary site. However, mechanisms involved in colonization of secondary tumors (MET) are not well studied in comparison to EMT that occurs at the initiation of metastasis.

1.3.3 Self renewal: breast cancer stem cells

The self-renewing ability of cancer cells is an important trait to reconstitute other subpopulations and maintain tumor heterogeneity. This property belongs to a subpopulation within tumors called CSCs. In breast tumors, these cells are known as breast cancer stem cells (BCSCs) [69]. There are some similarities between normal stem cells and CSCs in terms of gene expression but CSCs are not always generated from normal stem cells [70, 71]. Notch, hedgehog (Hh), and Wnt pathways are essential for maintaining normal tissue processes. However, dysregulation in these pathways can lead to transformation of normal stem cells into CSCs. In addition, CSCs can be generated from mutated cancer cells that acquire stem-like properties. BCSCs can be identified by their high expression of CD44, low expression of CD24, and high aldehyde dehydrogenase (ALDH) activity ($CD44^{+}CD24^{-}ALDH^{+}$) [69, 72]. Moreover, the combination of a high CD44/CD24 ratio and $ALDH^{+}$ on BCSCs is conserved during metastasis, from primary tumor to CTCs and the distant metastasis [73]. When transplanted into immunocompromised mice, BCSCs have the ability to self-renew and reconstitute other subpopulations and recapitulating the original heterogenous tumor [74, 75]. Metastatic cells with stem cell-like properties isolated from patient-derived xenograft models of BC have a tumor initiating capacity, leading to the formation of large tumors [76]. BCSCs are highly associated with increased invasiveness, tumor progression, and metastasis [77, 78]. BCSCs are known to be radiation and chemotherapy resistant [79–81]. Tumors with a high percentage of BCSCs generally have a worse prognosis [82] since as few as 1×10^{3} BCSCs can regenerate an entire tumor, including both $CD24^{-}$ and

$CD24^+$ cells [83]. Moreover, BCSCs are considered an independent prognostic factor for poor prognosis in TNBC [84].

EMT is associated with the formation of CSCs and the presence of CSCs promote EMT [77]. Induction of EMT markers such as TGFβ, TWIST and Snail can induce normal mammary cells to transform into CSCs [85]. In addition, TGFβ1 increases the BCSC population and promotes local tumor invasion and metastasis [86]. Consequently, EMT induced CSCs increase mammosphere formation where cells start to clump together. However, the promotion of CSC formation by EMT is also dependent on cell type during tumor progression [87].

CSCs isolated from the mammary gland or BC exhibit EMT properties [49, 88]. Specifically, E-cadherin mRNA is downregulated and mesenchymal vimentin, N-cadherin, and fibronectin mRNA are upregulated in $CD44^+CD24^-$ cells [49]. In addition, EMT-TF such as TWIST1, Snail 1, ZEB1, ZEB2, goosecoid, FOXC2, Y-box binding protein 1 (YB-1), ladybird homebox 1 (LBX-1), Six1 and hypoxia inducible factor (HIF) maintain the stemness of CSCs [89]. Similarly, microRNA miR200 maintains the stem cell state [90, 91]. Overall, EMT and CSCs together lead to formation of large tumors with the ability to invade, and survive therapy with a high chance of recurrence, which are a deadly combination for patients. In addition, CSCs migrate to the distant organs along with CTCs and contribute towards the initiation of tumor and metastases formation, where CSCs not only initiate the metastasis but also maintain the heterogeneity of the secondary tumor [92].

1.4 Obesity and its effect on breast cancer progression

Obesity is defined as an unequal distribution of body weight for height with high accumulation of adipose tissue that leads to mild, chronic, and systemic inflammation. According to the World Health Organization (WHO) standards, body mass index (BMI) ≥ 25 kg/m^2 is overweight and BMI of ≥ 30 kg/m^2 is obese. Over 2 billion people in the world are overweight or obese and it is estimated that by 2030 >3.3 billion (57.8%) of the adult world population will be overweight or obese [93, 94]. Obesity is now considered as one of the most important risk factors contributing to overall disease burden in the world [95]. Common health consequences of patients that are overweight or obese include cardiovascular diseases, diabetes, osteoarthritis, and some cancers including endometrial, ovarian, breast, prostate, liver, gall bladder, kidney, and colon [96, 97].

Over 40% of cancer patients are classified as overweight or obese [98, 99]. Obese women with BC have larger tumors and enhanced metastasis that contributes to a 30% increased risk of death [100–102]. Obesity is one of the various factors that influences BC progression in both pre-menopausal and post-menopausal women [103]. Obese post-menopausal women are at high risk for ER/PR positive BC whereas obese pre-menopausal women are at higher risk of developing TNBC compared to lean women [104]. Moreover, obese patients do not respond to therapy as well as lean patients, particularly when diagnosed with TNBC, also contributing to the overall worse prognosis [103, 104].

Body fat distribution plays an important role in disease progression. Adipose tissue (AT) is divided into two types: brown adipose tissue (BAT) and white adipose tissue (WAT). BAT depots are present in newborn babies and help maintain body temperature by thermogenesis. In infants, BAT is located in interscapular and perirenal regions where BAT in the interscapular region gradually decreases with age [105]. WAT not only stores energy but is also an endocrine organ that produces metabolites, hormones, and cytokines (adipokines). WAT depots are classified into visceral AT (VAT) and subcutaneous AT (SAT). WAT contained in the intra-abdominal, thoracic, and pelvic cavity surrounding the omentum, gut, kidney, heart and gonads is VAT. WAT depots beneath skin are SAT. SAT is widely distributed and divided into upper and lower SAT. Lower SAT is mainly located in the leg and hip regions where as upper SAT is located in face, arms, abdomen, and breast. Breast tissue is composed of 90% WAT is the only SAT with permanent interactions with epithelial cells and is involved in normal mammary gland development [106]. In addition, adipocytes constitute about 70% of bone marrow volume [107]. The number of adipocytes in bone marrow increase with both age and obesity [108].

WAT depots have different effects on the advancement of diseases such as metabolic syndrome or cancer based on the location. In comparison to SAT, VAT is more metabolically active, with accumulated inflammatory cells and cytokines [109]. Together, these contribute to cancer, including BC, and insulin resistance leading to several diseases such as metabolic syndrome and diabetes. Women with visceral obesity have a higher risk of BC occurrence than women with subcutaneous obesity [110]. Both obesity and TNBC are associated with visceral metastases development [27, 111]. In obese

patients with ovarian or prostate cancer, an increase in the number of bone marrow adipocytes is correlated to increased skeletal metastasis [112, 113]. The role of bone marrow adipocytes in metastasis of BC to bone has not yet been examined.

Obesity is characterized by the enlargement of WAT depots with excess engorgement of lipids in adipocytes. The increase in engorged adipocytes induces systemic changes such as increases in adipokines, secretion of inflammatory cytokines, lipid metabolites, fibrosis, and CSC, that can contribute to BC progression [114] (for details refer to 1.6.6, and 1.6.7). In obese BC patients, the increase in adipocyte size causes a stiffer ECM to be deposited by adipocyte stromal cells [115] (Fig 1.4). Chronic inflammation from obesity leads to secretion of cytokines such as interleukin-6 (IL-6) and tumor necrosis factor-α (TNF-α) that are known to affect cancer progression (for details refer to 1.6.6). When they occur together, obesity and TNBC are the worst combination for a patient's outcome, as obesity reduces the therapeutic response even further.

1.5 Tumor microenvironment and its effect on cancer progression

Genetic or epigenetic instability in cancer cells leads to activation of signaling networks, which interacts with neighbouring cells and ECM generating a tumor microenvironment (TME) convenient for tumor growth. The TME is one of the important extrinsic factors that contributes to the progression of BC. The TME is comprised of ECM proteins and several stromal cell types such as endothelial cells, fibroblasts, immune cells, adipocytes, and inflammatory cells that play a crucial role in tumor growth

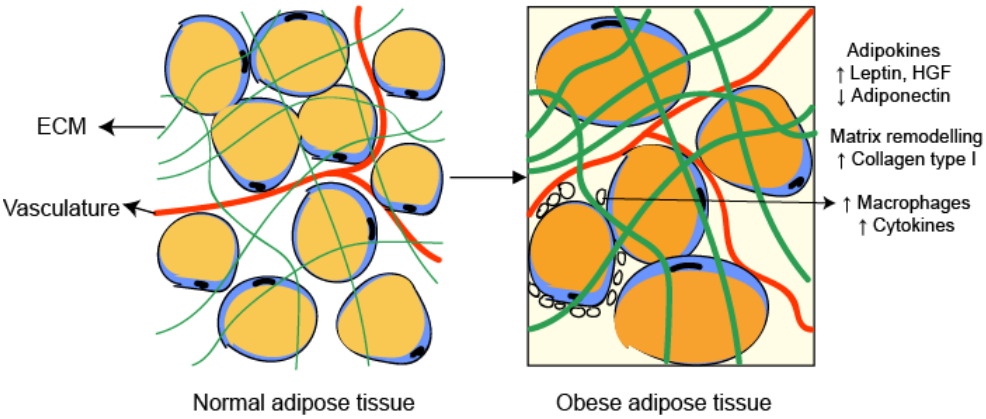

Figure 1.4: Schematic illustration of adipose tissue under normal and obese conditions:

Obesity induces both local and systemic changes where there is an increase in lipid content with in the cells, and macrophages that leads to accumulation of pro-inflammatory cytokines and adipokines such as leptin, and hepatocyte growth factor (HGF). Adipocytes under obese conditions accumulate collagen that leads to stiffening of the microenvironment. ECM shown in green, under obese conditions ECM is increased. Image was adapted from [131].

and development [116]. Abnormal conditions, like those seen in obesity, can contribute to BC progression by changing the TME [114].

In the normal breast, luminal and basal epithelium are surrounded by the basement membrane that constitutes of laminin-rich, collagen type IV, and proteoglycan based ECM. *In vitro*, mammary cells form acinar structures with a lumen and can functionally differentiate and produce milk proteins in *in vitro* 3 dimensional (3D) cultures but not 2D cultures, highlighting the importance of ECM in mammary development [117]. Laminins in the basement membrane maintain the polarity of epithelial cells [118]. In addition to structural support, the ECM involves in biochemical and mechanical cues that regulate cell behaviour. Viscous and elastic properties of ECM surrounding the cell contributes to the cell fate [119]. During tumor progression, an increase in ECM remodelling enzymes such as MMP 1, 2 and 9, and cathepsins by stromal cells degrade laminins and other ECM proteins changing the elasticity of ECM that contribute to contractility and motility of cells in EMT [50, 120–122]. In addition, there is an upregulation of fibrillar collagens I, III and V, matricellular proteins, glycosaminoglycans, and fibronectin that increase fibre crosslinking and induce a shift from the laminin rich normal breast tissue to a collagen rich tumor microenvironment. This increase in collagen leads to an increase in ECM stiffness [123, 124]. An increase in lysyl oxidase by BC cells, a copper-dependent amine oxidase that initiates the process of the intra and inter crosslinking of collagen strands leading to increase in ECM stiffness, also contributes to invasiveness of BC progression [125, 126]. ECM stiffness in turn promotes BC progression, increases pro-inflammatory cytokine secretion, and decreases

adipocyte lipolysis [127–129]. ECM stiffness leads to an upregulation of ERK signaling thereby leading to increases in BC cell proliferation. The increased ratio of stiffer ECM to adipocyte size in the mammary gland can also enhance cancer progression [115]. Stromal cells in the TME secrete several secretory factors such as cytokines, chemokines, growth factors and extracellular vesicles, and interact with tumor cells to contribute to breast cancer progression and invasion. Tumor-associated macrophages (TAM) promote angiogenesis and invasion by upregulating VEGF. In addition, TAM's secrete tumor promoting factors such as ECM-remodelling enzymes, growth factors, and inflammatory cytokines that contribute to tumor progression [130]. Fibroblasts when co-cultured with breast cancer cells, produce growth factors such as hepatocyte growth factor that promote tumor growth [132]. Moreover, adipocytes which are major component of the breast have both mechanical and biochemical interactions with BC cells that are involved in tumor progression (refer to section 1.7.4) [133].

1.6 Model systems: 2D and 3D culture systems

Cells in 2D cell culture lack the 3D organization of cells between each other or with the ECM as observed in organs and tissues *in vivo* [134]. *In vitro* 3D cell culture methods were thus developed to better mimic *in vivo* conditions and bridge the gap between *in vitro* and *in vivo* experiments [135–137]. Unlike cells in 2D cultures, cells grown in 3D obtain a more physiological morphology, displaying aggregate structures or spheroids with prevalent cell junctions. Moreover, cells in 3D obtain phenotypic heterogeneity with a varied cell proliferation rate, gene expression and differentiation within one population [138]. Exposure to nutrients, growth factors, or drugs is also

heterogeneous where cells on the outer side of a spheroid are more exposed compared to cells in the inner core, which is more similar to *in vivo* conditions. In addition, cells in 3D have greater viability, less susceptibility to external factors, and show increased resistance to drug-induced stimuli [139, 140]. Lastly, both EMT or MET are processes that need the matrix for invasion during transition . Therefore, these processes are better modeled in 3D culture systems compared to standard 2D culture systems [141].

The critical component of the *in vitro* 3D microenvironment is the matrix or scaffold that supports cells, allows nutrient and signal exchanges among cells, and mimics ECM. Natural matrices such as decellularized tissue, collagen, laminin, fibrin, alginate, gelatine or cellulose acetate as well as synthetic or artificial matrices such as hyaluronic acids, polyethanol glycol, polyurethane, Alvetex, or MapTrix Hygels, are used in *in vitro* 3D systems [137]. In addition, biological or synthetic hybrids such as polycaprotactone (PCL)-collagen, PCL-gelatine, metals, ceramic and bioactive glass, and carbon nanotubes are also used as scaffolds in 3D cultures [136]. Typically, co-culture studies that interrogate the influence of other cell types are conducted in Transwell systems or direct co-culture, where physical interactions between the cells and microenvironment is missing [142, 143]. 3D culture systems are used in different applications such as pharmacological studies, drug testing, differentiation studies, tumor models, gene and protein expression studies [136]. 3D culture is an effective way of testing drug genotoxicity or cytotoxicity at an early stage of drug screening and is more cost effective and ethical when compared to animal models.

1.7 Regulation of breast cancer progression

1.7.1 CD24

Cluster of differentiation 24 (CD24) is a heavily glycosylated surface marker which is linked to the plasma membrane via a glycosylphosphatidylinositol (GPI) anchor and localized in membrane lipid rafts [144]. CD24 was first identified 4 decades ago in 1978 [145]. CD24 is translated as a precursor protein of 76 or 80 residues in mice and human, respectively. Upon cleavage of the N-terminal signal sequence and C-terminal GPI anchor sequence, a mature peptide of 27 residues in mice and 32 residues in human is generated [144]. Since its initial discovery, sequencing efforts have revealed that CD24 orthologues are present in many species. However, the conservation of CD24 over the course of evolution has not been reported nor has the earliest known ancestor carrying the gene been identified.

CD24 is glycoprotein with varied molecular weight in different cell types, which is suggested to be due to glycosylation. Both Ser and Thr are potential sites for O-glycosylation and asparagine is site for N-glycosylation [146]. N-glycan analysis of CD24 protein in lymphoblastoma, neuroblastoma and astrocytoma revealed the presence of fucosylated and sialylated complex [147]. 50% of amino acids in mature CD24 protein consists of O- glycosylation sites [146].

The diversity in CD24 glycosylation can potentially be explained by the alternative splicing that generates eight transcript variants. Most of them differ at 3’ UTR region and one of them lacks 5’ UTR region. Transcripts, CD24-001, CD24-201, and

CD24-002 are considered as known protein coding sequences that translates into CD24a isoform pre-protein and CD24-007 is considered as putative protein coding sequence that translates into CD24b isoform, whereas the other transcripts, 004, 005, 003 and 005 are predicted transcript variants that do not have any NCBI ref ID [148]. In mouse, CD24 is designated as CD24a, CD24b and CD24c which are located on chromosome 10, 8 and 14, respectively. CD24a is very well studied, whereas CD24b and CD24c are considered as protein coding genes but nothing much is described about them. Moreover, *CD24* pseudogenes are present in both the mouse and human genome [149].

CD24 has various and diverse roles in cell adhesion and signaling, B-cell development, neuronal development, autoimmune diseases, and cancer [150]. In many cancers, such as colorectal, pancreas, and lung, high expression of CD24 is associated with enhanced proliferation, invasiveness and migration [82] and is also associated with metastasis. In stark contrast, forced expression of CD24 in $CD24^{-}/CD44^{+}$ breast cancer cell lines leads to a decrease in cell proliferation [151] and BCSCs with low expression of CD24 exhibit increased invasiveness and proliferation [79]. It has been shown that CD24 expression is dynamically regulated in both $CD24^{+}$ and $CD24^{-}$ cells, with $CD24^{-}$ cells gaining CD24 expression and *vice versa* in BC cells [74]. This dynamic regulation is associated with changes to the invasive phenotype and occurs both *in vitro* and *in vivo* [74].

Targeting the $CD24-/CD44^{+}$ population reduces BC progression and metastasis [77, 152]. Inhibition of the Notch signaling pathway reduces the CD24-/CD44+

population and brain metastasis from BC [153]. The anti-diabetic drug metformin, interestingly, regulates the EMT status in $CD24^{-}/CD44^{+}$ or $CD24^{+}/CD44^{+}$ cells [154] and also suppresses CD24 protein expression in TNBC [155]. In a similar manner, inhibition of the PI3K/Akt/mechanistic target of rapamycin (mTOR) pathway by quercetin suppresses the $CD24^{-}/CD44^{+}$ BCSC population [156]. Moreover, it has been previously shown that $CD24^{-}/CD44^{+}$ stem like cells can be generated from $CD24^{+}/CD44^{-}$ cells after activation of the oncogenic Ras pathway [85], but it was not clear if this was a direct effect of Ras signaling or a secondary effect of the transformed phenotype.

1.7.1.1 Regulation of CD24

CD24 expression can be regulated transcriptionally or post-transcriptionally. Transcriptionally, regulation of the CD24 promoter depends on GC-rich regions. For example, the specificity protein 1 (SP-1) binding site, and nuclear factor of activated T-cells 5 (NFAT5) binding sites were shown to promote transcription of CD24 in multiple sclerosis and hypertonicity of T-cells, respectively [157, 158]. Interestingly, the TWIST transcription factor family can upregulate or downregulate CD24 expression, with TWIST1 shown to downregulate CD24 transcription in BCSCs, and TWIST2 promoting CD24 transcription in human hepatocarcinoma [159, 160]. Moreover, the Wnt pathway represses CD24 via the T-cell factor 4 (TCF-4) transcription factor in mammary epithelial cells [161]. In addition, the CD24 promoter region contains a negative regulatory element (-983 to -1996 bp from transcription start site (TSS)) that can repress CD24 transcription via an unidentified transcription factor [162]. Bioinformatic analysis using the UCSC genome browser reveals a CpG island, a potential site for epigenetic silencing by

hypermethylation, between −828 to +430 bp, relative to the TSS [163]. Enhanced methylation of the CD24 promoter has been associated with decreased expression in glioblastoma cells and diseased conjunctiva [164, 165]. Post-transcriptionally, stability of CD24 mRNA depends on the two important *cis* elements in the 3'untranslated region (UTR). Deletion of either one of these elements leads to degradation of mRNA [166]. Destabilizing CD24 mRNA by deletion of a dinucleotide in the 3'UTR region leads to protection against autoimmune diseases [167]. Furthermore, the miR34a miRNA has been shown to repress CD24 mRNA expression via the 3' untranslated region [168].

1.7.1.2 Regulation of CD24 in breast cancer progression

CD24 expression is highly dynamic in various cancers but the molecular mechanism involved in the regulation of its expression is poorly understood. Hormones such as estrogen in BC cells and androgens in urothelial cancer can suppress CD24 expression [169, 170]. CD24 mRNA is up regulated by amino acid starvation in BC cells [171] while inhibition of signal transducer and activator of transcription 3 (STAT3) leads to dendritic cell mediated inhibition of CD24 in BC cells [172]. N- myc downstream regulated gene 2 (NDRG-2) down regulates CD24 in BC [173]. In addition, the expression of CD24 is upregulated by overexpression of terminal effector, truncated glioma associated oncogene homolog 1 (tGLI 1) of hedgehog pathway [174], and HIF1α binding to its promoter [175].

1.7.2 The Ras pathway

Ras is an oncogene with activating mutations present in approximately 30% of all human cancers, and is associated with poor prognosis [176]. The oncogenic role of Ras is very well established in many types of human cancers. Although, mutations in Ras are detected in only 5% of breast cancers, studies have shown that the epidermal growth factor receptor (EGFR)/Ras pathway is hyperactivated in >50% of TNBC [177, 178]. Ras activates numerous signaling pathways, such as the Raf, Ral guanine nucleotide dissociation stimulator (RalGDS), and PI3K pathways to promote a myriad of cellular functions such as cell proliferation, cell transformation and cell survival (Fig 1.5) [179]. Activation of RalGDS leads to activation of the RalA GTPases which leads to the subsequent activation of phospholipase D (PLD) to promote vesicle formation and membrane trafficking through the Golgi [180]. Activation of the Raf kinase downstream of Ras leads to the phosphorylation and activation of the MEK kinase (mitogen-activated protein kinase kinase 1), which subsequently phosphorylates and activates the mitogen activated protein kinase ERK (MAPK).The Raf/MEK/ERK pathway primarily regulates proliferation and apoptosis [181]. Activation of PI3K leads to phosphorylation of phosphatidylinositol phospholipids that recruit and promote the activation of Akt by the PDK1 (phosphoinositide-dependent kinase 1) and PDK2 (phosphoinositide-dependent kinase 2) kinases. The PI3K/Akt pathway promotes cell survival, growth, and metabolism in addition to regulating cell migration [181]. The PI3K pathway can also be activated independently of Ras activation and substantial cross-talk between the Raf and PI3K

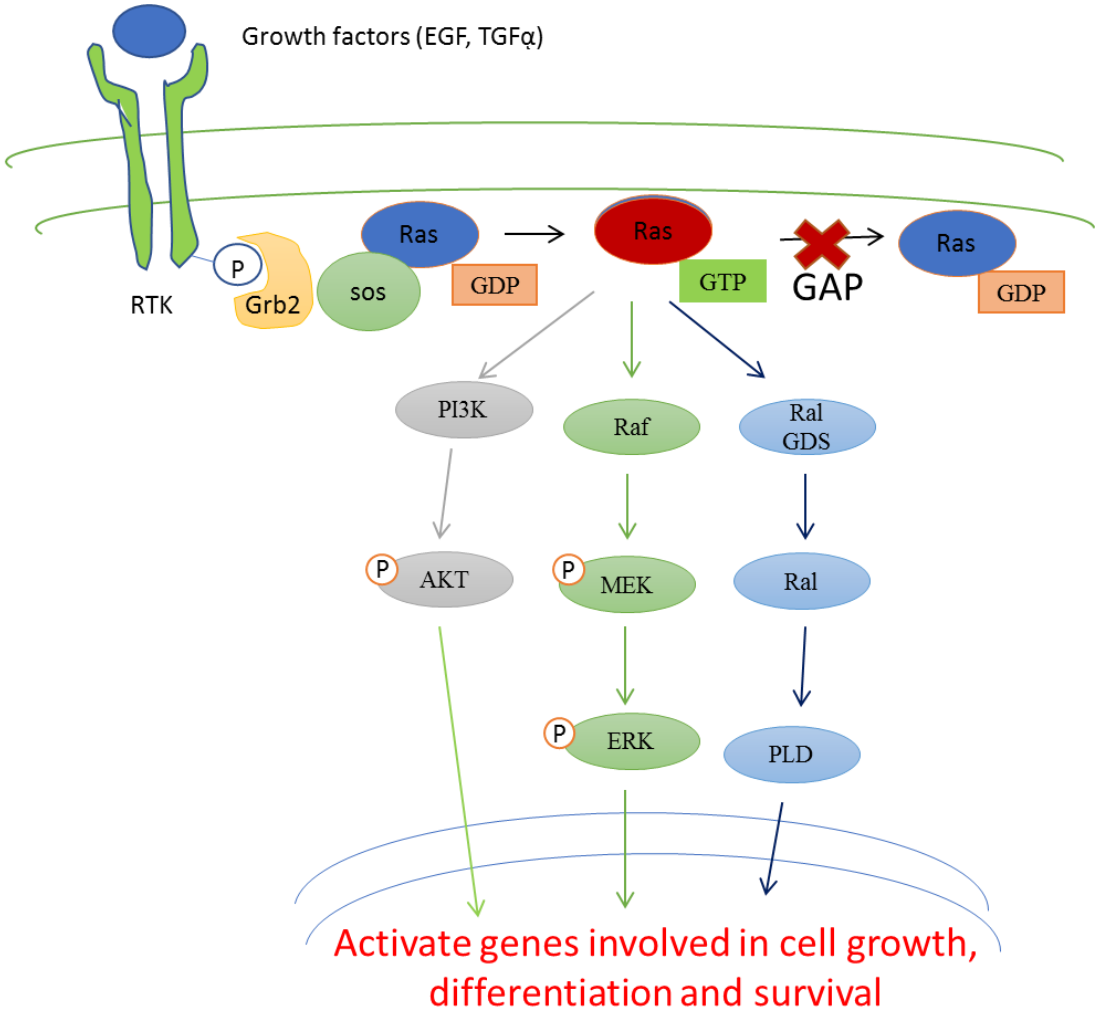
Growth factors (EGF, TGFα)
RTK
P
Grb2
sos
Ras
GDP
Ras
GTP
GAP
Ras
GDP
PI3K
Raf
Ral
GDS
P
AKT
P
MEK
Ral
P
ERK
PLD
Activate genes involved in cell growth,
differentiation and survival

Figure 1.5: Constitutive activation of Ras and its downstream targets:

Receptor tyrosine kinases (RTK) are activated by growth factors such as epidermal growth factor (EGF) or transforming growth factor β (TGF-β). Ras is a small molecular weight G protein which is regulated by switching on and off by exchange of nucleotide guanine phosphate. It is in an active state when bound to guanine triphosphate (GTP) and an inactive state when bound to guanine diphosphate (GDP). Growth factor receptor bound protein (Grb2) facilitates the catalysis by guanine exchange factors (GEFs) such as son of sevenless (SOS) where GDP is replaced by GTP. Activated Ras activates several downstream pathways such as Ras/MEK, Ras/PI3K, Ras/RalGDS which further activate genes involved in cell growth, proliferation and differentiation. Ras is a small GTPase protein which has the ability to hydrolyse GTP to GDP. Ras is inactivated by Ras GTPase activating protein (GAP) protein, which hydrolyses GTP to GDP.

pathways has been established [181]. In addition, oncogenic Ras activation leads to evasion of immune response, increased angiogenesis, and microenvironment remodeling [182]. Consequently, oncogenic Ras contributes to loss of cell polarity, and tumor invasion. Ras dependent signaling pathways such as the Ras/MAPK, Ras/PI3K, Ras/RAL GTPase and Ras/Rho GTPase pathways play essential roles in metastatic progression [183]. Moreover, the oncogenic Ras pathway activation leads to an increase in the $CD24^{-}$ /$CD44^{+}$ BCSC population [85].

1.7.3 EMT biomarkers

The process of EMT and MET, and the markers involved in induction of metastasis have been discussed in section 1.3. Importantly, markers associated with epithelial-like or mesenchymal-like states can indicate the status of cancer progression. Induction of EMT leads to destruction of cell-cell junction proteins, namely E-cadherin, CD44, claudins, occludins, and zonula occludens1 (ZO1), and modification of cytoskeletal proteins such as vimentin, β-catenin, and actin. These transitions are regulated by EMT-TFs, which also have an essential role in cancer progression. Interestingly, several studies have shown that activation or inhibition of a single EMT-TF is sufficient to induce partial EMT in cancer cells [184].

1.7.3.1 Cell-cell junction markers

Cadherins, specifically E-, N- and P-cadherin, are major components of epithelial cells. Loss of E-cadherin is a typical indication of EMT. Moreover, loss of E-cadherin is associated with the loss of cell differentiation and gain of invasiveness that leads to

metastasis [185]. In addition, a decrease in E-cadherin expression is significantly associated with basal-like or TNBC phenotype [186]. The switch from E-cadherin to N-cadherin expression is an important indicator of EMT status [187].

Integral transmembrane proteins such as claudins and occludin are important tight junction proteins that play a role in permeability and epithelial polarity [32]. In addition to cell polarity, tight junction proteins participate in different aspects of cancer progression. For instance, based on the claudin expression, a claudin-low molecular subtype of TNBC was identified. In the claudin-low BC subtype, claudins 3, 4, and 7 are suppressed with an associated increase in EMT characteristics [188]. Moreover, loss of claudin-7 is correlated to both histological high grade invasive ductal carcinoma and metastasis [189]. Silencing of occludin in BC cells leads to apoptotic resistance, suggesting a causative role in tumorigenesis [190]. Peripheral plaque proteins such as ZO-1, ZO-2, and ZO-3 are high in normal epithelial cells and maintain cell polarity. ZO-1 and ZO-2 are dysregulated in breast tumor cells, which contributes to metastasis [191].

CD44 is a cell surface protein that participates in cell-cell interactions and also regulates cell signaling via receptor tyrosine kinases. It is also a biomarker for BCSC as mentioned earlier [69]. Metastatic cells show higher expression of CD44 than non-metastatic cells. The CD44 variant (CD44v) isoform is switched to the CD44 standard (CD44s) isoform by epithelial splicing regulatory protein 1 during EMT, which is essential for promoting the EMT phenotype [192]. Broadly, cell-cell junction markers are not only correlated to initiation of EMT but also participate in overall BC progression.

1.7.3.2 Cytoskeletal markers

Vimentin is an intermediate filament protein present in mesenchymal cells that maintains cell integrity [193]. Vimentin is highly expressed in high grade invasive BC, and is correlated to invasion and poor prognosis of BC [194]. Downregulation of vimentin leads to impairment in migration and invasion of BC and colon cancer cells [195]. Switching between intermediate filament proteins is associated with cancer progression. For example, vimentin replaces cytokeratin in malignant BC cells [193]. The increase in vimentin is sufficient to induce changes in cell motility and shape typical of EMT [196]. Cortical organization of actin filaments is a hallmark of epithelial cells whereas actin stress fibers are detected in mesenchymal cells. Therefore, localization of actin is also an indicator of EMT status in cancer cells [197]. Depolymerization of the actin cytoskeleton leads to increase in E-cadherin expression and MET [198].

β-catenin is known for maintaining cell integrity by linking cadherins to the actin cytoskeleton. β-catenin is key factor in the Wnt pathway, which is involved in EMT. Localization of β-catenin from the cell membrane to the nucleus also defines EMT status [199]. Upon activation of the Wnt pathway, β-catenin dissociates from E-cadherin and localizes to the nucleus, thus dysregulating cell integrity and promoting subsequent initiation of EMT [200]. Overall, reorganization of cytoskeletal proteins enhances cell motility and migration and allows the BC cell to participate in invasion.

1.7.3.3 EMT-TFs

EMT-TFs are crucial mediators of cellular plasticity, favoring metastasis. EMT-TFs are complicated in cancer as they have additional functions that are tissue specific. For example, Snail initiates metastasis in BC progression whereas it has no effect on metastasis in pancreatic cancer [184]. EMT-TFs coregulate and functionally cooperate to target genes that enhance the mesenchymal phenotype and suppress the epithelial phenotype. Additionally, EMT-TFs activate MMPs 1, 9, and 14 to promote remodeling of the basement membrane and subsequent invasion [201]. The major EMT regulators are Snail, TWIST, and ZEB TFs, as mentioned earlier [202].

Overall EMT biomarkers act as major regulators of breast cancer progression and metastasis. Although, EMT-TFs are considered inducers of metastasis, the status of EMT can also be determined by the other EMT markers discussed above.

1.7.4 Adipocyte-derived factors

WAT is the major component of breast stroma and is known to contribute to BC progression, invasion and metastasis. Interaction between cancer cells and adipocytes leads to increased activity in adipocytes. Adipocytes activated by ovarian cancer cells show differential gene expression and changes in function that have been shown to contribute to tumorigenesis [203]. In addition, under obese conditions, adipocytes show elevated functional activity, leading to increases in factors related to pro-inflammation, hypoxia, angiogenesis, and ECM remodelling [204]. The adipocyte secretome is also modified when co-cultured with cancer cells, where an upregulation of MMP11,

osteopontin, TNF-α, and IL-6 has been observed [205]. Moreover, adipocyte cell size and cell number decrease when in the vicinity of the tumor compared to adipocytes that are distant from the tumor [206]. BC cells co-cultured with adipocytes in a transwell system also show reciprocal effects on adipocytes causing a decrease in lipid droplet (LD) number in adipocytes [207]. Moreover, there is an increase in fibroblast-like cells at the tumor site, suggesting a dedifferentiation of adipocytes [208].

WAT is composed of mature adipocytes, and cells found in the stromal vascular fraction (SVF) that includes adipocyte-derived stem cells, pre-adipocytes, immune cells, and fibroblast cells. Mature adipocytes contribute to 80% of the WAT secretome and shares 60% of these proteins with SVF [209]. WAT as an endocrine organ secretes a variety of factors such as metabolites (see section 1.6.5), enzymes, hormones, growth factors and cytokines called as adipokines involved in communication with the surrounding environment for growth and development. So far, more than 100 adipokines have been evaluated, of which only a few are thoroughly studied including leptin, adiponectin, reisistin, visfatin, insulin-like growth factor (IGF), HGF, TGF, TNF-α, and IL-6 [209].

1.7.4.1 Leptin

Leptin regulates energy balance by inhibiting food intake and suppressing hunger. Under obese conditions, serum leptin concentrations are increased but often the receptors for leptin become dysfunctional and do not respond to leptin. Furthermore, dysfunctional leptin receptors leads to excess food intake and thereby excess fat accumulation. BC cells also express leptin receptors. Excess leptin can bind and induce proliferation and growth

of BC cells. Leptin also induces pro-inflammatory responses by activating monocytes and macrophages, thus contributing to chronic inflammation [210]. Leptin participates in the tumor progression of both ER positive and ER negative BC cell lines [211] and acts as growth factor that enhances IDC and ILC progression [212]. In addition, leptin regulates different aspects of cell growth such as the cell cycle, signaling pathways, and apoptosis, which all contribute to BC progression [213, 214]. Leptin receptor expression in TNBC promotes E-cadherin expression and supresses vimentin expression suggesting a role in promoting MET [215].

1.7.4.2 Adiponectin

Adiponectin plays an important role in regulation of lipid and glucose metabolism. Under obese conditions, adiponectin is decreased, thereby leading to an accumulation of lipids and glucose, which promotes insulin resistance and obesity. Adiponectin has anti-inflammatory properties that modulate the inflammatory functions of immune cells and promote activation of anti-inflammatory macrophages [216]. Adiponectin supresses BC growth and invasion while enhancing apoptosis [217]. In addition, adiponectin inhibits PI3K activation and supresses cell proliferation. Adipocytes associated with cancer cells have been found to secrete low levels of adiponectin. [133]. Interestingly, a high leptin to adiponectin ratio is linked to increased risk of TNBC progression [218].

1.7.4.3 Other adipokines

IL-6 secreted by adipocytes not only regulates lipogenesis locally but also acts systemically [219]. Obesity leads to an increase of IL-6 in circulation, further adding to

inflammation [216]. Increased levels of IL-6 are correlated with poor prognosis, progression, and migration of BC [220]. TNF-α is an inflammatory cytokine and is primarily secreted by macrophages present in WAT. TNF-α is increased in TME and in obese humans, and an increase in TNF-α inhibits apoptosis of TNBC cells [216, 221]. Resistin is another adipokine shown to promote tumor growth, however, there is no direct link between resistin, obesity, and BC [222]. Autotaxin (ATX) is also secreted from adipocytes and is involved in fat expansion. ATX-lysophosphatidate signaling activates several cellular processes resulting in increased invasiveness and motility of BC cells [107]. Obesity is associated with increased levels of circulating IGF-1 resulting in increased risk of many cancers including premenopausal BC. BC cells express IGF-1 receptors, and binding of IGF-1 activates PI3K and MAPK pathways leading to cell proliferation [223–225]. Similarly, HGF is elevated by adipocytes during obesity and its receptor, c-Met, is expressed on BC cells, and their interaction during tumorigenesis leads to cell proliferation [226, 227].

1.7.4.5 ECM proteins and remodelling

Adipocytes secrete a wide variety of ECM components, especially different types of collagens needed for mechanical support, that can also regulate adipogenesis [228, 229]. Adipocytes are surrounded by basement membrane with collagen type VI and laminin as the major constituents [230]. Collagen type VI promotes the growth and survival of BC cells via NG2/chondroitin sulphate proteoglycan receptors [231] and the endotrophin component of the collagen VI protein promotes EMT and initiates metastasis [232].

Adipocytes also secrete matrix metalloproteinases such as MMP1, MMP7, MMP10, MMP11, and MMP14 which participate in remodelling the ECM [233]. MMP are also known as important regulators of tumor invasion, allowing cancer cells to migrate through the ECM. Specifically, expression of MMP11 induced in adipocytes by hepatocarcinoma cells promotes ECM remodelling and tumor invasion [234]. Moreover, MMP11 supresses adipocyte differentiation and enhances dedifferentiation, leading to an increase in fibroblast cells in the tumor microenvironment, which further amplifies tumor invasion [133].

Together, obesity and cancer completely change the gene expression and functional characteristics of adipocytes with reciprocal effects on cancer progression. Adipocytes communicate with cancer cells and can participate in the initiation of metastasis via secretory factors and ECM remodelling (Fig 1.6). The role of adipocytes in the colonization of tumors at local sites that can enhance micro-metastasis or at distant secondary sites is not well known. It is known that local adipocytes can trigger BC metastasis to the liver and lungs by paracrine signaling. Importantly, the presence of adipocytes at distant sites can intensify tumor metastasis, as in the case of bone marrow adipocytes [112, 113]. Bone marrow adipocytes secrete IL-1β, which is involved in the homing of BC cells to bone [235]. Therefore, adipocytes located at both the primary site and secondary sites can play a crucial role in the process of BC metastasis.

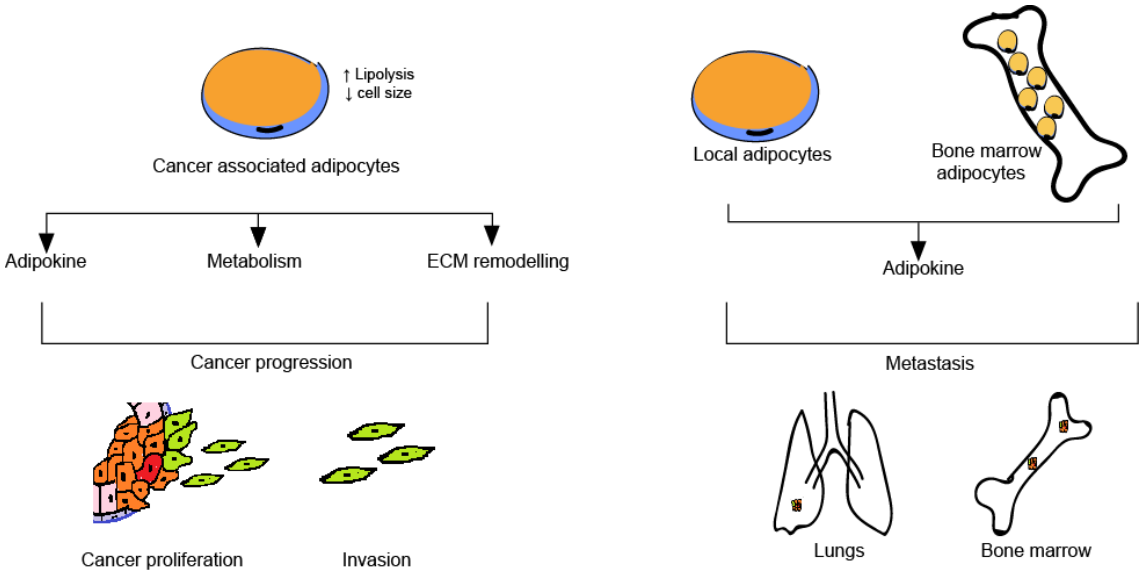

Figure 1.6: Schematic illustration of role of adipocytes in different stages of cancer: Cancer associated adipocytes (CAA) contribute to tumor progression via secretory factors such as adipokines and via remodeling the ECM. Metabolites from lipolysis of CAA also contribute to cancer cells proliferation. CAA can induce systemic and local changes that leads to increase in inflammatory adipokines that contribute to metastasis to organs such as lungs and liver. Local adipocytes in bone marrow also release adipokines such as leptin and IL-1β that leads tumor cell homing to bone marrow.

1.7.5 Lipid metabolites

Metabolic reprogramming is considered as an emerging hallmark of cancer cells [236, 237]. Cancer cells generate adenosine triphosphate (ATP) from aerobic glycolysis instead of mitochondrial oxidative phosphorylation; this change in metabolism is known as the Warburg effect [238]. The "reverse Warburg effect" is observed when cancer cells use the energy generated from stromal cells in the tumor microenvironment [239]. In addition to glucose, cancer cells take up free fatty acids and glycerol as a source of energy from stromal adipocytes. Martinez-Outshcoorn *et al.* [240] defined tumor cells "as metabolic parasites that rely on stromal sources for metabolic substrates such as lactate, glutamine and fatty acids via stimulation of glycolysis and lipolysis pathways in stromal cells". Uptake of glucose metabolites in cancer progression is well acknowledged [241], however, the involvement of lipid metabolites has not been well defined.

Reprogramming of lipid metabolism is part of the alterations in energy metabolism that occurs in cancer cells. Adipocytes regulate energy balance by storing triglycerides via lipogenesis and by production of diacylglycerol, monoacylglycerol, and free fatty acids via lipolysis within a cell. Highly proliferative cancer cells meet their energy requirements by synthesising lipids and cholesterol endogenously through lipogenesis or by obtaining them from the TME by stimulating lipolysis in adipocytes [229, 233]. To understand the adipocyte-tumor metabolic cross talk better, there has been an initiative for *in vitro* co-culture studies of BC cells and adipocytes or adipocyte-conditioned medium. Co-culture of adipocytes and BC cells increases lipolysis in adipocytes via

hormone sensitive lipase (HSL) and adipose triglyceride lipase (ATGL), resulting in release of free fatty acids that were transferred into adjacent BC cells as an energy source [243]. Moreover, a decrease in lipid droplet size and number has been reported in cancer-associated adipocytes (CAAs). Free fatty acids can be used for mitochondrial β-oxidation or as metabolic substrates that supports cancer proliferation and migration. Increases in lipid metabolites are reported for many cancers such as breast, prostate, glioblastoma, and hepatocellular carcinoma [242]. For instance, fatty acid binding protein (FABP) family proteins are expressed on cells involved in active lipid metabolism. One of the FABP protein, FABP4, which are involved in transport of fatty acids, are increased during BC progression [244].

Additionally, cancer cells utilize lipids for cell membrane formation, generation of lipid-derived bioactive molecules, and generation of exosomes. Free fatty acids and glycerol released from lipolysis can be used for biosynthesis of membrane lipids during BC proliferation [245]. Bioactive lipids such as steroid hormones, diacylglycerol, eicosanoids, phospholipids and sphingolipids also participate in metabolic reprogramming of cancer cells [237]. The fatty acid receptor CD36 is involved in initiation of metastasis in breast derived tumors and is associated with poor prognosis [246]. Adipocyte-derived exosomes, also known as adiposomes, can stimulate cell invasion and migration in melanoma cancer cells [247].

In addition to the tumor-stroma interactions mentioned earlier, reciprocal metabolic cross talk between adipocytes and BC not only drives pro-proliferative signaling but also

increases energy uptake by cancer cells. Previous literature has shownthat delipidation is observed in adipocytes co-cultured with cancer cells [206]. However, the mechanism involved in delipidation of CAAs is still elusive.

1.8 Hypotheses and objectives of this thesis

Hypothesis 1: The CD24 gene is conserved among various species.

Overall objective: Analyze the evolution of genomic structure and conserved peptide regions of CD24.

Specific objectives:

- **a.** Determine the genomic structure and evolution of CD24 among various species.
- **b.** Determine the conserved regions of CD24 peptide among various species.

Hypothesis 2: Oncogenic Ras downregulates CD24 promoter activity, mRNA, and protein expression independently via multiple downstream pathways to maintain the breast cancer stem cell population.

Overall objective: Identify the mechanisms involved in the downregulation of CD24 by oncogenic Ras in a model system and in human breast cancer cells.

Specific objectives:

- **a.** Determine the regulation of CD24 expression by the oncogenic Ras pathway in a model system.
- b. Evaluate promoter elements that repress CD24 transcription in response to constitutive activation of Ras.
- **c.** Determine the downstream targets of Ras that downregulate CD24 expression.
- d. Determine if inhibition of downstream targets, MEK, Raf and/or PI3K restores CD24 expression.

e. Identify the relationship between Ras pathway and CD24 gene expression in breast cancer subtypes.
f. Determine if inhibition of MEK or Raf restores CD24 expression in human breast cancer cell lines.

Hypothesis 3: Mature adipocytes contribute to the mesenchymal-to-epithelial transition of BC cells via secretions in 3D co-culture system.

Overall objective: Investigate the effect of reciprocal interactions between adipocytes, ECM and BC cells on mesenchymal-to-epithelial transition of BC cells in a 3D co-culture model.

Specific objectives:

a. Examine the effect of mature adipocytes on the morphology of mesenchymal TNBC cells.
b. Determine if the mature adipocytes affect the mesenchymal to epithelial transition, stemness and proliferation of TNBC cells via adipocyte secretions.
c. Determine the reciprocal effect of TNBC cells on adipocyte lipid content.
d. Examine if the mature adipocytes affect the epithelial state of ER/PR positive BC cells.

1.9 Publications associated with this thesis

1. Ayre, DC*, Pallegar, NK*, Fairbridge NF, Canuti, M, Lang, AS, Christian, SL. (2016) Analysis of the structure, evolution and expression of CD24, an important regulator of cell fate. Gene. [*Co-first authors]. 590(2):324-37

Figures 3.1-3.3 from chapter 3 are associated with this publication.

2. Pallegar NK, Ayre DC and Christian SL. (2015) Repression of CD24 surface protein expression by oncogenic Ras is relieved by inhibition of Raf but not MEK or PI3K. Frontiers in Cell and Developmental Biology. 5;3:47

Figures 4.1-4.6 and 4.11 from chapter 4 are associated with the above publication.

3. Pallegar NK, Garland CJ, Mahendralingam M, Viloria-Petit A, and Christian SL. (2018) Adipocytes promote a mesenchymal-to-epithelial-like transition in triple negative breast cancer cells in 3-dimensional co-culture. Journal Mammary Gland Biology and Neoplasia*, 23;1-13*

   Figures 5.1-5.6 from chapter 5 are associated with this publication.

.

Chapter 2. Materials and Methods

2.1 Methods corresponding to Chapter 3

2.1.1 Sequence and phylogenetic analysis

The nucleotide sequences for 106 *CD24* genes from 56 different species were obtained from the RefSeq Gene database (release 206, National Centre of Biotechnology Information (NCBI)) [148] and Ensembl genome database (release 25) (Appendix I) [248]. The DNA sequences corresponding to the mature peptide (lacking the signal sequence and the GPI-anchor signal sequence) were aligned with ClustalW multiple alignment using BioEdit software 7.2.5 [249]. Alignments were manually edited where needed and identities between sequence pairs were calculated (Supplementary file_1). For example, amino acids between 24-27 in tree shrew were creating gap when aligned with other species, these amino acids were deleted using BioEdit software. The evolutionary history of *CD24* and *CD24-like* (as named in NCBI database) genes was inferred by using the Maximum Likelihood method [250] based on the Kimura 2-parameter model [251], suggested as the best fitting model by model test analysis implemented in MEGA6 [252]. A discrete Gamma distribution was used to model evolutionary rate differences among sites (+*G*, parameter = 3.6287). All positions with less than 95% site coverage were eliminated. The robustness of branching was analyzed by the bootstrap method [253] with 1000 pseudo-replicates and a value greater than 60% considered as reliable. The human, mouse, and species present early in phylogenetic hierarchy such as turkey and green anole nucleic acid sequences corresponding to the

mature CD24 peptide were used to search for distant homologies via BlastN in the Ensembl database in platypus (*Ornithorhynchus anatinus*, version OANA5 [254]), opossum (*Monodelphis domestica*, version monDom5 [255]), Tasmanian devil (*Sarcophilus harrisii*, version Devil_ref v7.0 [256]) and wallaby (*Macropus eugenii*, version Meug1.0 [257]) genomes.

2.1.2 CD24 protein structure predictions

The CD24 pro-peptide and mature peptide consensus sequences were generated using BioEdit from the unique amino acid sequences (Supplementary file_2) and visualized using WebLogo [258]. These sequences were then analyzed by i-Tasser [259] and SPINE-D [260] for secondary structure predictions.

2.2 Methods corresponding to Chapter 4

2.2.1 Bioinformatics meta-analysis

Microarray data were obtained from the Gene Expression Omnibus (GEO) repository [261] (Table 2.1). Data were analyzed as per the platform. Background correction and RMA normalization of the data were done using the Bioconductor package oligo (v 1.26.6) [262], using R (v 3.0) [263]. The data were analyzed by hierarchical clustering by gene and sample using Genesis (v 1.7.6) [264]. The percentage of probesets representing selected Ras pathway genes (H-Ras, K-Ras, N-Ras, M-Ras, R-Ras, RAF1, ARAF, BRAF, MAPK1 (ERK2), PIK3C (phosphatidylinositol-4,5-bisphosphate 3-kinase, catalytic subunits) A-G, PIK3R (phosphatidylinositol-4,5-

Table 2.1. Datasets used for meta-analysis.

GEO Accession #	Cell type/Cell line	Treatment (n)	Platform
GSE26262 [265]	MDA-MB-231	siRNA against pin1 (3) siRNA against Lacz-control (3) siRNA against mutant p53 (3)	HG-U133A_2
GSE52262 [266]	MCF7 HCC1954 MC1 MCF10A Normal patient cells SUM149 SUM159	$CD24^{-}CD44^{+}$, $ALDH^{-}$ (1) $CD24^{-}CD44^{+}$, $ALDH^{+}$(1) $CD24^{+}CD44^{-}$, $ALDH^{-}$ (1) $CD24^{+}CD44^{-}$, $ALDH^{+}$ (1)	HG-U133A_2
GSE24592 [267]	MCF7	siRNA control vehicle – 4h (3) siRNA control – E2[a] – 4h (3) siRNA ERK2 vehicle – 4h (3) siRNA ERK2 – E2 – 4h (3) siRNA ERK1 vehicle – 4h (3) siRNA ERK1 – E2 – 4h (3) siRNA control vehicle – 24h (2) siRNA control – E2 – 24h (2) siRNA ERK2 vehicle – 24h (2) siRNA ERK2 – E2 – 24h (2) siRNA ERK1 vehicle – 24h (2) siRNA ERK1 – E2 – 24h (2)	HG-U133A_2
GSE7561 [224]	MCF7	Serum free medium control – 3h (3), 24h (3) IGF treated – 3h (3), 24h (3)	HG-U133A_2
GSE5116 [268]	MCF-10F	Untreated (3) Transformed by estradiol (3) Transformed outgrown cells (3)	HG-U133_plus_2

	Xenografts of transformed cells (3)

[a]Abbreviations: E2-Estradiol, IGF-Insulin like growth factor, HT-Hydroxytamoxifen, ER-Estrogen receptor, RAR-retinoic acid receptor

bisphosphate 3-kinase, regulatory subunits) 1-6, RAL-A, RAL-B, and RalGDS) that clustered with CD24 was then calculated.

2.2.2 Cell lines

NIH/3T3 cells expressing the empty pBabe vector (Control), or the pBabe vector containing RasV12, RasV12S35, RasV12G37, or RasV12C40 (Table 2.2) were gifts from Dr. Kensuke Hirasawa, Memorial University [269]. All cell lines were maintained in Dulbecco's Modified Eagle Medium (DMEM) supplemented with 10% fetal bovine serum (FBS), 1% anti-mycotic/antibiotic, 1% sodium pyruvate and maintained at 37°C in 5% CO_2. Control and RasV12 cells (2 x 10^5 cells/plate) were seeded in 35 mm plates. Based on the earlier studies and optimization in lab, cells were treated with the DMSO (dimethyl sulphoxide) vehicle control, 20 μM U0126 and/or 100 μM LY294002 (Calbiochem-Millipore, Billerica, MA) in complete medium [270, 271].

2.2.3 RNA isolation and RT-PCR

Cells were lysed using 1 ml TRIzol (Life Technologies Co., Burlington, ON), then the lysate was mixed vigorously after adding 0.2 ml chloroform followed by the centrifugation at 12,000 g for 15 min. The clear aqueous layer is collected, followed by addition of 0.5 ml of isopropanol and incubated for 10-12 min. Then centrifuge at 12,000 g for 10 min, discard the supernatant and add wash with 1ml 75% ethanol and centrifuge at 7,500 g for 5min. Remove the supernatant, air dry the pellet and resuspend in nuclease free water followed by DNase treatment using the Turbo DNA-free kit (Life

Technologies, Burlington, ON). RNA integrity was determined by running the sample on 1% agarose gel. RNA (500 ng) was reverse transcribed to cDNA using MMLV-RT (Life Technologies, Burlington, ON) with random hexamers, and then amplified with Taq DNA polymerase (Norgen Biotek, Thorold, ON) using the primers (selected using primer blast based in protein coding region)shown in Table 2.3. The PCR products were visualized on a 1% agarose gel after staining with ethidium bromide.

2.2.4 Quantitative RT-PCR (RT-qPCR)

RT-qPCR was performed in triplicate using Maxima SYBR Green qPCR Master Mix (2X) (Thermo Scientific) for *CD24* or *RPLP0* using the primers shown in Table 2.3 with the Eppendorf RealPlex^2 Real Time PCR machine. RPLP0 for NIH/3T3 cell lines and *GAPDH* for MDA-MB-231 BC cells were used as housekeeping genes based on previous studies [272, 273] Relative *CD24* mRNA levels were normalized using *RPLP0* or *GAPDH* were calculated using the ΔΔCt equation [274].

2.2.5 Fluorescent Activated Cell Sorting (FACS)

Single cell suspensions ($0.2 – 0.5 \times 10^6$ cells for NIH/3T3 derived cells) were obtained by scraping cells from plates into FACS buffer (1% heat inactivated FBS in phosphate-buffered saline (PBS, 137 mM NaCl, 2.7 mM KCl, 4.3 mM Na_2HPO_4, 1.4 mM KH_2PO_4, pH 7.4)). NIH/3T3 cells were incubated with 0.5 μg anti-CD24 (M1/69), or rat IgG2a κ isotype control, conjugated to APC (eBioscience, San Diego, CA, USA) for 30 min on ice, followed by three washes with FACS buffer then fixed in 4%

Table 2.2 Cell lines used for regulation of CD24 by Ras pathway.

NIH/3T3 Cell line	Vector transfected	Mutation	Constitutive activation of pathways
Babe/Control	Empty pBabe vector	No mutation	none
RasV12	pBabe with RasV12	D12V- Aspartic acid 12 Valine	Ras pathway
RasV12S35	pBabe vector with RasV12 and S35	T35S – Threonine 35 Serine	Ras-Raf pathway
RasV12G37	pBabe vector with RasV12 and G37	E37G- Glutamic acid 37 Glycine	Ras-Ral Pathway
RasV12C40	pBabe vector with RasV12 and C40	Y40C – Tyrosine 40 Cysteine	Ras-PI3K pathway

Table 2.3: Table showing the primers used in Chapter 4.

Gene/Region	Sequence (5'-3')	Efficiency	Amplicon size
RT-PCR			
mCD24	Forward -CTT CTG GCA CTG CTC CTA CC Reverse -AAC AGC CAA TTC GAG GTG GAC	N/A	300bp
mRPLP0	Forward -CGG CCC GTC TCT CGC CAG Reverse -CAG TGA CCT CAC ACG GGG CG	N/A	448bp
hCD24	Forward -AGA CGC CAT TTG GAT TGG GT Reverse -GCC AGC GGT TCT CCA AGC AC	N/A	369bp
hRas	Forward -ATG ACG GAA TAT AAG CTG GTG Reverse -TCA GGA GAG CAC ACA CTT GCA	N/A	570bp
hGAPDH	Forward -CCT GCT TCA CCA CCT TCT G Reverse -CCA TCA CCA TCT TCC AGG AG	N/A	576bp
RT-qPCR			
mCD24	Forward -ACT CAG GCC AGG AAA CGTCTCT Reverse -AAC AGC CAA TTC GAG GTG GAC	1.07	109bp

mRPLP0	Forward -TCA CTG TGC CAG CTC AGA AC Reverse -AAT TTC AAT GGT GCC TCT GG	1.03	101bp
hCD24	Forward -GAG CCA GCG GTT CTC CAA GCA Reverse -CTG CCC ATG TCC CCT CCG TC	1.11	71bp
hRPLP0	Forward- TGG ATG ATC TTA AGG AAG TAG TTG G Reverse – GCG TCC TCG TGG AAG TG	1.02	119bp
Promoter Amplification			
-688/+1	Forward -GTT GGA TGC TCC CGG GTA TGG Reverse -GGA GCG CGG CCG GCC GGC GG	N/A	688bp

[a]Abbreviations: N/A – Not applicable.

paraformaldehyde. Data were collected with a FACS Calibur (BD Biosciences, Mississauga, ON, Canada) and percentage of cell population expressing the protein on cells were analyzed using FlowJo software v10.0.5 (Ashland, OR, USA).

2.2.6 Western blot analyses

Cells were washed with PBS and then lysed in RIPA buffer (50 mM Tris-HCl (pH 7.6), 0.02% sodium azide, 0.5% sodium deoxycholate, 0.1% SDS, 1% NP-40, 150 mM NaCl) containing 1 µg/ml aprotinin, 1 mM PMSF and 1X HALT phosphatase inhibitor cocktail (Thermo Scientific, Waltham, MA, USA). Protein concentration was determined using a Bicinchoninic acid (BCA) protein assay (Thermo Scientific). The samples were subjected to 10% SDS polyacrylamide gel electrophoresis, followed by transfer procedure where the gel and nitrocellulose membrane are sandwiched between the filter paper and sponges and the current is passed in a way that the proteins are transferred from gel to the membrane, which was blocked in 5% skimmed milk in Tris-buffered saline (10 mM Tris base, 150 mM NaCl, pH 7.5) and 0.05% Tween-20 (TBST) for 1 hr. Primary antibodies to detect phosphorylated ERK (1:5000) (Cat #9101), phosphorylated Akt (1:2000) (Cat #9271), total ERK (1:5000) (Cat #4695), and total Akt (1:2000) (Cat #9272) were obtained from Cell Signalling Technologies, Inc. (Danvers, MA, USA). Goat anti-rabbit-HRP (1:2000) (Santa Cruz Biotechnology Inc (Dallas, TX, USA))secondary antibody was used for all the primary antibodies mentioned above . Both the primary and secondary antibodies were diluted in 5% bovine serum albumin in TBST. After blocking membrane was incubated with desired primary antibody for

overnight at 4° C, followed by the 3X washes for 10 min at RT. Then the membrane was probed with secondary antibodies for 1 hr at RT, followed by the 3X washes as mentioned above. Immobilon Western Chemiluminescent HRP substrate was used for detection (EMD Millipore, Darmstadt, Germany) followed by imaging with the ImageQuant LAS 4000 (GE Healthcare, Morgan Boulevard, Baie d'Urfe Quebec, Canada).

2.2.7 CD24 promoter analysis

Genomic DNA was isolated from a male C57BL/6N mouse liver using the Genomic DNA isolation kit (QIAGEN, Germantown, MD, USA). The *CD24* promoter region from -688 to -1 from the TSS (p688) was amplified from genomic DNA with the GC-Rich PCR system (Roche, Basil, Switzerland) using the primers indicated in Table 2.3. The promoter was cloned into the HindIII and BglII sites of the pGL4.17 vector (Promega, Madison, USA). The deletion constructs -469 to -1 (p469), -357 to -1 (p357) and -168 to -1 (p168) were generated using the Erase-a-base kit (Promega) according to the manufacturer's instructions. Briefly, p688 promoter was linearized by restriction digestion followed by digestion with of S1 nuclease reaction mix at 37° C. The nuclease digestion was stopped every 30 secs by collecting 2.5 µl of sample and mixing with Exo-III, digestion proceeds at about 450 bases/minute. The digested samples will be precipitated, and cleaned followed by re-ligation, and transformation. The positive colonies were selected followed by plasmid isolation. All sequences were verified by sequencing at The Centre for Applied Genomics (Toronto, ON, Canada).

The E-box elements on the p688 promoter region were mutated using the site directed mutagenesis kit (Promega) according to manufacturer's instructions. Briefly, every nucleotide in consensus sequence of the two E-box elements were checked for any change in the TF binding regions and selected the CACCTG→CGCCTG for E-1 and CACTTG→GACTTG for E-2 sequence. The mutations lead to one additional TF binding region on both E-1 and E-2 that are involved in regulation of cell cycle regulation and leukemia inhibitory factor, respectively. The primers were designed based on these mutations and amplified the p688 plasmid using these primers using the site directed mutagenesis kit. Amplified product was treated with DpnI to remove template, followed by transformation into XL-10 Gold ultra competent cells. The positive colonies were selected followed by plasmid isolation. All sequences were verified by sequencing at The Centre for Applied Genomics (Toronto, ON, Canada).

NIH/3T3 cells expressing empty vector (control) or RasV12 cells (30,000 cells/well in 24-well plates) were transfected with 1 µg of the pGL4.17 vector with or without the *CD24* promoter regions and 20 ng pRL-SV40 vector (Promega) using 2.5 µl Superfect transfection reagent (Qiagen), following the manufacturer's instructions. After 24 h, cells were lysed with 1X Passive Lysis Buffer and Firefly and Renilla Luciferase activity were measured using the Dual-Luciferase Reporter Assay kit (Promega).

2.2.8 Statistical analysis

Statistical analysis was performed in R v.3.3 [275] accessed through RStudio [276] (Appendix II). Significant differences in CD24 mRNA between experimental conditions

were determined by Student's t-test or One-Way ANOVAs with Tukey Honest Significant Differences (HSD) post-hoc analysis. Significant differences in CD24 surface protein expression were determined by One-Way ANOVA with Tukey HSD post-hoc analysis between the conditions. Differences were considered statistically significant at $P<0.05$.

2.3 Methods corresponding to Chapter 5

2.3.1 Cell lines

3T3-L1 pre-adipocytes (American Type Culture Collection, Burlington (ATCC), Burlington, ON) were maintained in high-glucose DMEM (Life Technologies Co, Burlington, ON) supplemented with 10% newborn calf serum and 1% penicillin/streptomycin (DMEM/NCS). MDA-MB-231, SUM159, Hs578t, and MCF7 cell lines were obtained from ATCC and maintained in Roswell Park Memorial Institute (RPMI) 1640 Medium (Life Technologies) supplemented with 10% FBS and 1% penicillin-streptomycin. All cells were confirmed to be mycoplasma-free using the MycoAlert^{TM} Plus Mycoplasma Detection Kit from Lonza (Basel, Switzerland). The breast cancer cell lines were authenticated by STR profiling by The Centre for Applied Genomics (The Hospital for Sick Children, Toronto, Canada). After thawing, all of the cell lines were used for up to 15 passages.

3T3-L1 cells were grown to confluency in 4-well chamber slides and adipogenesis was induced as previously described [272]. Briefly, pre-adipocytes were grown to confluency and then initiation medium containing 0.5 mM 3-isobutyl-1-

methylxanthine and 1 μM dexamethasone (Millipore, Darmstadt, Germany) in DMEM supplemented with 10% FBS (as it has additional growth factor and protein composition compared to NBCS that aids in adipogenesis) and 1% penicillin/streptomycin (DMEM/FBS) was added to the cells 48 h post-confluency. Initiation medium was replaced with progression medium (10 μg/ml insulin (Sigma-Aldrich, St. Louis, MI, USA) in DMEM/FBS) after 48h followed by replacement with DMEM/FBS 48h later. To obtain conditioned medium (CM), adipocytes were differentiated for 5 days and the medium collected 48 h after Matrigel was overlaid. Medium was refreshed and CM was collected again 48 h later. CM was mixed 1:1 with fresh medium and added to the breast cancer cells overlaid on Matrigel on day 6 and 8. Adipocyte and CM co-cultures were maintained for 5 days, and pre-adipocyte co-cultures maintained for 4 days, after plating BC cells on Matrigel. Note that there were no differences in colony structure or protein expression in breast cancer cells cultured on Matrigel for 4 or 5 days in the control cultures.

2.3.2 3D co-culture

We modified the 3D culture method initially developed by Dr. Mina Bissell [135] and adapted by Debnath *et al.* [277], as follows (Fig 2.1A). 3T3-L1 cells were differentiated for five days, at which point lipid droplets were clearly observable in >60% of the cells. On day six, 110 μl of Matrigel (9.1 mg/ml, BD Bioscience) was overlaid on top of mature adipocytes, or empty wells of a 4-well chamber slide and allowed to set for 1 h (Fig 2.1A). MDA-MB-231/ MCF7 (13,500 cells/450 μl), SUM159

(11,250 cells/450 µl), or Hs578t (18,000 cells/450 µl) were overlaid and incubated with

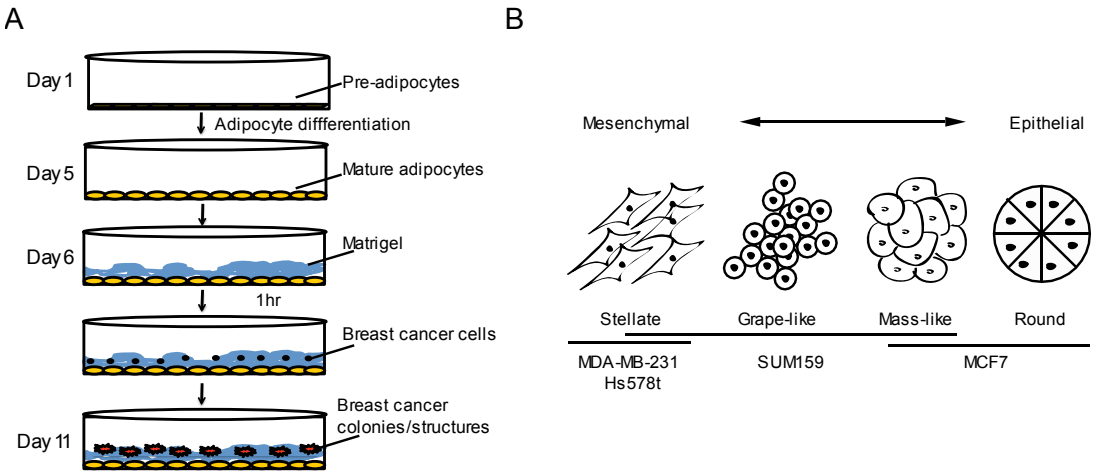

Figure 2.1 Schematic representation of the 3D co-culture system.

(A) Pre-adipocytes (3T3-L1 cells) are differentiated into mature adipocytes on chamber slides for five days. On day six, BC cells are overlaid in laminin-rich Matrigel and cultured in 3D for five days with 50% medium replacement every 48 h. Immunofluorescence detection of protein markers in the BC cells and direct staining for lipid droplets in the adipocytes was performed on day 11. (B) A representation of the morphology of BC cells used in this study when grown in 3D culture using Matrigel. MDA-MB-231 and Hs578t cells have stellate morphology, SUM159 cells adopt grape or mass-like structures, and MCF7 cells form round/mass-like structures [135, 278].

co-culture medium (mammary epithelial basal medium (MEBM) (Promo Cell, Heidelberg, Germany) containing epidermal growth factor (10 ng/ml), insulin (5 µg/ml), hydrocortisone (0.5 µg/ml), bovine pituitary extract (0.4%) and 2% Matrigel). BC cells were grown for an additional four-five days to allow colony formation. For the pre-adipocyte co-culture, pre-adipocytes were plated on day five, allowed to undergo growth arrest for 48 h, and then Matrigel and breast cancer cells were overlaid on day seven.

2.3.3 Immunofluorescence (IF)

Cells were fixed with 4% paraformaldehyde for 20 min at room temperature, followed by permeabilization in 1X PBS containing 0.5% Triton X-100 for 10 min at 4°C, then washed three times with PBS-glycine (100 mM glycine in 1X PBS) and blocked With 10% donkey serum in IF buffer (0.1% BSA, 0.2% Triton X-100, 0.05% Tween 20, 1X PBS) for 1 h at room temperature. Primary antibodies were diluted in blocking buffer as mentioned in the paragraph below, incubated overnight at 4°C and detected with appropriate secondary antibodies. Before and after secondary staining (as mentioned in the paragraph below), cells were washed three times with IF buffer. Co-cultures were then stained with 4’,6-diamidino-2-phenylindole (DAPI) (Life technologies) and/or boron-dipyrromethene (BODIPY) 493/503 (Life Technologies) for LD detection for 25 min at room temperature, then washed once with 1X PBS. The chambers were separated from the slide according to manufacturer’s protocol and any excess 1X PBS was gently removed. An even bead of silicone sealant (GE, Boston, MA, USA) was applied around the Matrigel layer to avoid compression of co-cultures by coverslips. Prolong Gold (Life

technologies) was used for mounting slides and placed in dark at room temperature to dry overnight. The slides were imaged using 20X and 40X objectives with the Nikon A1 confocal microscope with NIS elements imaging software.

Primary antibodies and dilutions used were as follows: vimentin (1:200; Cat #V2258; Sigma-Aldrich, St. Louis, MO, USA), ZO-1 (1:50; Cat #SC33725; SantaCruz Biotechnology Inc. Dallas, TX, USA), E-cadherin (1:200; Cat #610181; BD Biosciences, Franklin Lakes, NJ, USA), claudin7 (1:200; Cat #AB27487; Abcam, Cambridge, UK), CD24 (1:100; Cat #NBP1-46390; Novus Biologicals, Littleton, CO, USA), CD44 (1:25; Cat #M708201-2; Dako), and Ki67 (1:100; Cat #M724029-1; Dako, Denmark). Secondary antibodies used were AlexaFluor-647 anti-rat IgG (Cat #712-605-153; Jackson Immunoresearch Laboratories, West Grove, PA, USA), AlexaFluor-647 anti-rabbit IgG (Cat #711-605-152; Jackson Immunoresearch Laboratories), and DyLight 594 anti-mouse IgG (NBP1-75617; Novus Biologicals).

2.3.4 Image analyses

Colony morphologies were assessed by analysis of circularity using ImageJ v. 1.48 [279]. Structures present in three images per replicate (minimum 10 structures per replicate) were traced manually and the circularity measurement was obtained. A circularity value > 0.7 was classified as round/mass-like, 0.7-0.2 was classified as grape-like, and < 0.2 was classified as stellate (Fig. 2.1B).

Protein expression was analyzed using ImageJ by measuring the intensity of fluorescence of the whole image. Integrated density (IntDen) was determined to capture

the total fluorescence of each marker. Background was subtracted by taking measurements of selected areas where cells were absent as observed from the respective bright field images. The total fluorescence intensity of each marker was determined by normalizing IntDen of each marker to IntDen of DAPI and then the relative IntDen values of each marker per condition was determined relative to the control.

ImageJ was used to analyze the number and size of LDs [280] from five independent fields of view per biological replicate, where images from five different depths (Z-stack) were condensed to form a single 2D composite image of all BODIPY 493/503 stained LD. The composite image was converted to an 8-bit binary image followed by automatic threshold adjustment and then a watershed-based separation of closely spaced LD applied before calculation of LD area and number. The analyze particles command was used to measure the area and number of LD in ImageJ.

2.3.5 Statistical analysis

Statistical analysis was performed in R v.3.3 [275] accessed through RStudio [276] (Appendix II). Significant differences in lipid droplet area distributions between each experimental condition were determined using the Kolmogrov-Smirnov test. Significant differences in lipid droplet number were determined using a Student's t-test. Differences in the distribution of colony shape was determine by χ^2 analysis between control and experimental conditions. Significant differences in specific colony shape were determined using a 4 X 3 between subjects factorial ANOVA, followed by one-way

ANOVAs and Tukey HSD post-hoc analysis within each shape between conditions. Differences were considered statistically significant at $P<0.05$.

Chapter 3. Analysis of CD24 structure and evolution

CD24 is known for its diverse biological roles in cell differentiation and development [150]. However, little is known about CD24 genomic structure, conservation and evolution. Since its initial discovery, sequencing efforts have revealed that CD24 orthologues are present in many species. In addition, transcript variants of *CD24* in human have been recently identified [148], and *CD24* pseudogenes are present in both the mouse and human genomes [149]. However, the conservation of CD24 over the course of evolution has not been reported nor has the earliest known ancestor been identified. Therefore, here I have performed a phylogenetic analysis of the *CD24* gene. These analyses demonstrate that the sequence of the mature CD24 peptide, but not the genomic structure, is well-conserved from reptiles and birds through to mammals, and it suggests that glycosylation sites drive this conservation.

3.1 *CD24* genomic structure is diverse but the coding sequence is conserved.

The *CD24* gene has been well characterized in both the mouse and human systems at the functional and genomic levels [281], however, very little is known about *CD24* in other species. *CD24* homologue sequences, which were generally annotated as *CD24* or *CD24-like* (*CD24L*) with predicted genes given either designation, were thus analyzed.

Analysis of the genomic structure of 106 genes from 56 different species representing 17 unique orders (Appendix I) revealed that there are 5 general types of

structures based on the organization of introns and exons, and the presence of untranslated regions (UTRs) in the *CD24/CD24L* gene (Fig. 3.1). The first type consisted of one protein-coding exon lacking UTRs, while the second type consisted of one protein-coding exon along with either a 5'-UTR or both 5'- and 3'-UTRs (Fig. 3.1A-B). The third type consisted of 2 protein-coding exons lacking UTRs, while the fourth type also had 2 exons but also contained either both UTRs or a 3'-UTR (Fig. 3.1C-D). The fifth type had 3 exons with or without UTRs (Fig. 3.1E).

The designation of *CD24* or *CD24L* appeared to be unrelated to the genomic structure, as an approximately equal number of each designation possessed each type of genomic structure. The group with 2 exons contained the most evolutionarily diverse species of all the groups (Fig. 3.1D). Neither the ancestral genomic structure of *CD24* nor when the various gene structure types evolved could be determined. It appears that some *CD24* genomic structure variants might have lost introns and/or UTRs and others might have gained additional introns. Moreover, the evolutionarily higher organisms, such as human, marmoset, and green monkey, were more likely to have gained the additional exon (Fig 3.1E).

CD24 is translated as a precursor protein of approximately 80 amino acids, depending on the species. In human, mouse, and rat, three distinctive regions of the CD24 precursor protein can be identified: the signal peptide for endoplasmic reticulum (ER)/golgi localization, the mature core peptide, and the GPI anchor peptide [144, 282].

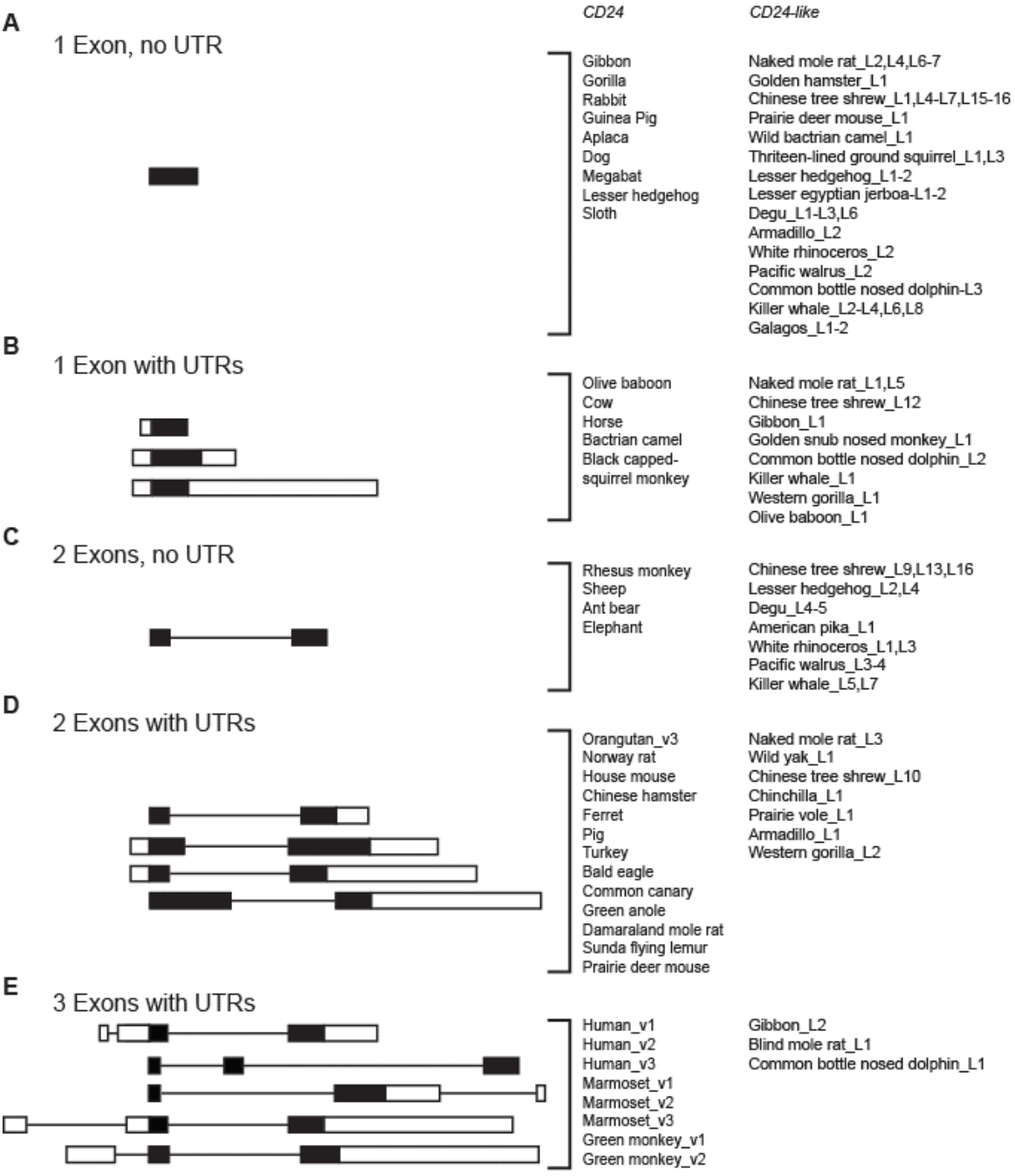
A
1 Exon, no UTR
B
1 Exon with UTRs
C
2 Exons, no UTR
D
2 Exons with UTRs
E
3 Exons with UTRs
CD24
CD24-like
Gibbon
Gorilla
Rabbit
Guinea Pig
Aplaca
Dog
Megabat
Lesser hedgehog
Sloth
Naked mole rat_L2,L4,L6-7
Golden hamster_L1
Chinese tree shrew_L1,L4-L7,L15-16
Prairie deer mouse_L1
Wild bactrian camel_L1
Thriteen-lined ground squirrel_L1,L3
Lesser hedgehog_L1-2
Lesser egyptian jerboa-L1-2
Degu_L1-L3,L6
Armadillo_L2
White rhinoceros_L2
Pacific walrus_L2
Common bottle nosed dolphin-L3
Killer whale_L2-L4,L6,L8
Galagos_L1-2
Olive baboon
Cow
Horse
Bactrian camel
Black capped-squirrel monkey
Naked mole rat_L1,L5
Chinese tree shrew_L12
Gibbon_L1
Golden snub nosed monkey_L1
Common bottle nosed dolphin_L2
Killer whale_L1
Western gorilla_L1
Olive baboon_L1
Rhesus monkey
Sheep
Ant bear
Elephant
Chinese tree shrew_L9,L13,L16
Lesser hedgehog_L2,L4
Degu_L4-5
American pika_L1
White rhinoceros_L1,L3
Pacific walrus_L3-4
Killer whale_L5,L7
Orangutan_v3
Norway rat
House mouse
Chinese hamster
Ferret
Pig
Turkey
Bald eagle
Common canary
Green anole
Damaraland mole rat
Sunda flying lemur
Prairie deer mouse
Naked mole rat_L3
Wild yak_L1
Chinese tree shrew_L10
Chinchilla_L1
Prairie vole_L1
Armadillo_L1
Western gorilla_L2
Human_v1
Human_v2
Human_v3
Marmoset_v1
Marmoset_v2
Marmoset_v3
Green monkey_v1
Green monkey_v2
Gibbon_L2
Blind mole rat_L1
Common bottle nosed dolphin_L1

Figure 3.1: Genomic structure of CD24 orthologues.

Species with *CD24* and *CD24-like* (*CD24L*) genes are listed on the right of the representative gene structure. Labels with 'v' followed by number represent transcript variant numbers while 'L' followed by numbers represent paralogues of *CD24L* genes within a species. The genomic structures shown are (A) one protein-coding exon with no untranslated regions (UTRs), (B) one protein-coding exon with 5'- and/or 3'-UTRs, (C) two protein-coding exons with no UTRs, (D) two protein-coding exons with 5'- and/or 3'-UTRs, and (E) three protein-coding exons with or without UTRs. Exons are shown as boxes, with protein coding regions in black and UTR regions in white.

As with all GPI-anchored proteins, the signal peptide and GPI-anchor peptide are lost prior to surface expression of CD24. This processing generates the mature peptide, which ranges from 26 to 41 residues with a mean and median length of 32 residues. To assess the evolutionary history of CD24 genes, we analyzed the nucleic acid sequences coding for the mature core peptide. Overall, we found 34 orthologues for human *CD24* distributed across 26 species, including reptiles, birds, and placental mammals. Within these genes, transcript variants were identified in 4 species (human, marmoset, Sumatran orangutan, and green monkey) (Fig 3.2). In the remaining 22 species, the sequences were annotated as *CD24L*; 14 of these had paralogues identified at different locations in the genomes (Appendix I). No sequences with similarity to CD24 were identified in the available marsupial or monotreme genomes.

Two clear branches that divide reptiles and birds from placental mammals were resolved on the phylogenetic tree (Fig. 3.2). Despite the low bootstrap numbers, which are most likely due to the short length of the alignment, sequences tended to be organized by taxonomic order. Some exceptions were observed such as for the sequences retrieved from galagos, which did not cluster together with sequences from other primates. We found that the *CD24L* genes were not phylogenetically distinct from the *CD24* genes, indicating that these should not be distinct classifications. Furthermore, in some species, such as the naked mole rat, all *CD24L* genes were in one clade, while *CD24L* genes from other species, such as dolphin and whale, were present in separate clades. In some species, such as the prairie deer mouse, gibbon, and hedgehog, both a *CD24* gene and a *CD24L* gene were present in the same clade.

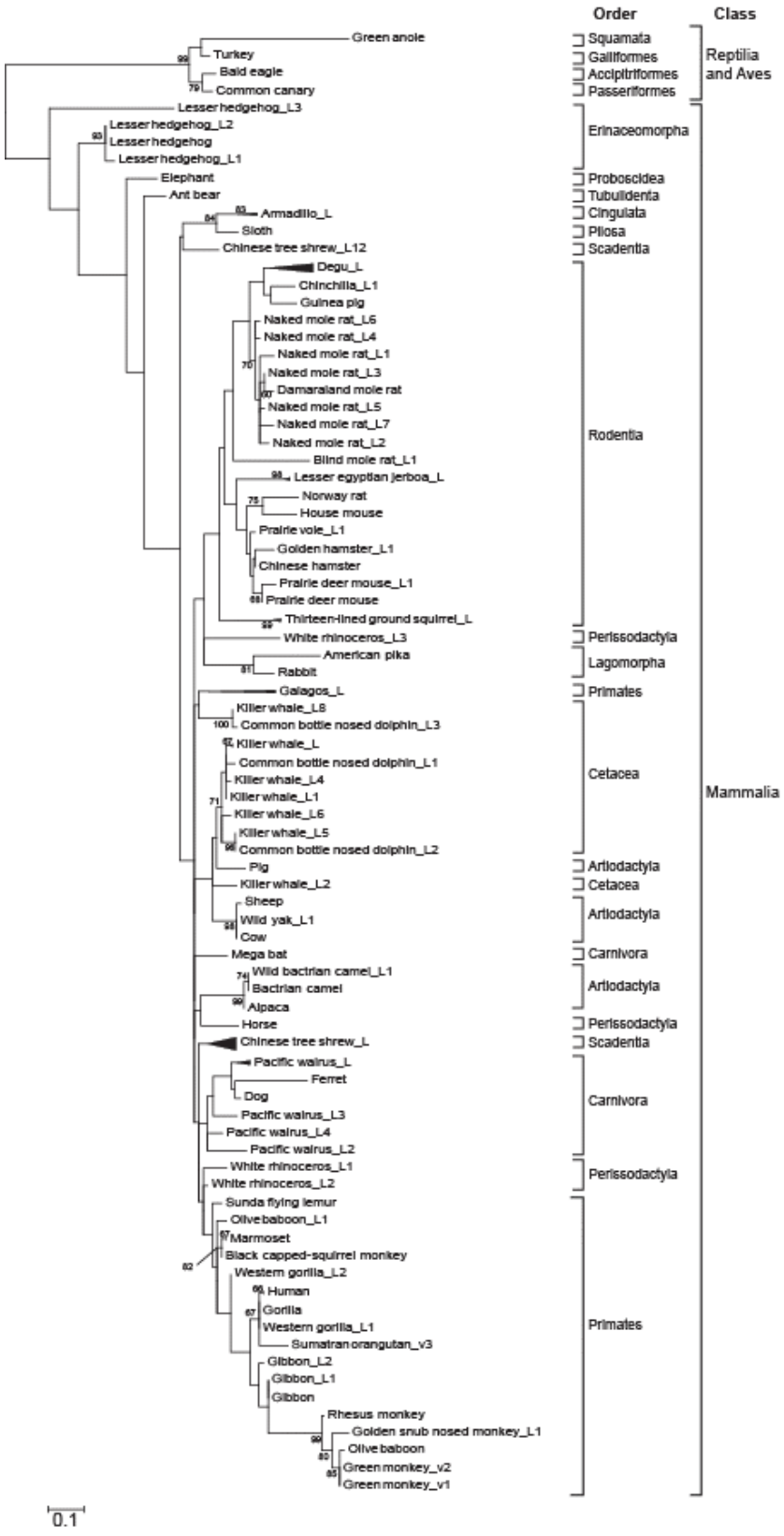
Order
Class
Green anole
Turkey
Bald eagle
Common canary
Lesser hedgehog_L3
Lesser hedgehog_L2
Lesser hedgehog
Lesser hedgehog_L1
Elephant
Ant bear
Armadillo_L
Sloth
Chinese tree shrew_L12
Degu_L
Chinchilla_L1
Guinea pig
Naked mole rat_L6
Naked mole rat_L4
Naked mole rat_L1
Naked mole rat_L3
Damaraland mole rat
Naked mole rat_L5
Naked mole rat_L7
Naked mole rat_L2
Blind mole rat_L1
Lesser egyptian jerboa_L
Norway rat
House mouse
Prairie vole_L1
Golden hamster_L1
Chinese hamster
Prairie deer mouse_L1
Prairie deer mouse
Thirteen-lined ground squirrel_L
White rhinoceros_L3
American pika
Rabbit
Galagos_L
Killer whale_L8
Common bottle nosed dolphin_L3
Killer whale_L
Common bottle nosed dolphin_L1
Killer whale_L4
Killer whale_L1
Killer whale_L6
Killer whale_L5
Common bottle nosed dolphin_L2
Pig
Killer whale_L2
Sheep
Wild yak_L1
Cow
Mega bat
Wild bactrian camel_L1
Bactrian camel
Alpaca
Horse
Chinese tree shrew_L
Pacific walrus_L
Ferret
Dog
Pacific walrus_L3
Pacific walrus_L4
Pacific walrus_L2
White rhinoceros_L1
White rhinoceros_L2
Sunda flying lemur
Olive baboon_L1
Marmoset
Black capped-squirrel monkey
Western gorilla_L2
Human
Gorilla
Western gorilla_L1
Sumatran orangutan_v3
Gibbon_L2
Gibbon_L1
Gibbon
Rhesus monkey
Golden snub nosed monkey_L1
Olive baboon
Green monkey_v2
Green monkey_v1
Squamata
Galliformes
Accipitriformes
Passeriformes
Erinaceomorpha
Proboscidea
Tubulidenta
Cingulata
Pilosa
Scadentia
Rodentia
Perissodactyla
Lagomorpha
Primates
Cetacea
Artiodactyla
Cetacea
Artiodactyla
Carnivora
Artiodactyla
Perissodactyla
Scadentia
Carnivora
Perissodactyla
Primates
Reptilia and Aves
Mammalia
0.1

Figure 3.2: Phylogenetic analysis of the nucleotide sequence encoding the mature CD24 peptide.

Sequences are labeled as described for Figure 1. The triangular shaped branches represent multiple sequences from the species indicated, where the size of the triangle is relative to the number of sequences present. The order and class of each species are shown on the right. Bootstrap values above 60% are shown.

No strict correlation between the genomic structure and the phylogenetic relationship amongst sequences could be detected. We observed that all genes identified from birds and reptiles, whose sequences form a separate clade, possessed the same genetic structure. However, we cannot rule out the possibility that other genome structures may exist in these groups and will be identified as more detailed genome annotations become available. In most cases, all sequences from the same species or order of animals clustered together in spite of possessing different genomic structures. For example, three different gene structures were found in gibbon (Fig. 3.1A, B and E) but all of these sequences clustered together in the tree (Fig. 3.2). The same pattern could be observed for most of the primates. This might suggest that the duplication of the original CD24 sequence occurred after the separation of the lineages. However, in other cases sequences from the same species but with different gene structures appeared in separate clusters, such as for common bottle-nosed dolphin. These observations suggest that some duplications might also have occurred before the separation of some lineages. Overall, it appears that *CD24* orthologues and paralogues have evolved through a combination of both evolutionarily recent and distant within-lineage duplications.

3.2 CD24 peptide organization and structure

Note: Analysis in this section was performed by Craig Ayre, while interpretation was performed in collaboration.

The consensus sequence of CD24 derived from the alignment of the previously analyzed species was used to predict secondary structure and organization at the protein

level. The consensus sequence was longer than the sequence for any individual species as it includes rare and unique amino acid insertions from each species added into the single sequence. Secondary structure prediction of the precursor CD24 protein using i-Tasser suggested that there are two alpha-helical regions (Fig. 3.3A). One is in the N-terminal region, from residues 3 to 29, which corresponds to the signal sequence. The second is in the C-terminal domain, from residues 86 to 96, which corresponds to a portion of the GPI-anchor signal sequence. No secondary structure could be predicted for the region of the precursor protein that corresponds to the mature peptide between residues 42 to 77. As the N- and C-terminal regions are cleaved from the mature peptide during post-translational processing [150], we also analyzed the mature core peptide in isolation (Fig. 3.3B). Similarly, no discrete secondary structure was predicted for the mature peptide in isolation. As expected from the secondary structure prediction results, no tertiary structure was confidently predicted for either the precursor or the mature peptide.

In agreement with the secondary structure prediction, analysis of the intrinsic disorder of the CD24 precursor protein via SPINE-D revealed that this protein is likely to be highly intrinsically disordered, with an average probability score of 0.62 (Fig. 3.3A). In the N-terminal region of the precursor protein, the region from residues 24 to 37 has a probability of disorder of 0.32, indicating it is likely an ordered region. This area partially overlaps with the alpha-helical domain predicted by i-Tasser (Fig. 3.3A). In the C-terminal region, there is another ordered region from residues 88 to 97, with a probability of disorder of 0.42, overlapping with the predicted alpha-helical region of the GPI-anchor signal sequence. The central domain of the precursor protein containing the mature core

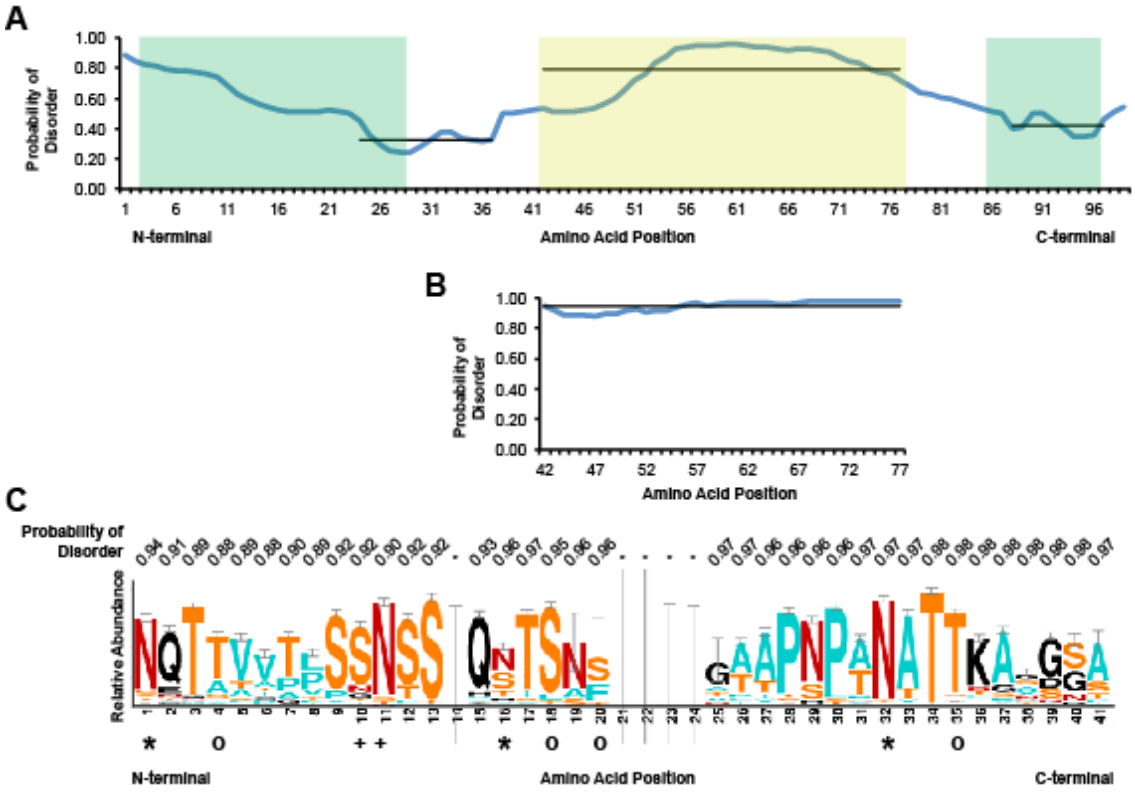
A
Probability of Disorder
1.00
0.80
0.60
0.40
0.20
0.00
1 6 11 16 21 26 31 36 41 46 51 56 61 66 71 76 81 86 91 96
N-terminal
Amino Acid Position
C-terminal
B
Probability of Disorder
1.00
0.80
0.60
0.40
0.20
0.00
42 47 52 57 62 67 72 77
Amino Acid Position
C
Probability of Disorder
Relative Abundance
N-terminal
Amino Acid Position
C-terminal

Figure 3.3: Visualization of CD24 secondary structure motifs and sequence alignment.

The predicted secondary structures of the CD24 (A) pro-peptide and (B) mature peptide were assessed using i-Tasser and SPINE-D. The predicted disorders of the pro- and mature peptide are represented with a blue line. Areas predicted by i-Tasser to contain alpha-helical domains are shown in green. Black bars represent the average probability of disorder predicted by SPINE-D for two ordered domains in the N- and C-terminal regions and the mature peptide. (C) A graphical representation of the mature CD24 peptide alignment is shown. Letter height indicates relative abundance of a given amino acid in each position. Error bars show a Bayesian 95% confidence interval. Asn and Arg residues are shown are red, while Ser and Thr residues are shown in orange. Hydrophobic amino acids are in blue and all other amino acids are in black. Known *Mus musculus* N-glycosylated residues are indicated with * and known O-linked glycoslyations are indicated with °. Potential N-linked glycosylation sites are shown with $^{+}$, based on the Asn x(Ser/Thr) glycosylation motif. Amino acid positions 14 and 21-24 are shown as gaps as they do not align or are not present in the majority of sequences analyzed (Supplementary file_2). The likelihood of a given residue existing in a disordered state was predicted using SPINE-D and the probability of disorder is shown above the sequence.

peptide from positions 42 to 77 had a high average probability of disorder value of 0.80. Furthermore, when analyzed in isolation, we found that the intrinsic disorder of the mature peptide increased to an average of 0.94, primarily due to a loss of order at the N-terminus (Fig. 3.3B). Therefore, post-translational processing of the CD24 protein causes reduced order in the peptide core, however, it is not precisely known how the addition of glycosylations and/or the GPI-anchor influence the structure or disorder of the surface protein.

Visualization of the alignment of the mature core peptide clearly reveals that several of the known O-glycosylation sites, as well as known and predicted N-glycosylation sites [146], are highly conserved (Fig. 3.3C). Specifically, there were 12 highly conserved Ser or Thr residues that could be modified by O-linked glycosylation, and five highly conserved Asn residues that can be N-glycosylated, based on the consensus sequence of Asn-X-(Thr/Ser) where X can be any amino acid except proline [283]. Of the potentially glycosylated residues, there are three highly conserved residues that are known to be N-linked, and four highly conserved residues that are likely to be O-linked, at least in the case of erythrocyte-derived mouse CD24 [284]

In addition to the glycosylation sites, there are two clearly identifiable regions with highly conserved sequences, from positions 9 to 19 and 28 to 35 of the mature protein. The second, a proline-rich region, partially overlaps with the CD24 domain as annotated by the Pfam database (PF14984) [285], which begins at position 26 and ends within the GPI-anchor signal peptide at position 75. However, as the Pfam domain PF14894 includes the GPI-anchor peptide, it does not accurately represent the mature core peptide. Nevertheless, the high conservation of key glycosylation residues supports previous work showing that glycosylation of CD24 dictates ligand specificity and therefore function of CD24 [286–288].

3.3 Discussion

This is the first comprehensive analysis of CD24 with regards to its distribution, genomic structure, and evolution. Although the mature CD24 peptide is only between 26 and 41 residues, it was possible to use phylogenetic analysis to evaluate the evolutionary relationships amongst the *CD24* genes from 56 species. The evolution of the *CD24* genomic structure has been dynamic, with apparent gains and losses of intronic regions as well as UTRs. However, there was no correlation between the presence or absence of either the intronic regions or the UTRs and the evolutionary relationships of the species with *CD24* genes. The *CD24* 3'-UTR can regulate *CD24* transcript stability in COS cells [166] and intronic regions can contain regulatory regions that regulate expression level. Therefore, further investigation of these regions and their role in regulating CD24 expression may reveal novel regulatory mechanisms and clarify the role and evolution of these non-coding sequences.

This analysis provides evidence that *CD24* arose prior to the divergence of reptiles and birds from mammals approximately 200 million years ago [289], with subsequent loss of the gene from non-placental mammals. The CD24 gene was not annotated in any of the monotreme or marsupial genomes, nor were we able to detect it using the human, mouse, turkey or green anole *CD24* mature peptide sequence as the query. There are two possibilities to explain the absence of the *CD24* gene in these animals. The first is that the *CD24* genes were not represented in the genomes currently available from these species and that with further sequencing efforts *CD24* orthologues will be found. The second possibility is that *CD24* was lost in an ancestor of the non-

placental mammals. While this possibility is intriguing given the presence of CD24 in the placenta [290] and on vesicles secreted into the amniotic fluid from the fetus [291], the presence of *CD24* in egg laying reptiles and birds does not support a divergent role of CD24 in placental-based gestation. Further work is necessary to determine if the function of CD24 is conserved in egg-laying animals, as well as to investigate potential roles of CD24 in placenta-based gestation. There is currently limited availability of *CD24* sequences from birds and reptiles (three and one, respectively) and therefore the evolutionary history of this gene in these groups is not clear.

Analysis of the predicted structure of the consensus mature peptide sequence did not reveal any secondary structure for CD24. As such, CD24 may be considered an intrinsically disordered protein. Intrinsically disordered proteins represent a comparatively new paradigm in understanding protein structure and the suggestion is that many proteins exist without a defined secondary or tertiary structure as a basis of their molecular function [292]. Protein functions thought to depend on intrinsic disorder include flexible linker domains and phosphorylation sites [292, 293]. Given that CD24 is heavily glycosylated in its mature form, it is also plausible that this disorder gives the mature protein additional flexibility to maximize its glycosylation potential through minimizing steric interactions. The glycosylations may also impose order on the structure, thereby making structure prediction from the amino acid sequence alone not possible.

As mentioned, the amino acid sequence of CD24 possesses conserved glycosylation sites, as well as a proline-rich domain near the C-terminal region of the mature peptide. The conservation of glycosylation sites strongly suggests that they are critical regions that define the biological activity of CD24, including the localization of CD24 to the extracellular surface of the plasma membrane. Interestingly, the sites and degree of glycosylation can also vary within and between species. For example, the comparison of CD24 between humans and mouse reveals human CD24 is enriched in Ser and Thr, and missing two Asn residues, compared to mouse [287]. This may result in greater O-linked and fewer N-linked glycosylations. The mature core protein only contributes approximately 3.5 kDa, with the remaining and variable mass of CD24 made up by differing glycosylations [150, 287] . Thus, while the presence of multiple potential glycosylation sites is maintained, the number and type varies in a cell- and species-dependent manner.

Physically, the gain or loss of these glycosylation sites may have a significant impact on the size or shape of the mature CD24 peptide. O-linked glycans may contribute up to 2.5Å to total protein length [294]. Thus, mouse CD24 would be predicted to extend at least 10Å beyond the plasma membrane. The presence of significantly more O-linked glycosylation sites in the human sequence suggests that it may be held in a more rigid conformation and extend even further from the cell surface. The evolution of the conserved glycosylation sites in CD24 suggests that the function of the protein is critically dependent on its status as a glycophosphoprotein, with additional flexibility depending on the nature of the individual glycosylations [295].

Overall, this analysis has clearly shown that CD24 evolution predates the divergence between birds, reptiles and mammals, and is conserved across the placental mammals. Also, the CD24 protein exists in an intrinsically disordered state and that the most evolutionarily constrained regions are related to sites of N- and O-linked glycosylation, which mediate CD24-ligand interactions and possibly affect the protein structure.

Chapter 4 The effect of intrinsic factors on breast cancer progression

Preliminary data from Dr. Christian's lab suggested a potential link between Ras and CD24 gene expression [296]. Moreover, previous studies have shown that activation of oncogenic Ras in BC cells leads to generation of $CD24^{-}/CD44^{+}$ stem-like cells from $CD24^{+}/CD44^{low}$ cells [85]. Despite evidence that overexpression of oncogenic Ras can repress CD24 surface expression [85], the mechanism for this regulation of CD24 is not known. Here, I examined the regulation of CD24 mRNA and protein levels, as well as promoter activity in a model of oncogenic Ras activation and in BC cells with oncogenic Ras activation. To analyze the regulation of CD24 expression by oncogenic Ras, I used a model system in which constitutively active H-Ras, containing a G12 to V12 mutation (RasV12), was stably expressed in the mouse embryonic fibroblast NIH/3T3 cell line [297]. To narrow down the downstream regulators of Ras, I used Ras effector mutants that constitutively activate either Raf or PI3K or Ral-GDS pathways. I examined the pathways regulated by Ras to show that either the PI3K or Raf pathways can repress CD24 expression. Surprisingly, inhibition of Raf but not MEK or PI3K significantly increased CD24 surface expression. Finally, to determine if there is a similar effect in BC cells, I performed a meta-analysis and selected MDA-MB-231 cells that have an inverse relation between Ras pathway genes and CD24 to further determine the effect of Raf on CD24 surface expression.

4.1 Regulation of the BCSC marker CD24 by Ras pathway in a model system

4.1.1 RasV12 down regulates CD24 mRNA and surface protein expression.

Initially, the level of *CD24* mRNA expression in NIH/3T3 cells stably transfected with empty vector (control cells) or containing the constitutively active Ras gene was analyzed by RT-PCR and RT-qPCR (Fig 4.1A-B). I observed a clear suppression of *CD24* mRNA expression (Fig 4.1A) with more than 1000-fold decrease in RasV12 cells compared to Babe cells (Fig 4.1B).

Similarly, analysis of CD24 surface protein by flow cytometry showed a statistically significant reduction in the percentage of $CD24^{+}$ cells in RasV12 population compared to control cells (Fig 4.1C-D). Therefore, I conclude that the reduction of expression is due to the majority of RasV12 cells losing CD24 expression entirely. Together, these data show that constitutively active Ras significantly downregulates CD24 at both the mRNA and surface protein expression levels. Residual levels of CD24 are due to a small portion of the population retaining surface expression.

4.1.2 Ras-mediated repression of *CD24* at the level of the promoter.

I next analyzed the activity of the *CD24* promoter region comprising the 688 nucleotides upstream of the TSS (p688) [162]. I found that this region is active in both RasV12 and control cells compared to the promoterless control (Fig 4.2A). However, the activity was reduced in RasV12 cells compared to control cells. To determine if this difference was statistically significant, I analyzed the relative activity in RasV12 versus

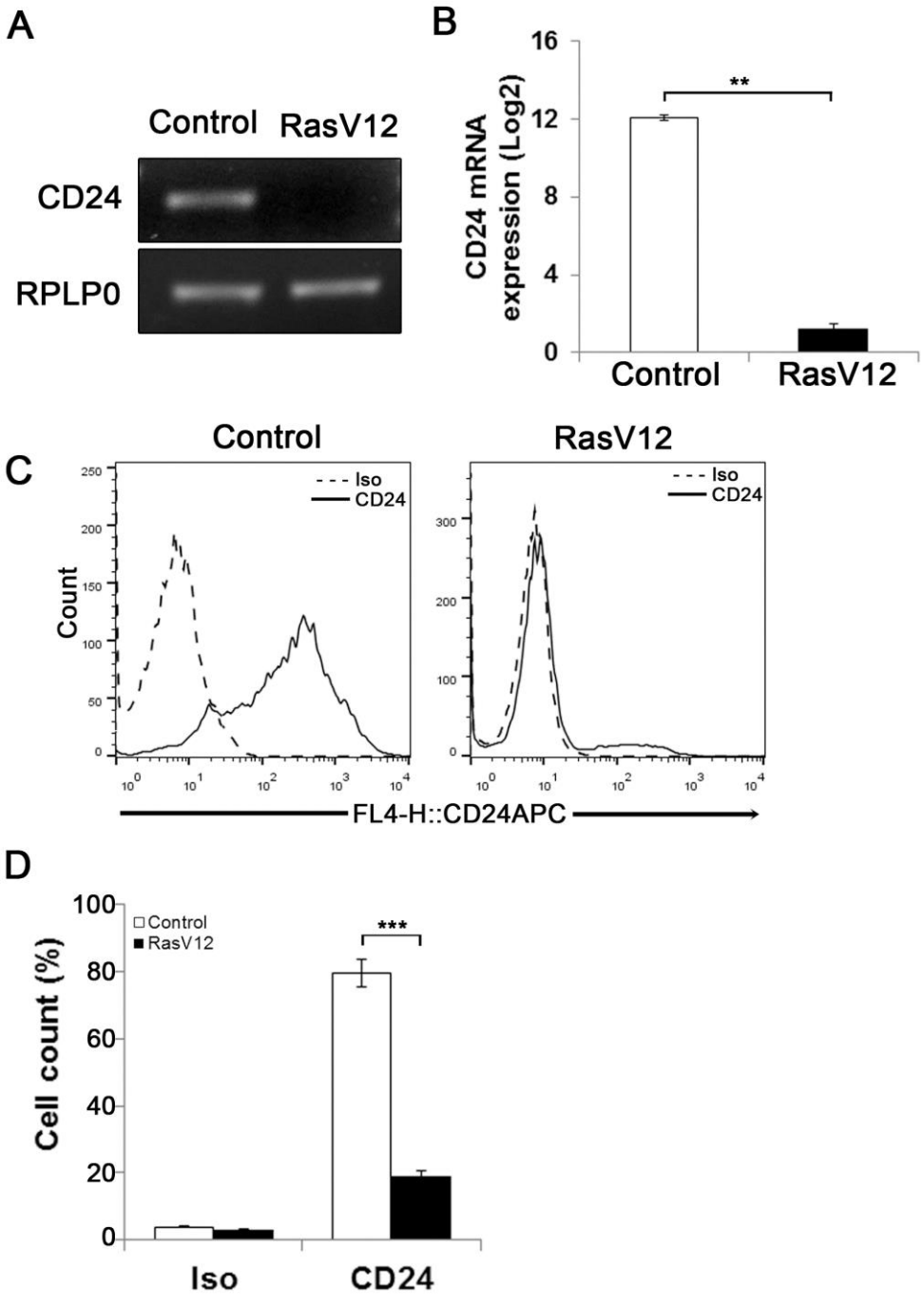
A
Control
RasV12
CD24
RPLP0
B
CD24 mRNA expression (Log2)
16
12
8
4
0
**
Control
RasV12
C
Control
RasV12
Iso
CD24
Count
FL4-H::CD24APC
D
Control
RasV12
Cell count (%)
100
80
60
40
20
0
***
Iso
CD24

Figure 4.1: Oncogenic Ras downregulates CD24 expression in NIH/3T3 cells:

CD24 mRNA expression in vector control (Control) and RasV12 cells was determined by (A) RT-PCR and (B) RT-qPCR. *RPLP0* was used as the loading and normalization control. *CD24* mRNA levels shown as mean ± s.e.m. (C) Surface CD24 protein was determined by flow cytometry in Control and RasV12 cells. One representative histogram of isotype (Iso) and CD24-stained cells is shown. (D) Quantification of CD24 surface protein expression as mean ± s.e.m percentage of $CD24^+$ cells. Significance was determined by Student's t-test, n=3, **P<0.01, ***P<0.001.

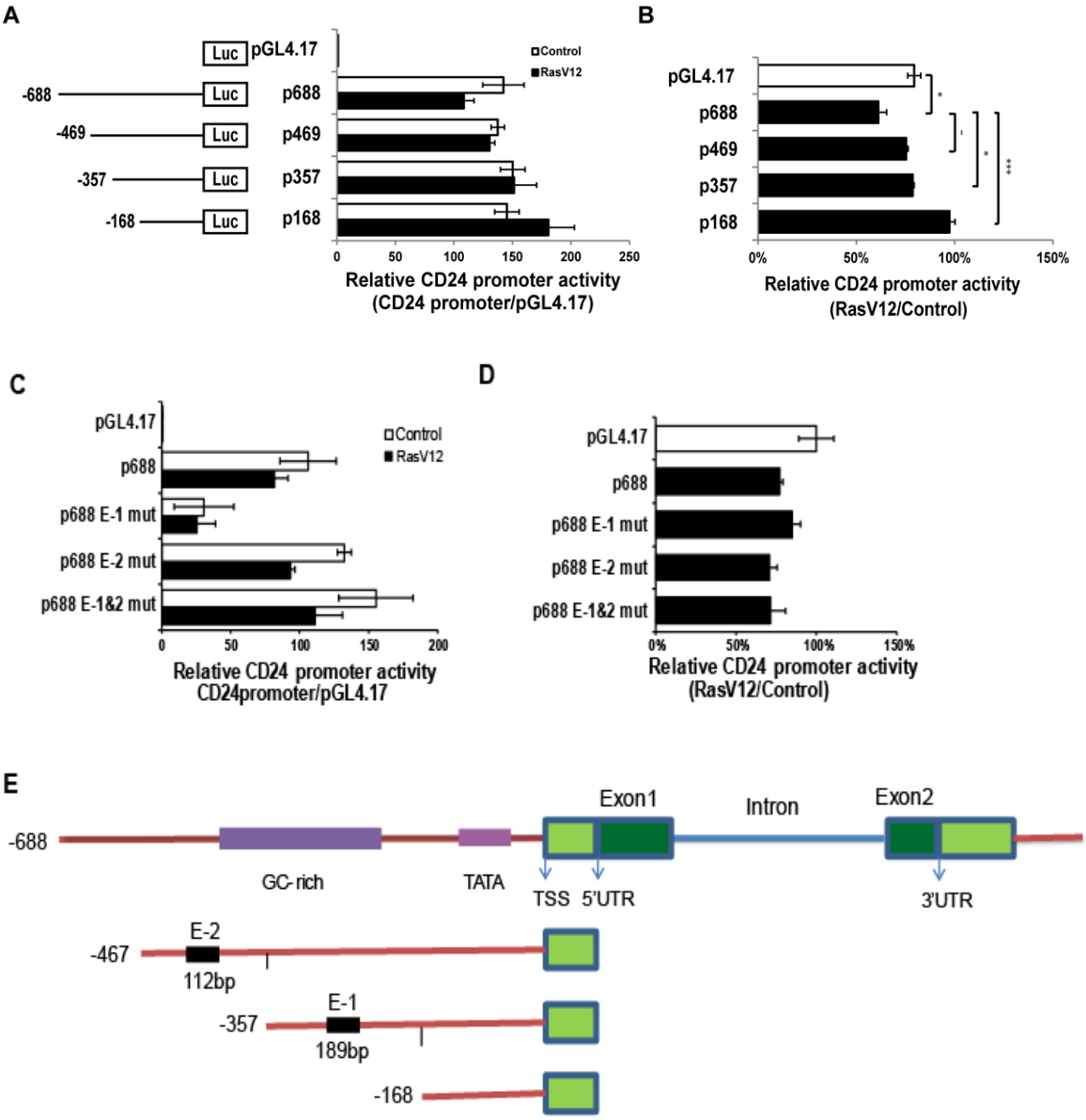
A
Luc
pGL4.17
-688
Luc
p688
-469
Luc
p469
-357
Luc
p357
-168
Luc
p168
Control
RasV12
0
50
100
150
200
250
Relative CD24 promoter activity
(CD24 promoter/pGL4.17)
B
pGL4.17
p688
p469
p357
p168
0%
50%
100%
150%
Relative CD24 promoter activity
(RasV12/Control)
C
pGL4.17
p688
p688 E-1 mut
p688 E-2 mut
p688 E-1&2 mut
Control
RasV12
0
50
100
150
200
Relative CD24 promoter activity
CD24promoter/pGL4.17
D
pGL4.17
p688
p688 E-1 mut
p688 E-2 mut
p688 E-1&2 mut
0%
50%
100%
150%
Relative CD24 promoter activity
(RasV12/Control)
E
-688
Exon1
Intron
Exon2
GC-rich
TATA
TSS
5'UTR
3'UTR
-467
E-2
112bp
-357
E-1
189bp
-168

Figure 4.2: RasV12 represses *CD24* promoter activity:

(A, C) Relative promoter activity in vector control and RasV12 is shown compared to promoterless vector (pGL4.17). Schematic diagram of promoter deletion constructs are shown on the left. Promoter length is indicated by the position upstream of the TSS. (B, D) Relative promoter activity in RasV12/Control cells for each reporter construct. Significant differences were determined by one-way ANOVA with Tukey Honest Significant Difference post-hoc analysis, n=3, $^{-}P<0.1$ (not significant), $*P<0.05$, $***P<0.001$, all data are shown as mean ± s.e.m. (E) Schematic diagram showing CD24 gene structure and the presence of E- box elements 1 and 2 on the repressed region of CD24 promoter. E-1-E-box1 and E-2 – E-box2

control cells in comparison to the promoterless vector, which represents basal activity levels in the two cell types (Fig 4.2B). I found that there was a significant repression of the promoter activity in the RasV12 cells. To further narrow down the responsive region, I analyzed a series of *CD24* promoter deletion mutants (Fig 4.2A-B). I found the relative promoter activity in RasV12 versus control cells increased in each deletion mutant compared to the full promoter. This increase in p469 promoter region (-469 to -1) activity was modest and was not significantly different from control. The relative promoter activity in p357 promoter region (-357 to -1) reached significance and was further increased when the promoter included only the region from -168 to -1 from the TSS (p168). Therefore, both the 112 bp region from -469 to -357 and the 189 bp region from -357 to -168 contain repressive elements that are regulated by RasV12. However, the sequence within -357 to -168 promoter region appears to contribute more to the suppression of *CD24* than the sequence within the -469 to -357 region.

I have analyzed the repressive elements for the transcription factors that might bind and regulate *CD24* transcription. The bHLH proteins bind to enhancer- box (E-box) elements that have the consensus sequence CANNTG [298]. TWIST family, bHLH TFs regulate CD24 expression, where TWIST1 downregulates CD24 transcription and TWIST2 upregulates CD24 transcription [159, 160]. There are two E-box elements, E-box 1 and E-box 2 on the p688 promoter region of CD24 in between -357 to -168 region and -469 to -357 region, respectively (Fig 4.2E). However, promoter analysis of mutated E-box elements did not relieve the CD24 promoter repression by Ras pathway (Fig 4.2C-D). Using JASPAR- a database of TF binding profiles [299], I identified 45 putative TF

binding sites located in regions that are repressed by oncogenic Ras. I further narrowed down the TF binding sites based on the preliminary microarray data where the genes were regulated in presence and absence of U0126 in RasV12 cells [296]. I also performed a literature review and found that SPIB, FOXP1, FOXO3, Sox5, and Sox17 TFs might play a role in repressing the CD24 promoter (Table 4.1). Overall, these data show that E-box elements do not repress CD24 promoter activity in response to oncogenic Ras, and that further analysis of other TFs is necessary to fully elucidate this interaction.

4.1.3 Activation of either the Raf or the PI3K pathway is sufficient to downregulate CD24 expression.

Since I observed that CD24 mRNA and protein expression are downregulated by Ras, I next asked which pathways downstream of Ras are sufficient to suppress CD24 expression. Ras activates three major pathways, the Raf, RalGDS, and PI3K pathways, all of which contribute to the fully transformed phenotype of cancer cells [300]. I made use of NIH/3T3 cells expressing the Ras effector mutants RasV12G37, RasV12S35 and RasV12C40 [301–303], in which only one pathway is activated. Specifically, RasV12G37 activates only RalGDS but not PI3K or Raf. In a similar manner, RasV12S35 selectively activates the Raf pathway, and RasV12C40 selectively activates the PI3K pathway.

I observed a downregulation in *CD24* mRNA expression in RasV12S35 and RasV12C40 effector mutants compared to control cells by RT-PCR (Fig 4.3 A). In

Table 4.1: List of predicted transcription factors and their role in regulation of genes.

Transcription factor	Family	Consensus sequence	DNA binding site uptream of 3'TSS	Relationship with Ras pathway	Role	Ref
SPIB	SPI subclass of ETS family	GGAA/T	347 - 341	ERK1 phosphorylates SPIB which decreases its stability, which inactivates transcription by SPIB	Activator	[304, 305]
FOXP1	P subclass of forkhead family	TATTT(G/A)T	349 - 336	PI3K/Akt increases FOXP1 activity via p70s6k	Repressor	[306]
FOXO3	O subclass of forkhead family	GTAAACA (FOXO consensus sequence)	345 - 335	PI3K/Akt inactivates FOXO proteins by phosphorylation further decreasing DNA binding ability of FOXO proteins	Activator	[307]
Sox5	SRY related HMG-box related family	AACAAT	342 - 336	Inhibition of MEK by U0126 increased Sox5 mRNA expression	Activator	[296]

Sox17	SRY related HMG-box related family	(A/T)(A/T) CAA(A/T)	341 - 333	Inhibition of MEK by U0126 increased Sox17 mRNA expression	Activator	[296]

[a]Abbreviations: FOXP1-forkhead box P1, FOXO3 – forkhead box O3, SOX – SRY related HMG box

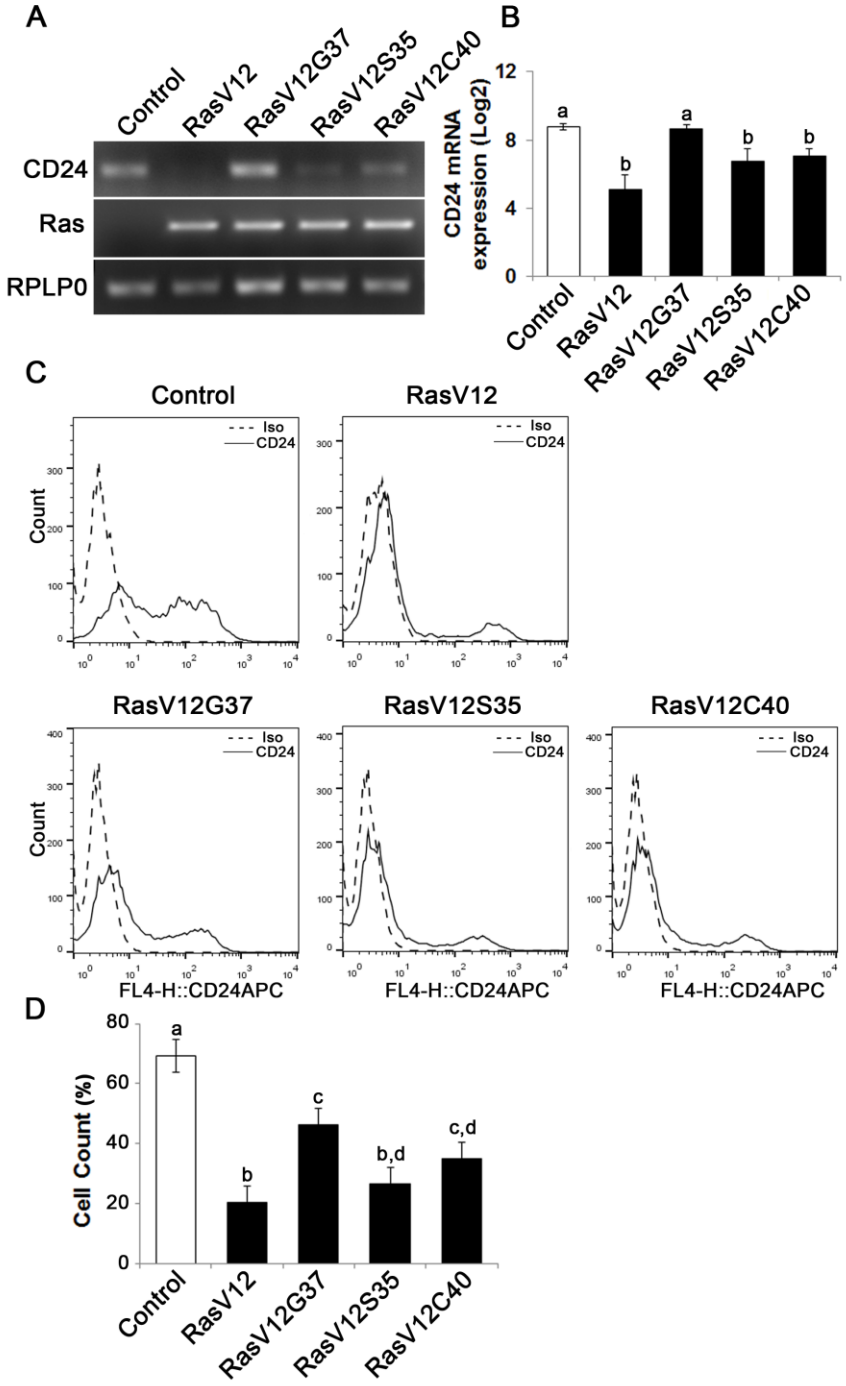
A
Control
RasV12
RasV12G37
RasV12S35
RasV12C40
CD24
Ras
RPLP0
B
CD24 mRNA expression (Log2)
12
8
4
0
a
b
a
b
b
Control
RasV12
RasV12G37
RasV12S35
RasV12C40
C
Control
RasV12
RasV12G37
RasV12S35
RasV12C40
Iso
CD24
Count
FL4-H::CD24APC
D
Cell Count (%)
80
60
40
20
0
a
b
c
b,d
c,d
Control
RasV12
RasV12G37
RasV12S35
RasV12C40

Figure 4.3: The Raf and PI3K pathways downregulate *CD24* mRNA expression while the Raf pathway is primarily responsible for downregulation of CD24 surface protein expression:

(A) *CD24* mRNA expression in Control, RasV12, RasV12G37, RasV12S35 and RasV12C40 cells was determined by RT-PCR. *H-Ras* mRNA expression was used to verify expression of ectopic Ras. *RPLP0* was used as the loading control. (B) RT-qPCR was used to quantify *CD24* mRNA expression with *RPLP0* used as the normalization control. (C) Surface CD24 protein was determined by flow cytometry. One representative histogram of isotype (Iso) and CD24-stained cells is shown. (D) Quantification of CD24 surface protein expression as mean ± s.e.m percentage of $CD24^+$ cells. Significance was determined by one way ANOVA with Tukey Honest Significant Difference analysis, n=4, different lower case letters indicating different groups at $P<0.01$.

contrast, the RasV12G37 cells had a similar level of *CD24* mRNA expression as the control cells (Fig 4.3A). Quantitative analysis of *CD24* mRNA by RT-qPCR revealed the change in *CD24* mRNA expression levels in RasV12S35 and RasV12C40 cells to be statistically significant when compared to control cells and RasV12G37 but not different from RasV12 cells (Fig 4.3B).

I then determined if CD24 surface protein expression was also affected in Ras effector mutant cells (Fig 4.3C). I found that there was a significant and substantial reduction in the percentage of cells expressing CD24 surface protein in RasV12 and RasV12S35 cells (Fig 4.3D). RasV12G37 and RasV12C40 expression had an intermediate effect on reducing the percentage of cells expressing CD24, compared to control cells. Therefore, activation of the Raf kinase pathway, the PI3K pathway, or the RalGDS pathway downstream of Ras are sufficient to decrease the $CD24^+$ population. However, activation of the Raf pathway was sufficient to decrease the $CD24^+$ population to the same low level as RasV12 suggesting that the Raf pathway is the major regulator of CD24 expression in these cells. Moreover, Raf and PI3K could decrease both CD24 mRNA and surface expression while RalGDS only partially affected surface expression.

4.1.4 Inhibition of MEK or PI3K does not fully restore *CD24* mRNA expression.

Since we observed that both CD24 mRNA and protein were significantly and substantially downregulated by the Raf and PI3K pathways, I next determined if inhibition of either or both of these pathways could restore *CD24* expression in RasV12 cells at the mRNA level. The major downstream effectors of Raf are the MEK1/2 kinases

[308], which can be inhibited specifically with the chemical inhibitor U0126 [270]. PI3K can be inhibited directly using LY294002 [270, 271]. Considering the duration of transcription and translation, I incubated the cells with inhibitors for 16 h for mRNA expression and for 24 h for protein expression. I evaluated the inhibition of Raf/MEK/ERK and PI3K/Akt pathways using western blot analysis of phosphorylated ERK (P-ERK) and phosphorylated Akt (P-Akt), respectively (Fig 4.4A). I found that RasV12 cells treated with U0126 had reduced phosphorylation of ERK with no effect on Akt phosphorylation. Similarly, RasV12 cells treated with LY294002 had reduced phosphorylation of Akt with no effect on ERK phosphorylation. Treatment with both U0126 and LY294002 inhibited phosphorylation of both ERK and Akt. I found that treatment of RasV12 cells with U0126 had a modest, but significant 6-fold increase in *CD24* mRNA expression (Fig 4.4B-C). Surprisingly, treatment with LY294002 alone or in combination with U0126 suppressed *CD24* mRNA expression to below the levels seen in RasV12 cells (Fig 4.4B-C).

Since U0126 modestly increased *CD24* mRNA levels, I next determined the effect of U0126 on CD24 surface protein in control cells and RasV12 cells. Unexpectedly, I found that U0126 increased the percentage of $CD24^+$ cells in the control cell population (Fig 4.4D-E). In contrast, there was a modest but not statistically significant increase in the percentage of $CD24^+$ RasV12 cells treated with U0126 (Fig 4.4D-E). Therefore, even though the Raf pathway is sufficient to decrease CD24 mRNA and protein, inhibition of oncogenic Raf/MEK signaling does not restore CD24 expression to the level of control cells at the mRNA or protein level.

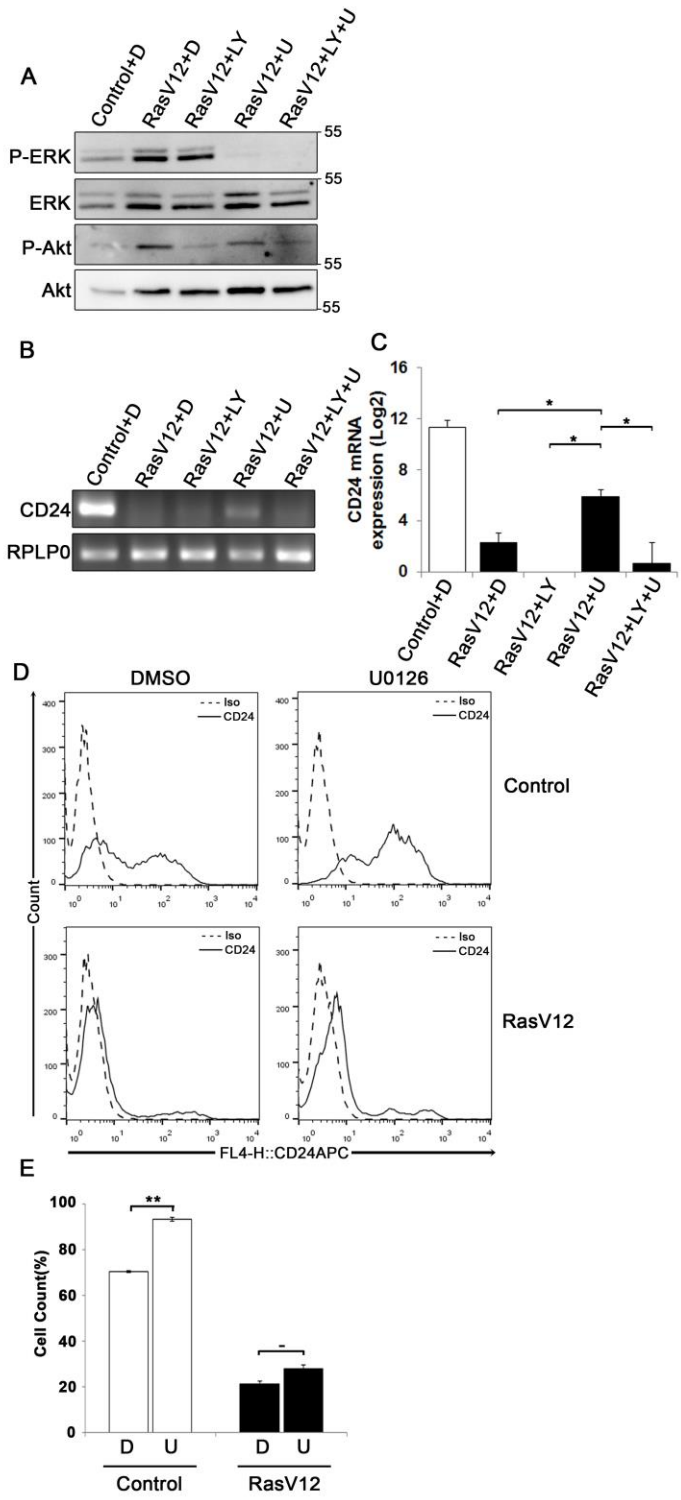
A
Control+D
RasV12+D
RasV12+LY
RasV12+U
RasV12+LY+U
P-ERK
ERK
P-Akt
Akt
55
B
CD24
RPLP0
C
CD24 mRNA expression (Log2)
16
12
8
4
0
D
DMSO
U0126
Iso
CD24
Control
RasV12
Count
FL4-H::CD24APC
E
Cell Count(%)
100
80
60
40
20
0
D
U
Control
RasV12

Figure 4.4: Inhibition of the Raf/MEK/ERK pathway is sufficient to partially restore *CD24* mRNA but not protein expression in RasV12 cells:

(A-C) RasV12 cells were treated for 16 h with DMSO (D), or U0126 (U) and/or LY294002 (LY). (A) Western blot analysis was performed to detect phosphorylated ERK (P-ERK), and phosphorylated Akt (P-Akt). Total ERK and total Akt were used as loading controls. Molecular mass standards are shown in the right of each image. One representative experiment from three replicates is shown. *CD24* mRNA expression in Control and RasV12 cells was determined by (B) RT-PCR and (C) RT-qPCR. *RPLP0* was used as the loading and normalization control. Significance was determined by one-way ANOVA with Tukey Honest Significant Difference post-hoc analysis, *P<0.05. (D) Surface CD24 protein was determined by flow cytometry with Control or RasV12 cells treated for 24 h as above. One representative histogram of isotype (Iso) and CD24-stained cells is shown. (E) Quantification of CD24 surface protein expression as mean ± s.e.m percentage of $CD24^+$ cells. Significance was determined by Student's t-test, n=4, ¯P<0.1, **P<0.01.

4.1.5 Inhibition of Raf partially restores CD24 cell surface protein expression in cells expressing oncogenic Ras but not control cells.

Since I observed that inhibition of MEK partially restored *CD24* mRNA with no significant effect on protein levels, I next determined if inhibition of Raf directly could restore CD24 expression levels. Raf is the major downstream target of Ras and can be directly inhibited by sorafenib, which does not inhibit MEK or ERK [309]. I evaluated the inhibition of Raf/MEK/ERK pathway by sorafenib at different concentrations using western blot analysis of phosphorylated ERK (P-ERK) and phosphorylated Akt (P-Akt) as measures of efficacy and specificity (Fig 4.5A). I found that sorafenib reduced ERK phosphorylation in RasV12 cells at all concentrations examined. I also found that both phosphorylated and total Akt was reduced with 10 and 20 μM sorafenib. Sorafenib is known to inhibit additional kinases such as EGFR, PDGFR, c-Kit and FLT-3 [309, 310], therefore, it is not surprising to observe inhibition of additional pathways with this inhibitor. However, I found that treatment of RasV12 cells with sorafenib had no effect on *CD24* mRNA expression (Fig 4.5B-C).

I next determined the effect of Raf inhibition by sorafenib on CD24 surface protein in control cells and RasV12 cells. We found that treatment with 20 μM but not 5 or 10 μM sorafenib significantly increased the percentage of $CD24^+$ cells within the RasV12 cell population (Fig 4.5D-E). In contrast to MEK inhibition, there was no change in the percentage of $CD24^+$ cells in the control cells after treatment with sorafenib (Fig 4.5D-E). Therefore, inhibition of Raf significantly increases the proportion of

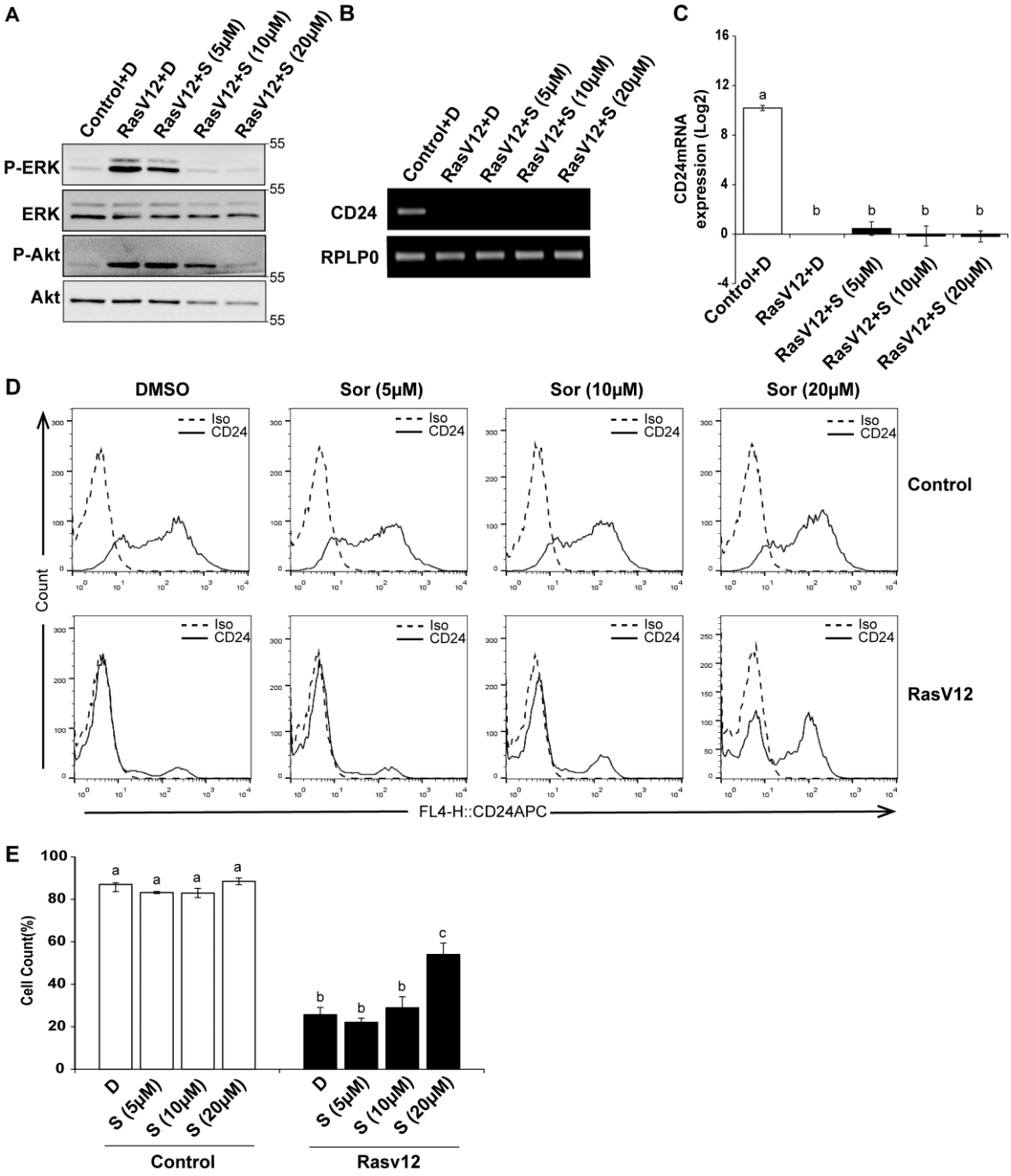
A
Control+D
RasV12+D
RasV12+S (5μM)
RasV12+S (10μM)
RasV12+S (20μM)
P-ERK
ERK
P-Akt
Akt
55
B
CD24
RPLP0
C
CD24mRNA expression (Log2)
D
DMSO
Sor (5μM)
Sor (10μM)
Sor (20μM)
Iso
CD24
Control
RasV12
Count
FL4-H::CD24APC
E
Cell Count(%)
D
S (5μM)
S (10μM)
S (20μM)
Control
Rasv12

Figure 4.5: Inhibition of Raf is sufficient to increase CD24 cell surface protein but not mRNA expression in RasV12 cells:

(A-C) Rasv12 cells were treated for 16 h with DMSO (D) or 5µM, 10µM and 20µM sorafenib (S). (A) Western blot analysis was performed as in figure 4.4. One representative experiment from three replicates is shown. *CD24* mRNA expression in Control and RasV12 was determined by (B) RT-PCR and (C) RT-qPCR as in figure 4.4. Significance was determined by one-way ANOVA with Tukey Honest Significant Difference post-hoc analysis, n=3. (D) Surface CD24 protein was determined by flow cytometry with Control and RasV12 treated for 24 h as above. One representative histogram of isotype (Iso) and CD24-stained cells is shown. (D) Quantification of CD24 surface protein expression as mean ± s.e.m percentage of $CD24^+$ cells. Significance was determined by one way ANOVA with Tukey Honest Significant Difference analysis, n=3, different lower case letters indicate different groups at $P<0.001$.

$CD24^+$ cells in the absence of changes at mRNA level, but only in cells expressing oncogenic Ras.

4.1.6 Inhibition of PI3K does not synergize with Raf inhibition to affect *CD24* mRNA or surface protein expression.

I next determined if inhibition of both PI3K and Raf together could further restore CD24 expression in RasV12 cells at the mRNA and surface protein levels. I evaluated the inhibition of PI3K/Akt and Raf/MEK/ERK pathways using western blot analysis of phosphorylated ERK (P-ERK) and phosphorylated Akt (P-Akt), respectively, as previously discussed (see section 4.1.4) (Fig 4.6A). Similar to previous observations, I found that treatment of RasV12 with LY294002 reduced phosphorylation of Akt with no effect on phosphorylation of ERK. Treatment with both LY294002 and sorafenib inhibited phosphorylation of both ERK and Akt, as expected. I found that treatment with both LY294002 and sorafenib did not increase *CD24* mRNA expression (Fig 4.6B-C).

I found that treatment of RasV12 cells with LY294002 alone did not affect the percentage of $CD24^+$ cells in either control or RasV12 cells (Fig 4.6D-E). Moreover, addition of LY294002 did not affect the sorafenib-induced increase in the percentage of CD24+ cells (Fig 4.6E). Together, these data indicate that even though activation of either the PI3K or Raf pathway is sufficient to decrease CD24 mRNA and protein expression, inhibition of both PI3K and Raf together is not sufficient to restore CD24 surface protein or mRNA expression.

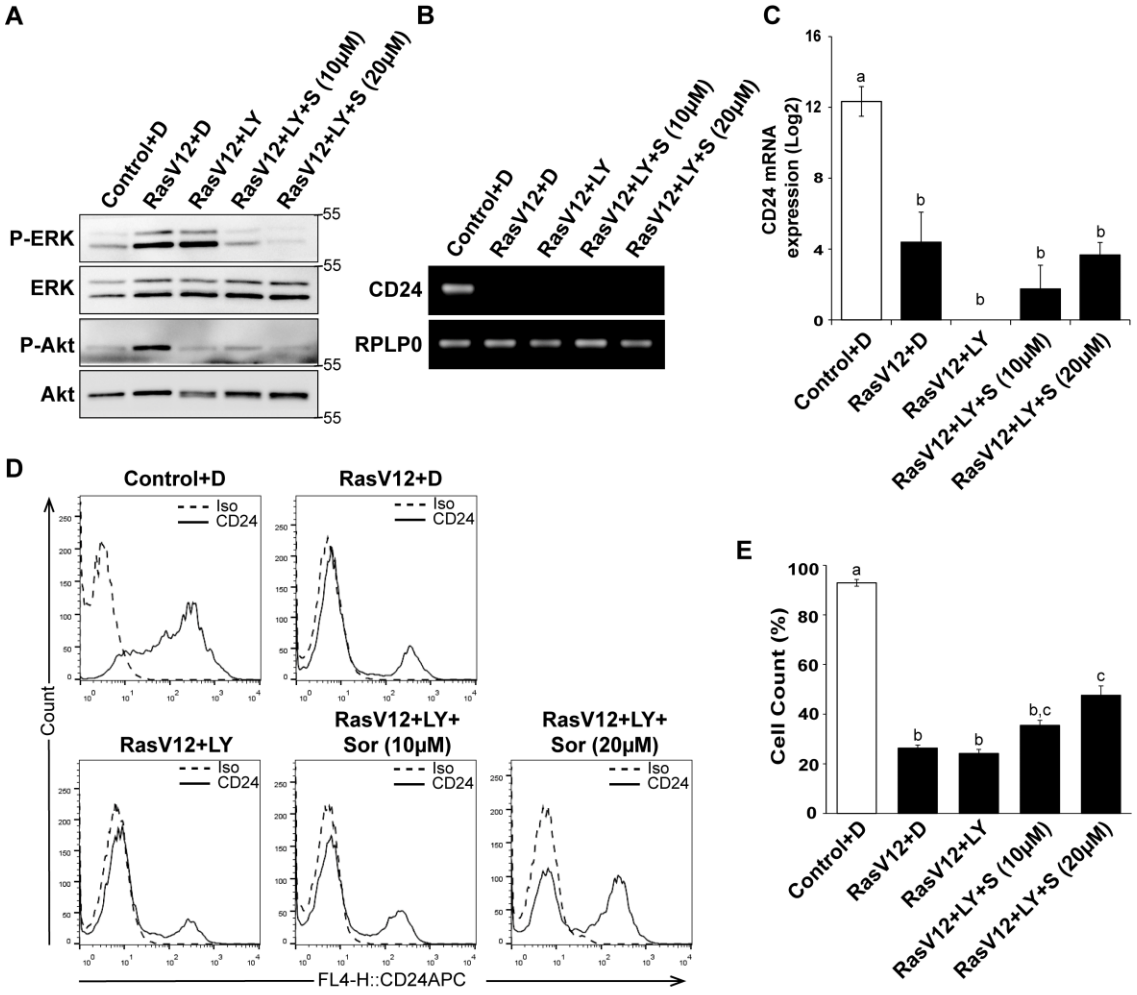
A
Control+D
RasV12+D
RasV12+LY
RasV12+LY+S (10μM)
RasV12+LY+S (20μM)
P-ERK
ERK
P-Akt
Akt
55
B
CD24
RPLP0
C
CD24 mRNA expression (Log2)
16
12
8
4
0
a
b
b
b
b
D
Control+D
RasV12+D
RasV12+LY
RasV12+LY+ Sor (10μM)
RasV12+LY+ Sor (20μM)
Iso
CD24
Count
FL4-H::CD24APC
E
Cell Count (%)
100
80
60
40
20
0
a
b
b
b,c
c

Figure 4.6: Inhibition of PI3K did not alter the Raf-mediated inhibition of CD24 expression:

(A-C) Rasv12 cells were treated for 16 h with DMSO (D), 100µM LY294002 (LY) and/or 10µM or 20µM sorafenib (S/Sor) with LY. (A) Western blot analysis was performed as in figure 4.4. One representative experiment from three replicates is shown. *CD24* mRNA expression in Control and RasV12 was determined by (B) RT-PCR and (C) RT-qPCR as in figure 4.4. Significance was determined by one way ANOVA with Tukey Honest Significant Difference post-hoc analysis, n=3, $^{a,b}P<0.01$. (D) Surface CD24 protein was determined by flow cytometry with Control and RasV12 for 24 h as above. One representative histogram of isotype (Iso) and CD24-stained cells is shown. (D) Quantification of CD24 surface protein expression as mean ± s.e.m percentage of $CD24^{+}$ cells. Significance was determined by one way ANOVA with Tukey Honest Significant Difference analysis, n=3, different lower case letters indicating different groups at $P<0.001$.

4.2 Regulation of BCSC marker, CD24 by Ras pathway in BC cell lines

4.2.1 Relationship between CD24 and Ras pathway gene expression in human breast cancer.

To select cell lines that have an inverse relationship between the Ras pathway genes and CD24, we analyzed previously published DNA microarray datasets [224, 265–268] from 9 different BC cells or normal cells (Table 2.1). An inverse relationship was confirmed by considering the datasets, where the cells under different conditions showed alterations in expression of Ras pathway genes and CD24. Ten of the gene expression profiles were obtained using the Affymetrix HG-U133A_2 array, while one used the HG-U133_plus_2 array (Table 4.2). Both of these platforms share the same strategy of interrogating the 3' region of mRNA transcripts and, therefore, can be compared directly, as well as being the most commonly used platform for analyzing whole genome expression data from breast cancer cells in the GEO repository [261]. I performed unsupervised hierarchical cluster analysis of CD24 along with genes in the three major pathways downstream of Ras, and the different Ras isoforms (Fig 4.7). All of the probesets representing all the isoforms of each gene in a gene family (i.e. all Ras isoforms) were evaluated for their presence in the same cluster as the CD24 probeset in each cell type/treatment (Fig 4.7).

The cells analyzed were separated into three broad categories: 1) cells expressing ER, PR or HER-2, 2) TNBC cells, and 3) normal or immortalized cells [9, 311, 312].

Table 4.2: The total number probesets representing the Ras pathway genes and CD24 from each platform.

Gene/Gene family	Number of probesets	
	HG-U133A_2	HG-U133_plus_2
CD24	6	6
Ras	10	15
Raf	3	7
MAPK1	5	6
Ral/Ral GDS	2	7
PIK3C	12	27
PIK3R	10	12

A1

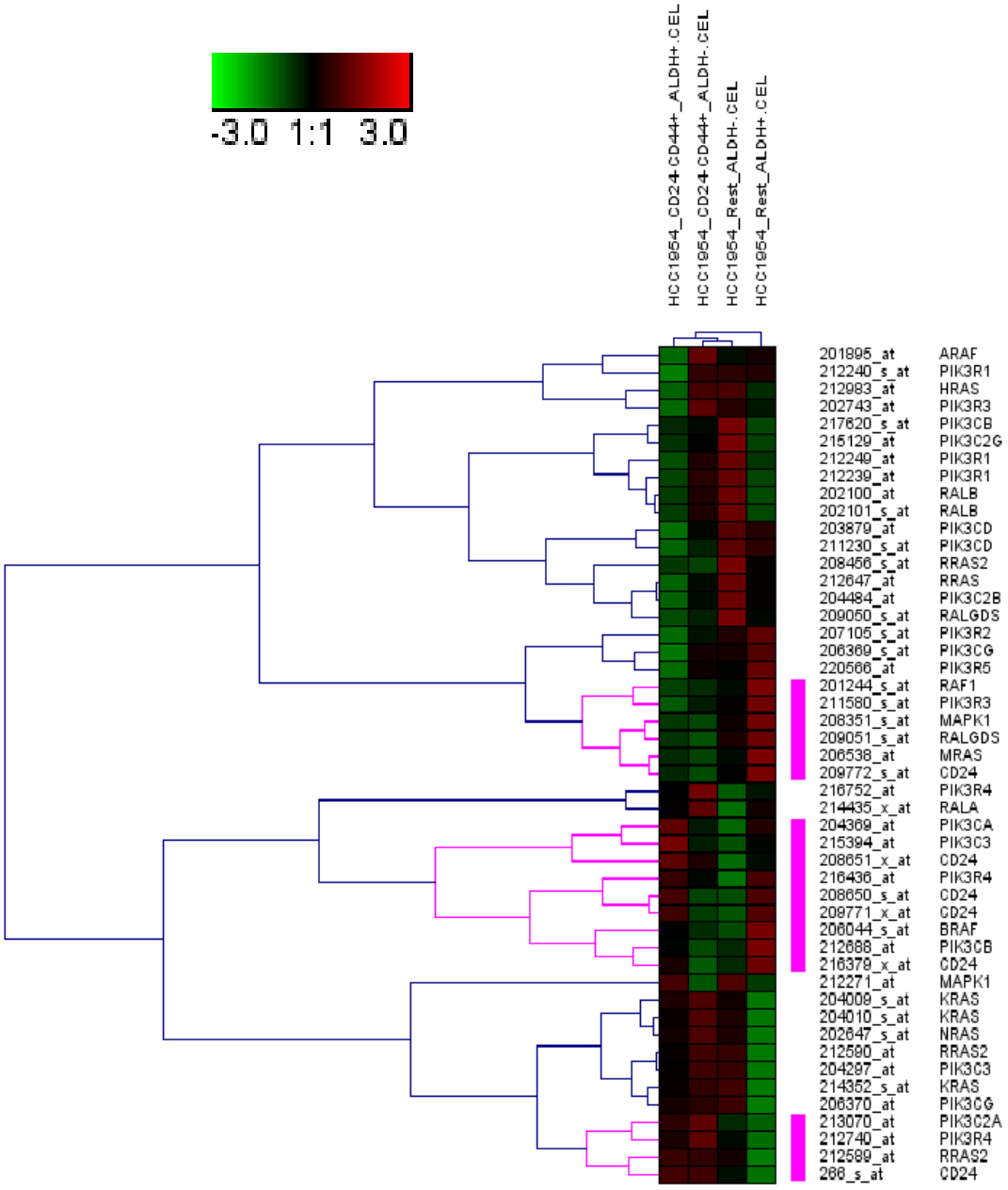

HCC1954
GSE52262

A2

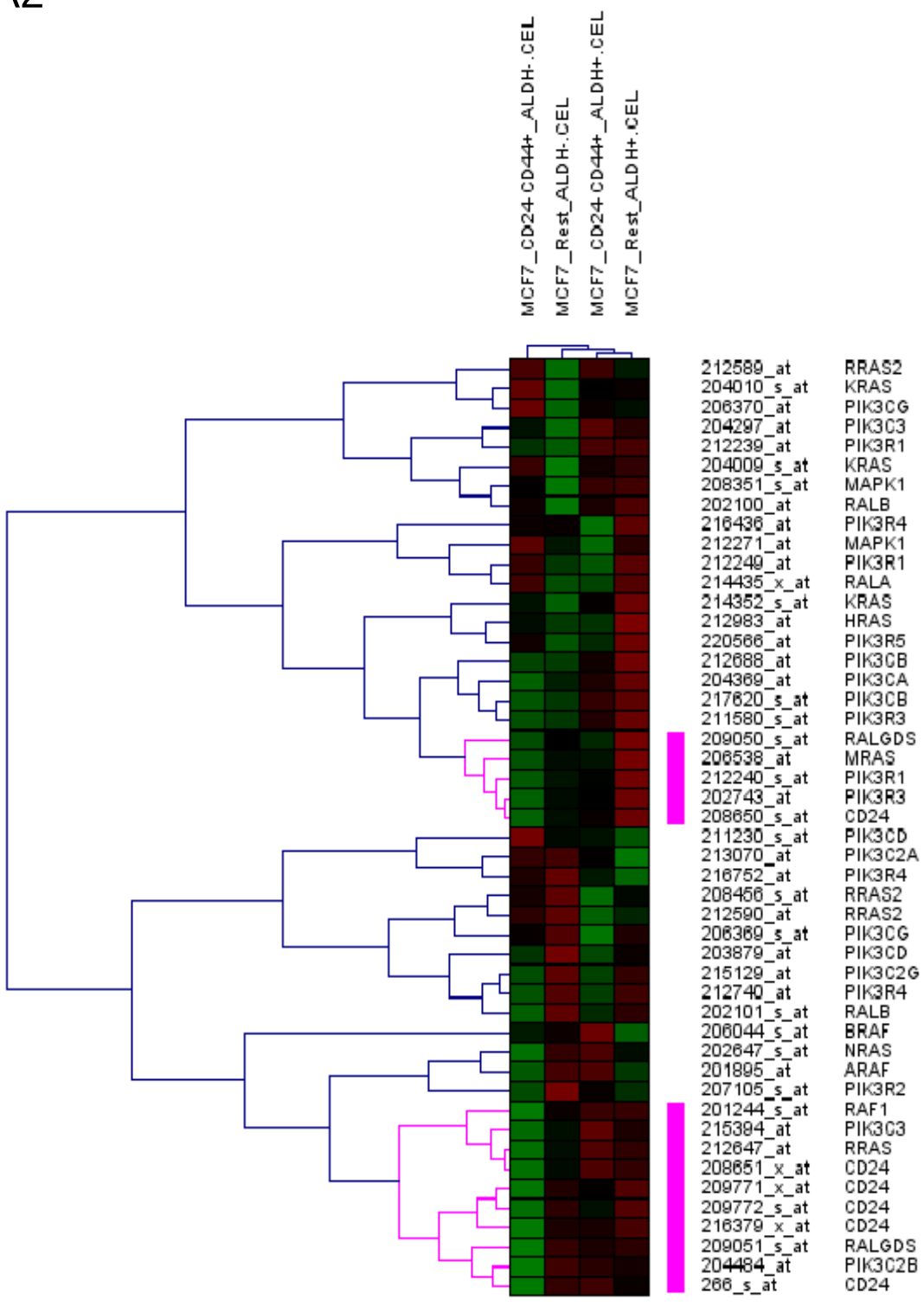

MCF7
GSE52262

A3

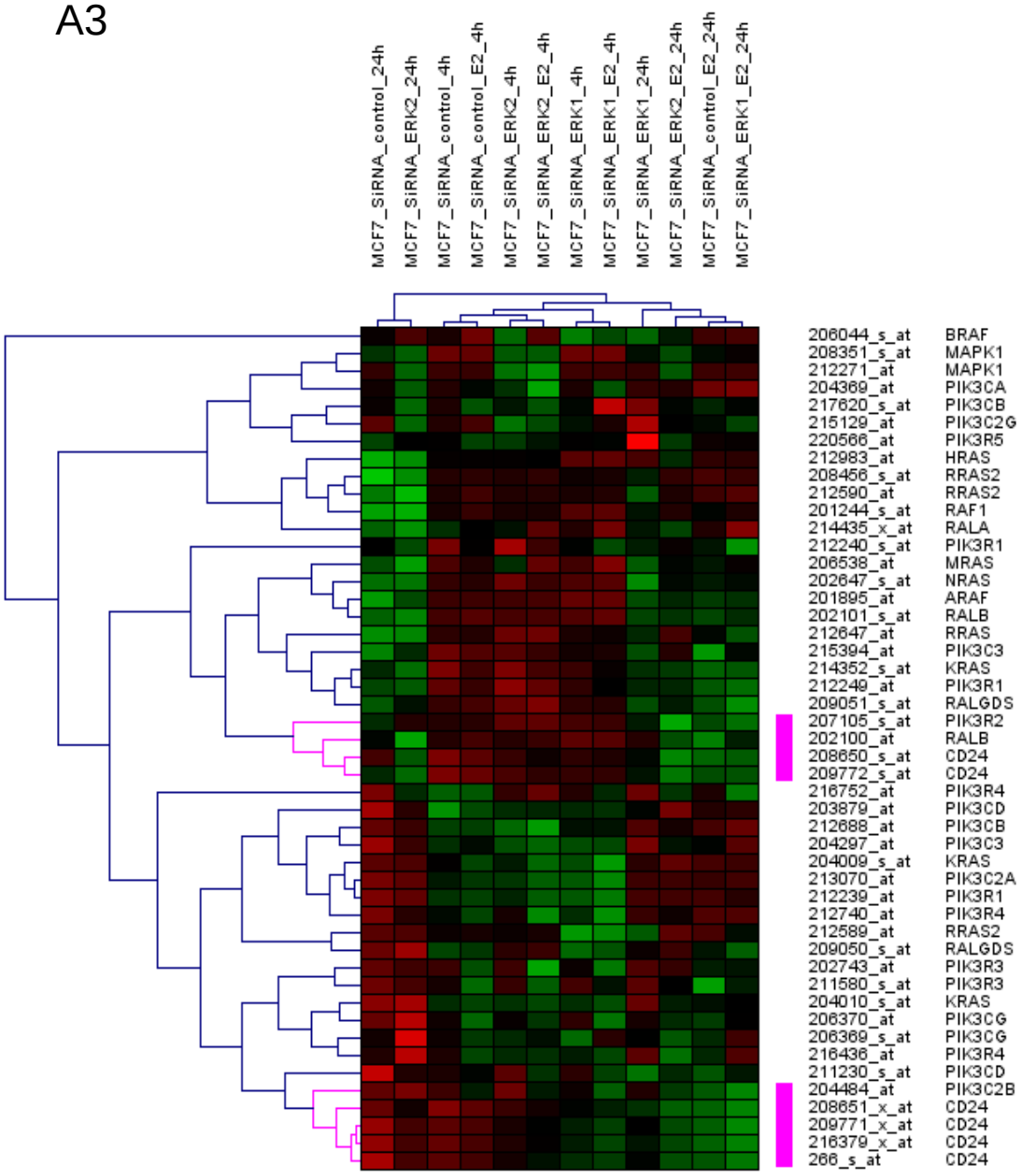

MCF7_estradiol
GSE24592

A4

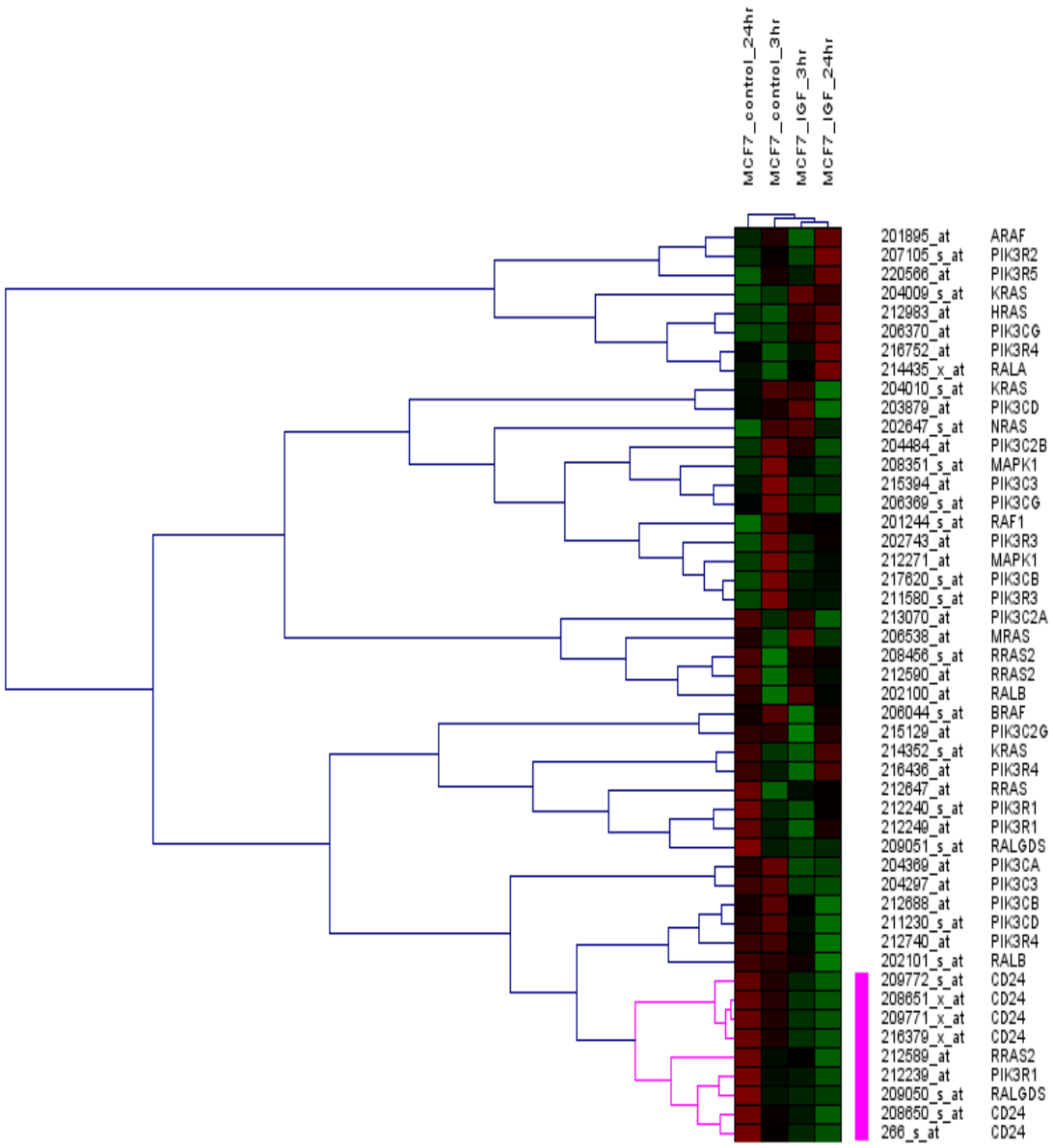

MCF7_IGF
GSE7561

B1

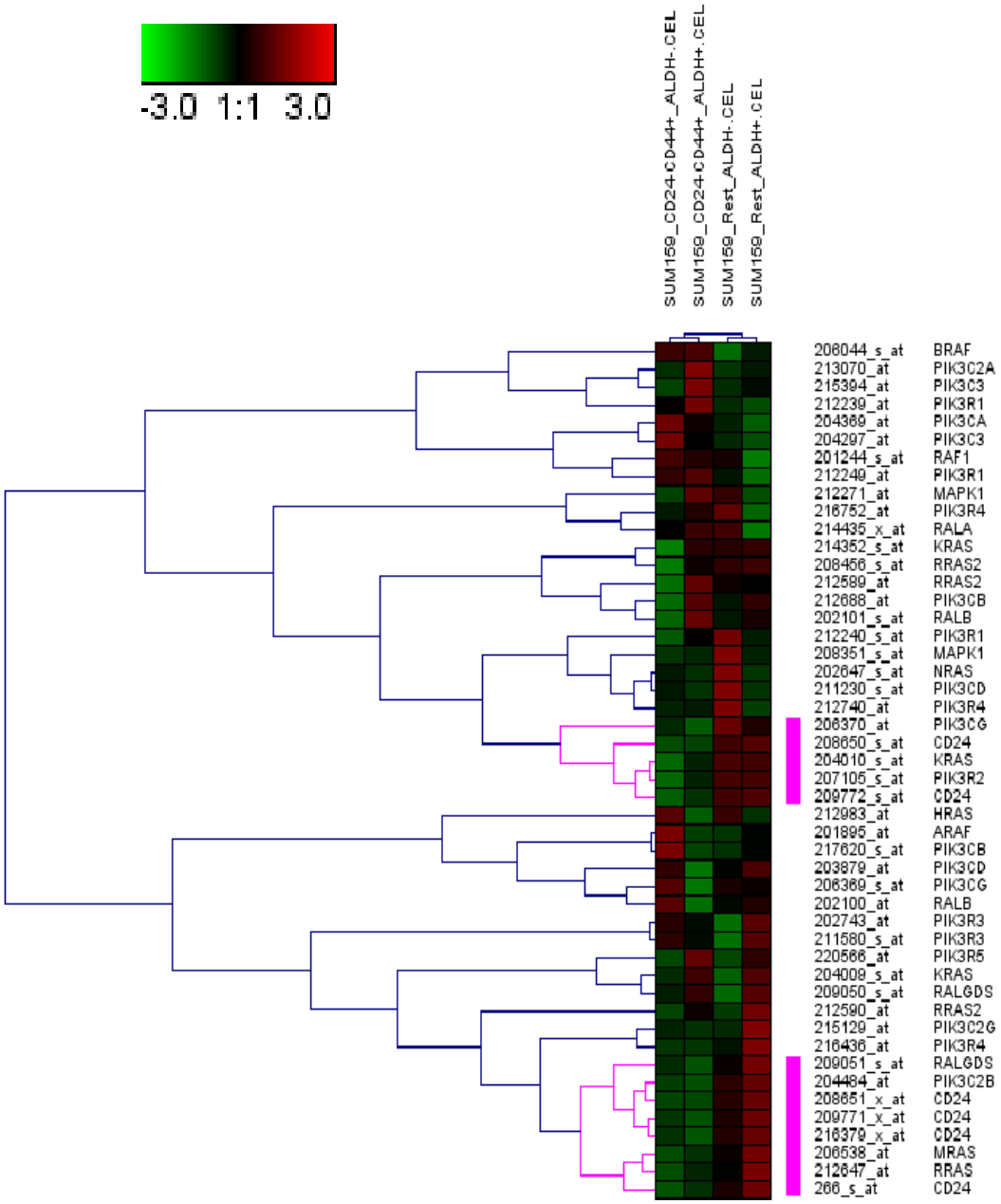

SUM149
GSE52262

B2

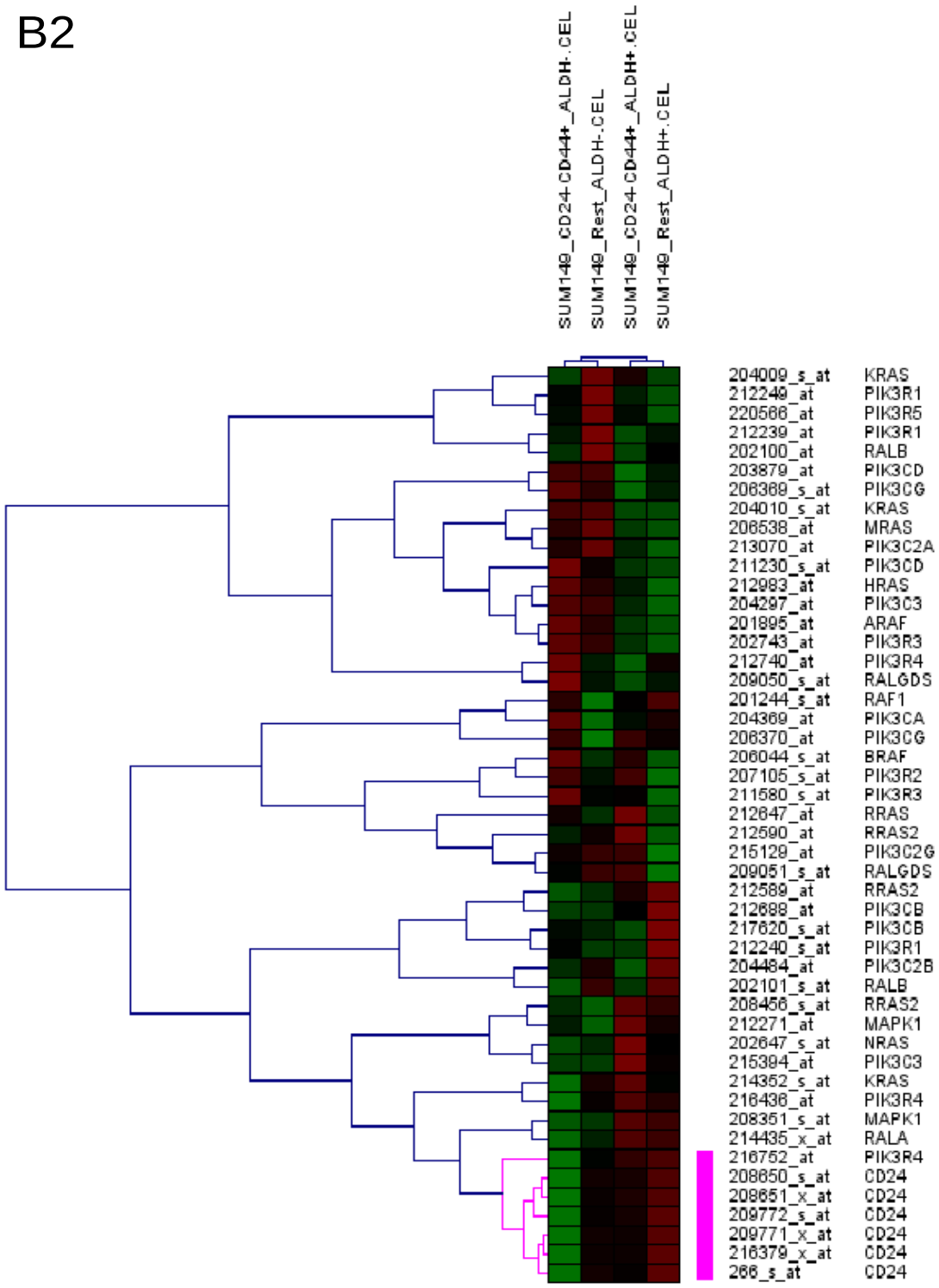

SUM159
GSE52262

B3

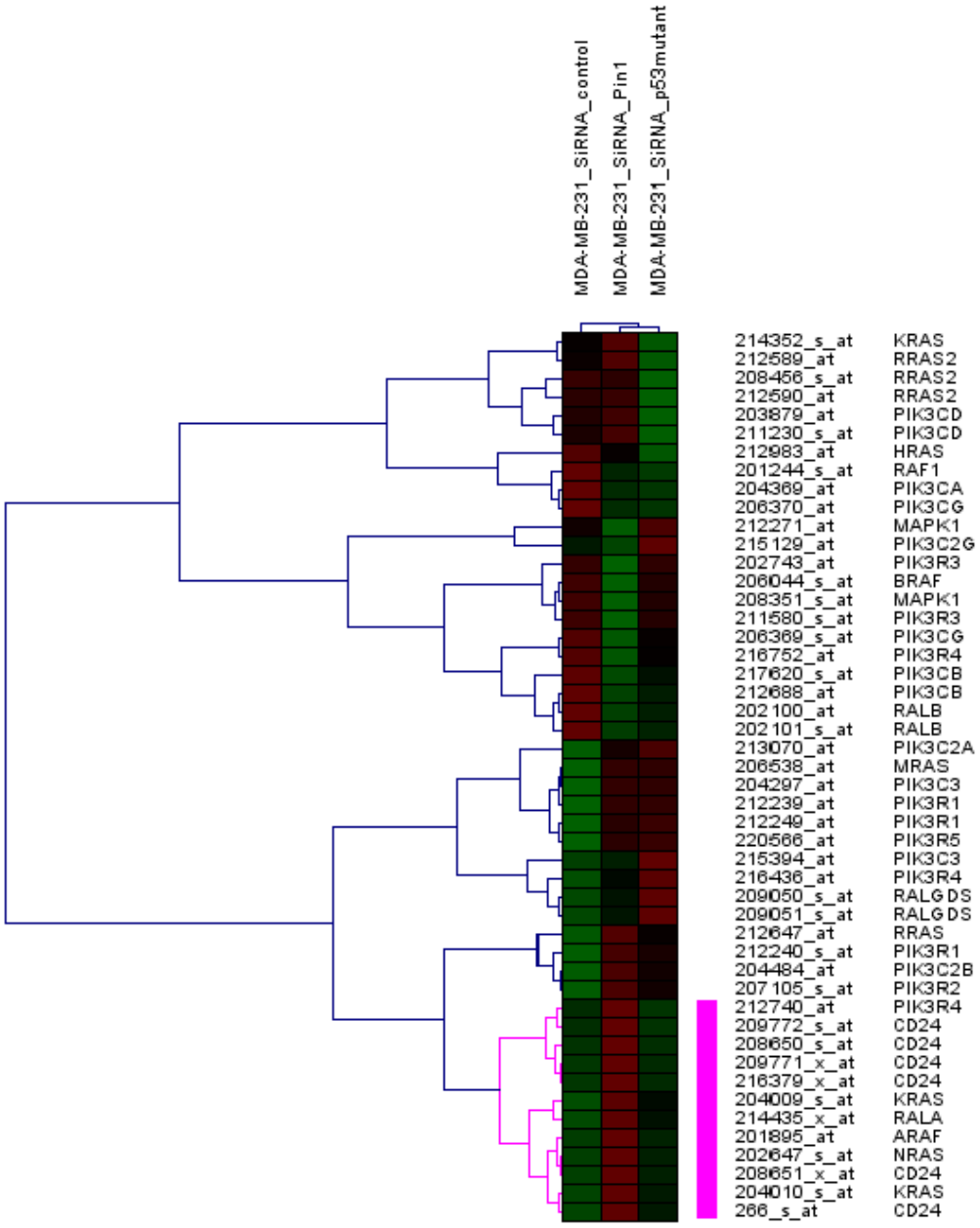

MDA-MB-231
GSE26262

B4

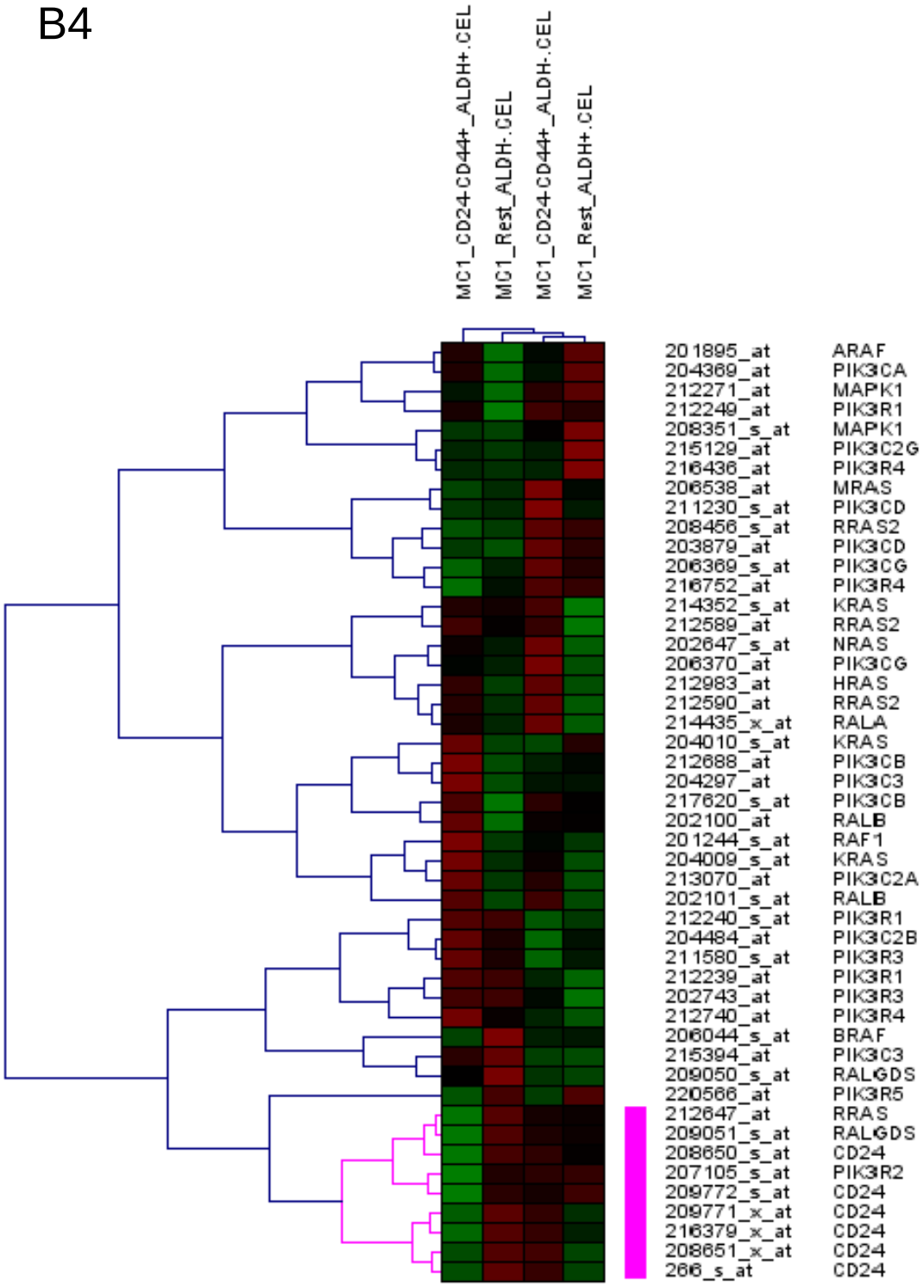

MC1
GSE52262

C1

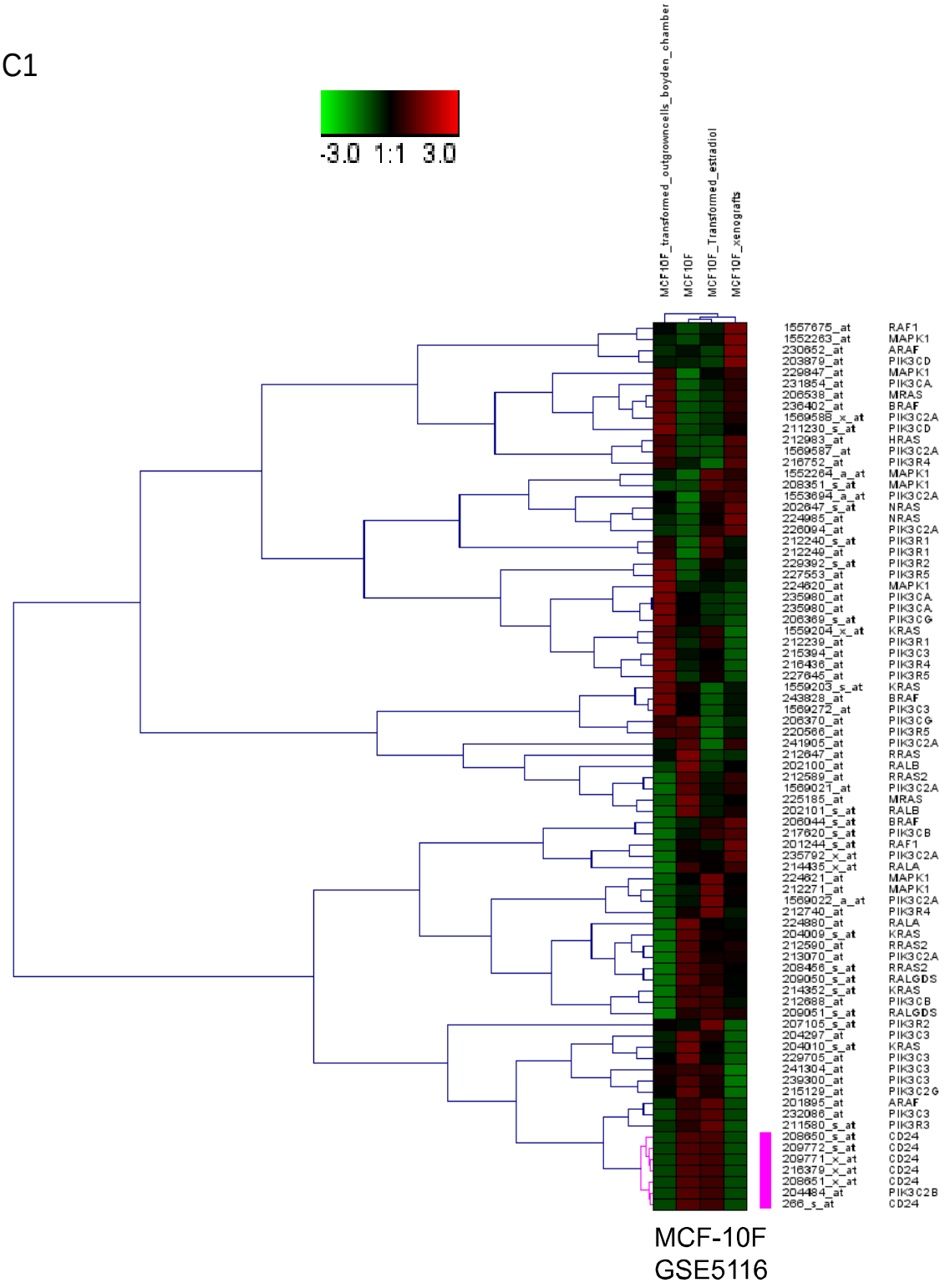

MCF-10F
GSE5116

C2

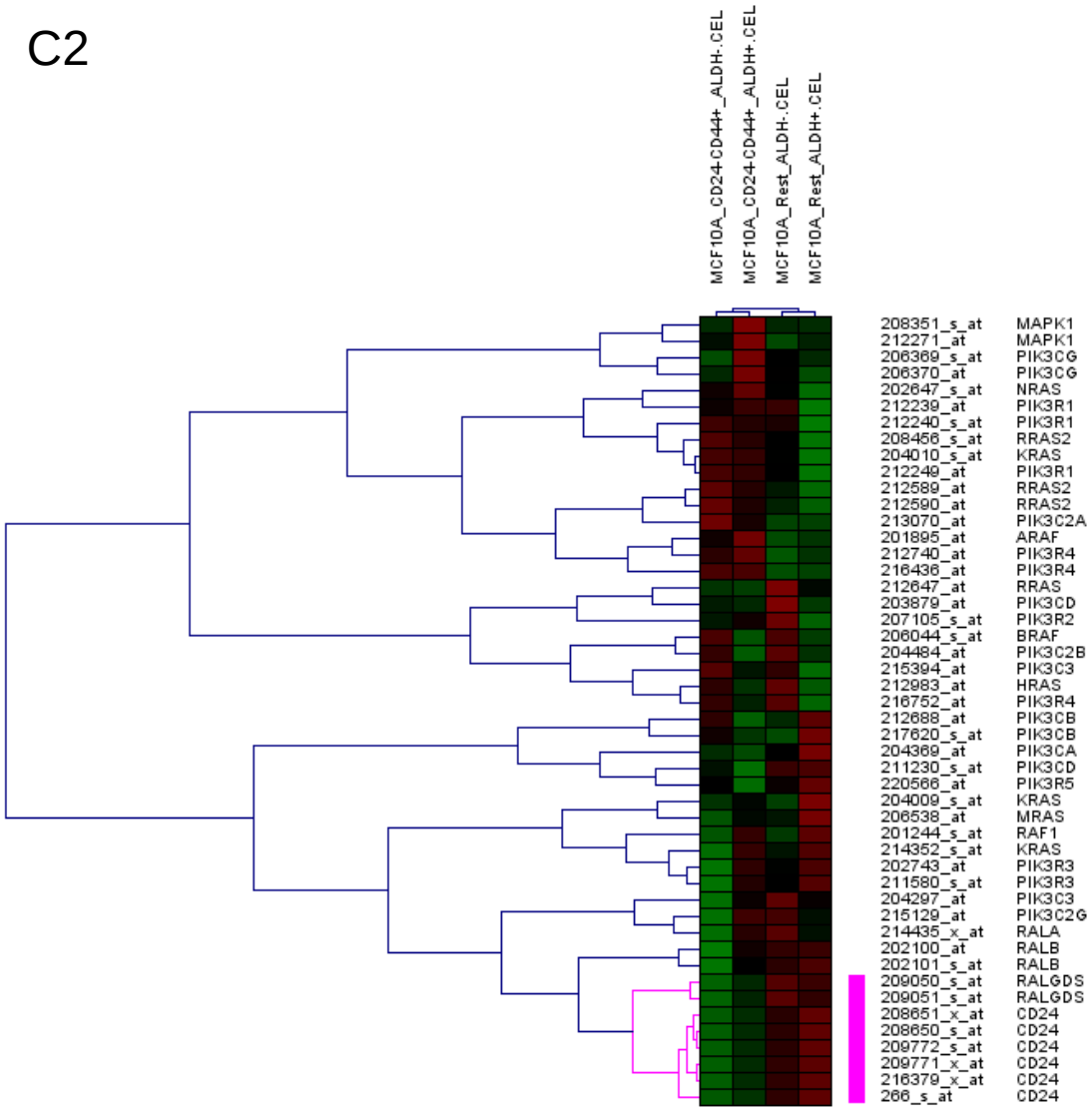

MCF-10A
GSE52262

C3

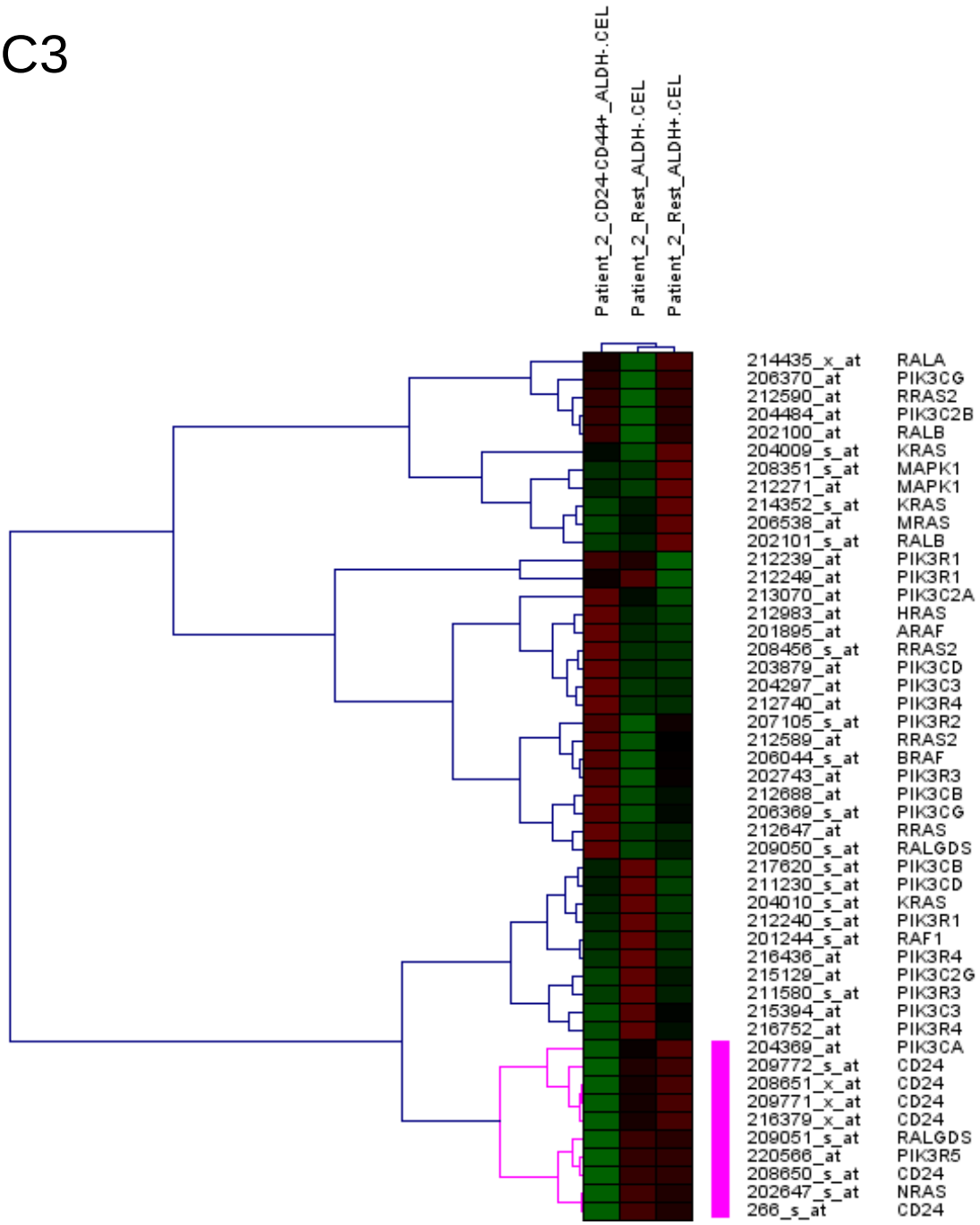

Patient (sorted normal cells)
GSE52262

Figure 4.7: Hierarchical cluster analysis of Ras pathway genes and CD24 expression in ER/PR or HER2 positive, TNBC and normal/immortalized cells. Analysis of gene expression by unsupervised hierarchical clustering by gene and sample of (A1-4) ER/PR or HER2 positive, (B1-4) TNBC and (C1-3) normal/immortalized cells or cell lines. Clusters containing any CD24 probeset are highlighted in pink. Gene expression levels, normalized to median, are coloured by expression as indicated. High gene expression is shown in red and low expression is shown in red.

Overall, based on the cluster that have similar expression with CD24, I found that ER, PR and HER-2 expressing cells tended to have the highest association of CD24 with Ras pathway genes, followed by TNBC and then normal/immortalized cells (Fig 4.8).

HCC1954 HER2-positive breast cancer cells sorted on the basis of CD24, CD44 and ALDH protein expression, demonstrated the highest association of Ras pathway genes with CD24, with all of these genes clustering with CD24 (Fig 4.8). Similarly, ER-positive MCF7 cells sorted on the basis of CD24, CD44 and ALDH protein expression, showed a highly positive correlation with Ras pathway genes with all gene families, except MAPK1, clustering with CD24 (Fig 4.8A).

In addition, with the exception of the $CD24^{-}CD44^{+}$ALDH- population, CD24 expression was generally high in MCF7 cells (Fig 4.7). However, when ER-positive MCF7 cells were treated with inhibitors or activators in a way that upregulates the Ras pathway genes, the association with CD24 was substantially reduced. In the case where MCF7 cells were treated with siRNA against ERK1 and ERK2 individually, followed by treatment with estradiol (E2), there were few Ras related genes that clustered with CD24, with only genes in the Ral/RalGDS, PIK3C and PIK3R gene families represented (Fig 4.7A3). However, knockdown of ERK1 with or without E2 treatment dramatically altered the expression profiles of the Ras pathway genes and CD24, with the combination resulting in an obvious decrease in CD24 expression levels and increase in Ras pathway gene expression (Fig 4.7A3). Similarly, MCF7 cells treated with insulin-like growth factor (IGF) upregulate Ras pathway genes resulting in an overall low percentage of Ras pathway genes clustering with CD24, with only Ras, Ral/RalGDS, and PIK3R gene

A

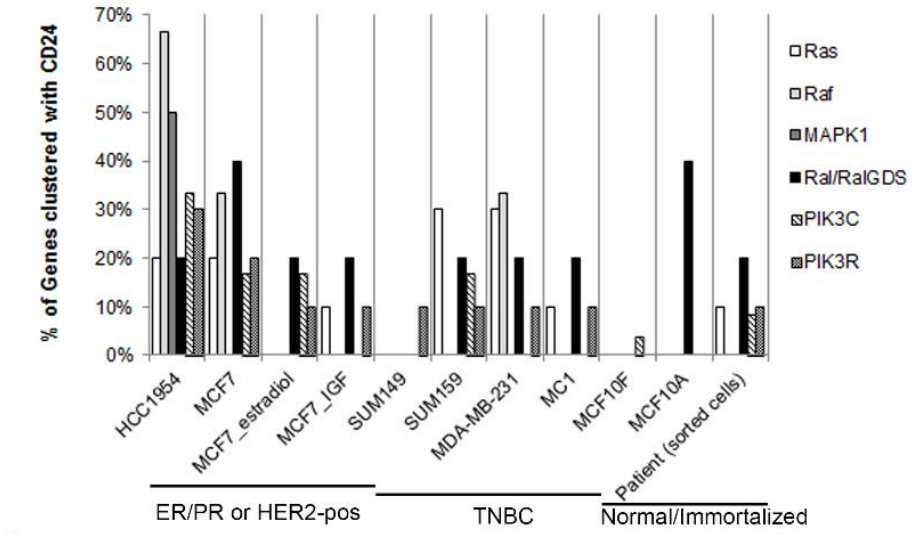
% of Genes clustered with CD24
70%
60%
50%
40%
30%
20%
10%
0%
Ras
Raf
MAPK1
Ral/RalGDS
PIK3C
PIK3R
HCC1954
MCF7
MCF7_estradiol
MCF7_IGF
SUM149
SUM159
MDA-MB-231
MC1
MCF10F
MCF10A
Patient (sorted cells)
ER/PR or HER2-pos
TNBC
Normal/Immortalized

B

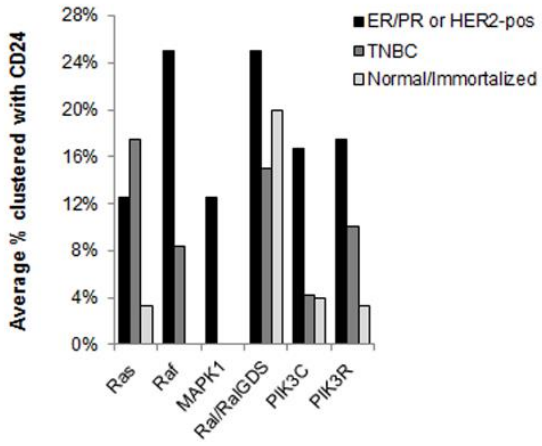
Average % clustered with CD24
28%
24%
20%
16%
12%
8%
4%
0%
ER/PR or HER2-pos
TNBC
Normal/Immortalized
Ras
Raf
MAPK1
Ral/RalGDS
PIK3C
PIK3R

Figure 4.8: Summary of meta-analysis showing clustering of Ras pathway gene probesets with CD24 from DNA microarray datasets obtained from ER/PR or HER2 positive, TNBC and normal/immortalized cells. (A) The percentage of probesets representing Ras pathway associated genes that clustered with CD24 in ER/PR or HER2 positive (HCC1954, MCF7), TNBC (SUM149, SUM159, MDA-MB-231 and MC1), normal/immortalized (MCF-10F, MCF-10A and patient (sorted cells)) cell lines is shown. (B) The average percentage of Ras pathway genes clustered with CD24 genes in ER/PR or HER2 pos, TNBC and normal/immortalized cells is shown.

families clustered with CD24 (Fig 4.8). In the untreated cells, over half of the Ras pathway genes had high expression levels and were similar to CD24, but upon treatment, CD24 levels were substantially reduced along with many, but not all, of the Ras pathway genes reduced as well (Fig 4.7A4).

Non-tumorigenic cells, including MCF-10F, MCF-10A and normal patient cells, sorted by CD44, CD24 and ALDH, gene expression showed the strongest inverse relationship between Ras pathway genes and CD24, with only four out of 6 gene families clustering with CD24 (Fig 4.8). Ral/RalGDS showed the highest direct association with CD24 in these cells but neither MAPK1 nor Raf showed any association with CD24.

Cells with the TNBC phenotype (MC1 cells derived from primary xenografts, SUM149, SUM159, and MDA-MB-231) showed an intermediate association with Ras pathway genes and CD24 compared to that seen with immortalized/normal cells or the ER/PR and HER-2 positive cells. In addition, all but the MAPK1 gene family never clustered with CD24 in TNBC group. Interestingly, in MDA-MB-231 cells that were treated with siRNA against Pin1, which is a protein that cooperates with Ras [313], a cluster of Ras pathway genes was downregulated while CD24 expression increased, suggesting that alterations in the Ras pathway can alter CD24 expression in this cell line. In a similar manner, when MDA-MB-231 cells treated with siRNA against p53, upregulation in Ras-related genes such as BRAF, MAPK1 and downregulation in CD24 expression was observed (Fig 4.7 B3).

In summary, this meta-analysis showed that the untreated ER-positive (MCF7) and HER-2 positive (HCC1954) cells had, on average, a positive association of Ras

pathway genes with CD24, while the normal and TNBC cells had fewer genes and fewer different gene families associating with CD24 (Fig 4.8B). Of note, in TNBC and normal cells, MAPK1 (ERK2) never clustered with CD24, and Ral/RalGDS clustered the most often with CD24. In addition, these data suggest that TNBC cells, sorted by BCSC markers, are more similar to normal cells than ER/PR or HER-2 positive cells, with respect to this set of genes.

4.2.2 Inhibition of Ras/MEK/ERK increases CD24 mRNA but not protein expression in MDA-MB-231 $CD24^-$ breast cancer cells.

MDA-MB-231 cells are TNBC and considered to model BCSC since the majority of the cells are $CD44^+CD24^-ALDH^+$ [79]. In addition, K-Ras is constitutively active in these cells [314, 315]. The above meta-analysis revealed an inverse correlation between CD24 and Ras pathway genes in MDA-MB-231 cells, which was enhanced by the lack of the Ras pathway associated gene, Pin1. Therefore, I reasoned that this cell line may respond to manipulations of the Ras pathway by altering CD24 levels. I first confirmed that, in comparison with MCF7 BC cells, MDA-MB-231 have a low level of CD24 mRNA expression (Fig 4.9A). To determine if inhibition of the Ras/MEK/ERK pathway was sufficient to increase CD24 expression, I treated MDA-MB-231 cells with the MEK inhibitor U0126 and analyzed CD24 mRNA expression (Fig 4.9B, C). I found that CD24 mRNA expression increased in response to inhibition of the Ras/MEK/ERK pathway, which was statistically significant when analyzed by RT-qPCR (Fig 4.9C). This suggests

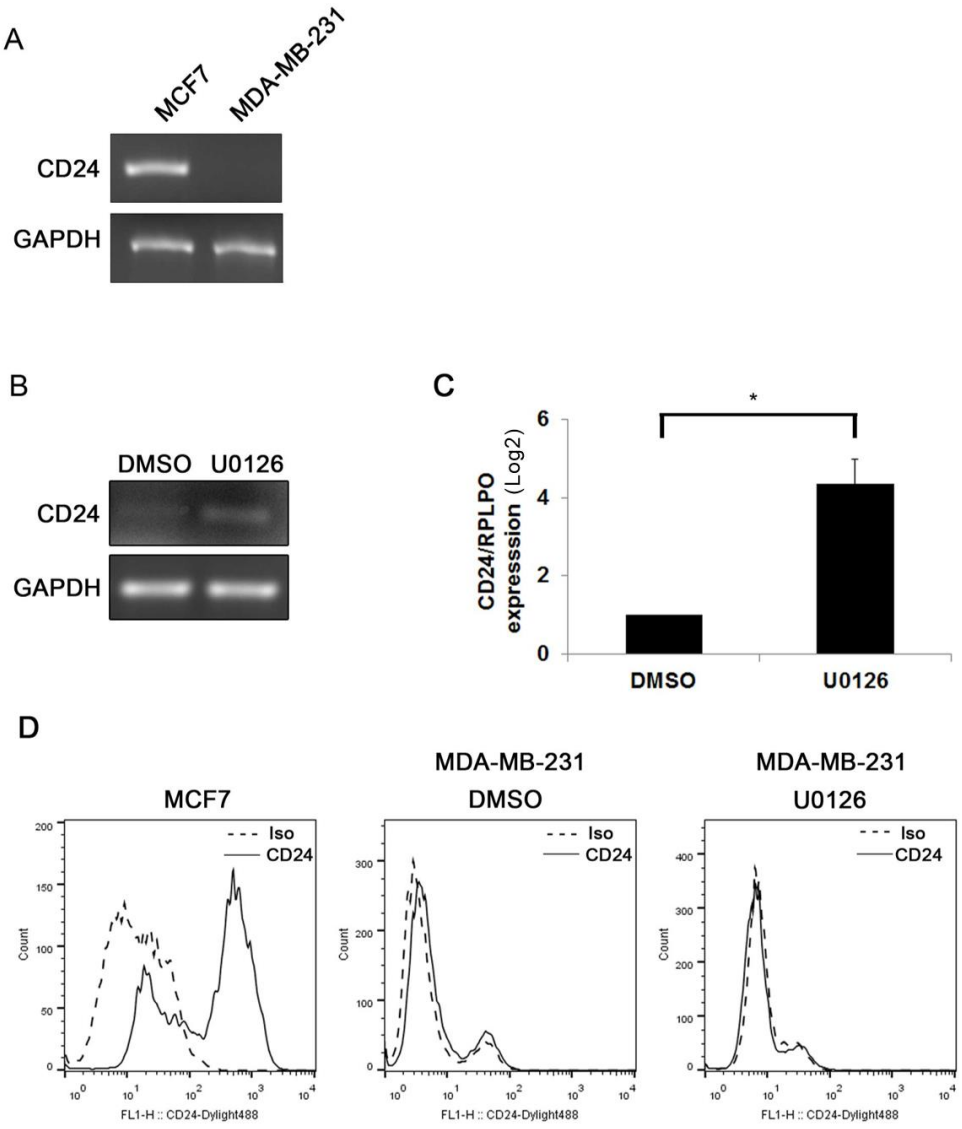
A
MCF7
MDA-MB-231
CD24
GAPDH
B
DMSO
U0126
CD24
GAPDH
C
*
CD24/RPLPO expresssion (Log2)
6
4
2
0
DMSO
U0126
D
MCF7
MDA-MB-231
DMSO
MDA-MB-231
U0126
Iso
CD24
Count
FL1-H :: CD24-Dylight488

Figure 4.9: Regulation of CD24 mRNA but not protein by inhibition of the Ras/MEK pathway in MDA-MB-231 breast cancer cells. (A) CD24 mRNA expression in MCF-7 and MDA-MB-231 breast cancer cell lines was determined by RT-PCR. (B) MDA-MB-231 cells were treated for 24 h with U0126 or the DMSO as the vehicle control and then CD24 mRNA levels determined by RT-PCR and (C) qRT-PCR. GAPDH was used as the loading control. Significance was determined by Student's T-test, n=4, *P<0.05. Mean ± s.e.m. is shown. (D) Surface CD24 protein levels were determined by FACS on MCF7 cells and MDA-MB-231 with or without treatment with U0126 for 24 h. One representative experiment of three replicates is shown.

that the Ras/MEK/ERK pathway actively suppresses CD24 mRNA expression in these cells.

I then analyzed the level of CD24 surface protein to determine if the increase in CD24 mRNA translated to increases in CD24 surface protein. Using flow cytometry, I observed that inhibition Ras/MEK/ERK was not sufficient to upregulate CD24 protein on the cell surface (Fig 4.9D). Therefore, this suggests that similar to RasV12 cells, cancer cells continue to suppress CD24 surface expression via other pathways or mechanisms.

4.2.3 Inhibition of Raf does not restore CD24 cell surface protein expression in breast cancer cells with oncogenic Ras.

Since U0126 modestly increased *CD24* mRNA levels in MDA-MB-231 BC cells but had no effect on CD24 surface protein expression, which is similar to RasV12 cells, I next determined if inhibition of Raf could restore CD24 surface protein expression as observed in RasV12 cells. I examined an additional BC cell line, SUM159 which also has constitutively active Ras and a high proportion of BCSC population [316]. T47D and MCF7 BC cell lines were used as positive controls for CD24. I evaluated the inhibition of Raf/MEK/ERK pathway by sorafenib for 24h as previously discussed using western blot analysis (see section 4.1.4) (Fig 4.10A). Although the sensitivity to sorafenib among different cell lines varied, I found that sorafenib reduced ERK phosphorylation in MDA-MB-231, SUM159, MCF7, and T47D BC cells at all concentrations examined, while Akt phosphorylation varied across the cell lines. In MCF7 and SUM159 BC cells sorafenib reduced Akt phosphorylation at all concentrations. In contrast, sorafenib treatment

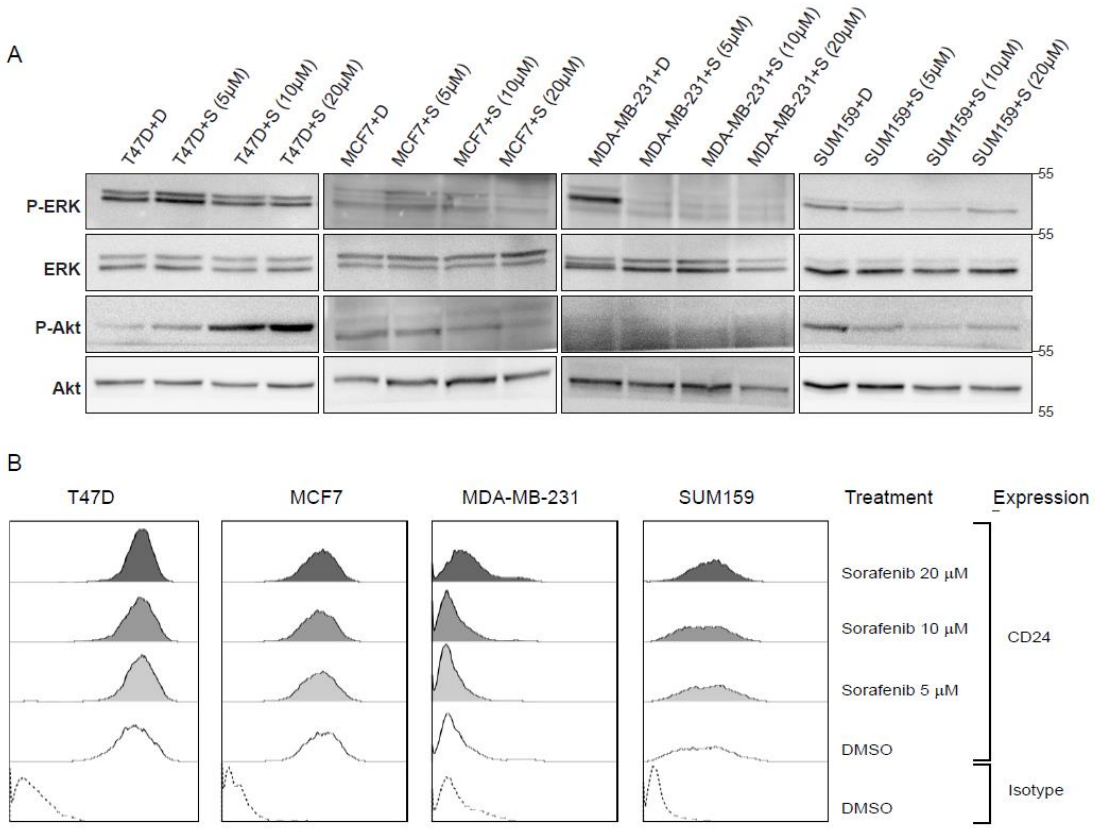

Figure 4.10: Regulation of CD24 protein by inhibition of the Ras/Raf pathway in T47D, MCF7, MDA-MB-231 and SUM159 breast cancer cells. T47D, MCF7, MDA-MB-231 and SUM159 BC cells were treated for 24 h with DMSO (D) or 5μM, 10μM and 20μM sorafenib. (A) Western blot analysis was performed to detect phosphorylated ERK (P-ERK), and phosphorylated Akt (P-Akt). Total ERK and total Akt were used as loading controls. Molecular mass standards are shown in the right of each image. One representative experiment from two replicates is shown. (B) Surface CD24 protein was determined by flow cytometry with Controls, T47D and MCF7 or MDA-MB-231 and SUM159 BC cells treated as above. One representative histogram of isotype (Iso) (dotted line) and CD24-stained cells is shown. n=2.

increased Akt phosphorylation in T47D BC cells. However, MDA-MB-231 cells have low or no activation of Akt even in control samples [317, 318] (Fig 4.10A).

I determined the effect of Raf inhibition by sorafenib on CD24 surface protein in MDA-MB-231, SUM159, MCF7 and T47D cells. I found that there was no change in the percentage of $CD24^+$ cells in the MDA-MB-231 and SUM159 BC cells after treatment with sorafenib (Fig 4.10B). Therefore, inhibition of Raf significantly increases the proportion of $CD24^+$ cells exclusively in model systems that have constitutive activation of oncogenic Ras human BC cells must have additional mutations that regulate CD24 gene expression.

4.3 Discussion

Here, I have demonstrated that expression of oncogenic Ras is sufficient to directly downregulate the expression of CD24 at the mRNA and protein levels, as well as repress promoter activity in model systems. In addition, activation of either the Raf or PI3K pathway is sufficient to downregulate CD24 expression at both the mRNA and protein levels (Fig 4.11). Surprisingly, inhibition of the Raf pathway, at the level of MEK or Raf, or the PI3K pathway, at the level of PI3K, either separately or together, was not sufficient to fully restore CD24 expression in the model system. However, inhibition of Raf directly was able to partially restore CD24 surface protein expression without affecting mRNA levels. Moreover, I have shown that cell lines with high ER/PR or HER-2 expression tend to have a positive association between CD24 and Ras pathway genes, while normal or TNBC cells have an inverse correlation of Ras pathway gene and CD24.

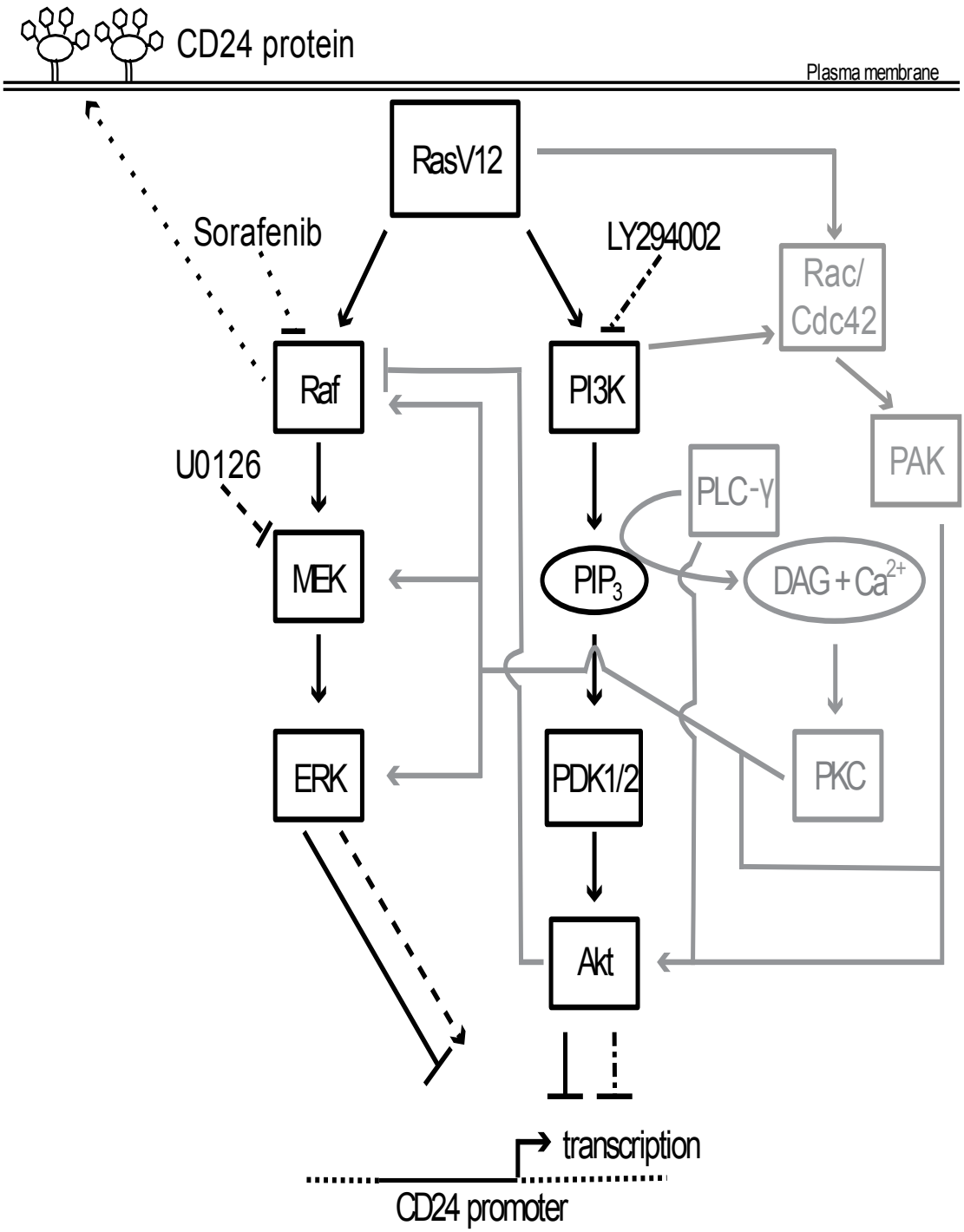
CD24 protein
Plasma membrane
RasV12
Sorafenib
LY294002
Rac/
Cdc42
Raf
PI3K
PAK
U0126
PLC-γ
MEK
PIP3
DAG + Ca2+
ERK
PDK1/2
PKC
Akt
transcription
CD24 promoter

Figure 4.11: Schematic representation of the regulation of CD24 by Ras/Raf and Ras/PI3K pathways. Rectangles represent proteins and ovals represent lipids and second messengers. Protein activation is indicated by solid arrows and inhibition indicated by solid lines with blunt ends. Potential mechanisms for cross-talk are shown in grey. The effect of U0126 and LY294002 on MEK and PI3K and on *CD24* transcription is indicated by dashed lines and dash dot dash lines, respectively. The effect of sorafenib on Raf and on CD24 surface protein expression is indicated by dotted lines. The *CD24* promoter is indicated with a solid line flanked by genomic DNA depicted with a dotted line. The transcription start site is indicated by a bent arrow. Abbreviations not in the main text: PLC-γ, phospholipase C- γ; PIP_3, phosphotidylinositol-3,4,5-trisphosphate; DAG, diacylglycerol; PKC, protein kinase C; PAK, p21-activated kinase; Cdc42, cell division cycle 42.

Interestingly, inhibition of downstream targets of Ras was not sufficient to increase $CD24^+$ cells in TNBC population. Therefore, oncogenic Ras uses additional mechanisms to regulate CD24 surface protein expression in both model system and TNBC cell lines.

Experimental analysis of the *CD24* promoter region revealed that repression of *CD24* promoter activity by oncogenic Ras was primarily mediated by the 189 bp region between -168 and -357. In addition, a 112 bp region between -357 and -469 also appears to contribute to this repression. Therefore, I have identified a novel negative regulatory region between -168 and -357 that may act independently or in cooperation with additional elements between -357 and -469 to regulate *CD24* transcription in response to oncogenic Ras.

Computational analysis of the 112 bp region revealed more than 300 potential transcription factor binding sites, including 5 sites that can bind TWIST transcription factors. However, deletion of these sites did not affect the repression of *CD24* promoter by Ras (Fig 4.2C-D). Moreover, 5 TF binding sites on the CD24 promoter region were predicted by JASPAR database and are potentially regulated by Ras directly or indirectly (Table 4.1). While regulation of the *CD24* promoter by methylation has been reported in diseased conjunctiva [165] and glioblastoma cell lines [164], there was no evidence of promoter methylation of *CD24* in breast cancer cell lines or in patient tumors in previous study [7]. Therefore, further work is necessary to validate TFs predicted from computational analysis and the other 189 bp region in order to identify the precise regulatory mechanism used by Ras to repress *CD24* transcription.

To narrow down which of the Ras-activated pathways represses CD24 expression I made use of the Ras effector mutants and found that activation of either the PI3K or the Raf pathway is sufficient to decrease *CD24* mRNA expression but the Raf pathway is the major repressor of CD24 expression at both the mRNA and protein levels. Unexpectedly, when I performed the complementary loss-of-function experiments using either the MEK inhibitor U0126 or the Raf inhibitor sorafenib in the presence or absence of the PI3K inhibitor LY294002, we were unable to restore *CD24* mRNA expression to the level of the control cells. Of note, U0126 treatment partially restored CD24 mRNA levels in RasV12 cells, suggesting that this partial restoration is common to our model mouse cell line. Treatment with U0126 caused a 13-fold increase in RasV12, which is still 100-fold lower than the mRNA levels present in control cells, and therefore may be responsible for the modest but not statistically significant increase in CD24 surface expression. In contrast, sorafenib treatment did not alter *CD24* mRNA levels. Inhibition of PI3K alone did not alter *CD24* mRNA levels but in combination with MEK inhibition prevented the U0126-mediated increase in *CD24* mRNA expression. Thus, these data suggest that the inhibition of the PI3K pathway could potentially activate a repressor or inhibit an activator of *CD24* mRNA expression to block the effects of U0126 treatment. Consistent with this hypothesis, significant cross-talk between the PI3K and Raf pathways has been shown, including the ability of Akt to inhibit Raf. As we did not observe an increase in ERK phosphorylation, the possible relief of Akt-mediated inhibition of Raf did not override the U0126-mediated block in MEK activation. Thus, inhibition of the PI3K

pathway may relieve the Akt-mediated inhibition of Raf and promote Raf mediated suppression of CD24 (Fig 4.11).

Interestingly, sorafenib treatment significantly increased the proportion of $CD24^+$ RasV12 cells while U0126 treatment significantly increased $CD24^+$ cells only in the control cell population. This suggests that regulation at the level of Raf regulates CD24 expression in oncogenic conditions, while MEK can regulate CD24 expression in response to basal growth conditions. In both situations ERK phosphorylation is equally inhibited, therefore. the regulation of CD24 surface expression cannot be downstream of ERK activation. Together, these data demonstrate that the regulation of CD24 surface protein expression is regulated in a Raf-dependent, MEK-independent manner in model system.

Meta-analysis revealed that Ras pathway genes tended to cluster with CD24 in ER/PR and HER-2 positive. In contrast, both TNBC and normal cells had low percentage of Ras-associated genes that correlated with CD24. In particular, MAPK1 did not correlate with CD24 in any of the TNBC or normal cells. The Ral/RalGDS genes showed the highest correlation with CD24 overall, which supports previous observations that the Ral pathway can positively regulate CD24 expression [319]. In agreement with these data, I found that the activation of Ral pathway was not sufficient to downregulate CD24 mRNA expression. Overall, this meta-analysis supports the apparent paradox that CD24 is pro-proliferative in some cancers but anti-proliferative in other cancers [82], and supports previous expression profile analysis of breast cancer cells showing that the

mRNA expression levels of oncogenic Ras pathway genes is higher in $CD24^-$ cells isolated from populations of primarily $CD24^+$ cells [320].

Next, I found that MDA-MB-231 that carries the oncogenic G13D K-Ras mutation [314, 315], and SUM159 cells that carry both H-Ras and PI3CA mutation have low CD24 expression. Furthermore, overexpression of oncogenic H-Ras as part of the sequential transformation of primary human mammary epithelial cells resulted in the downregulation of CD24 surface expression [85]. Therefore, the downregulation of CD24 expression at the mRNA and surface protein levels in response to oncogene activation appears to be common to different oncogenic Ras isoforms but, according to the meta-analysis, likely restricted to TNBC-like cells.

Similarly, U0126 treatment did not increase surface expression of CD24 in MDA-MB-231 cells even though there was a significant 4-fold increase in mRNA expression. In contrast, sorafenib treatment Raf inhibition had no effect on $CD24^+$ cells among MDA-MB-231 and SUM159 cell populations. These data suggest that downregulation of CD24 is dependent on more than Raf or MEK in human BC cells. In BC cells where not only Ras but also other oncogenes such as PIK3CA and BRAF and tumor suppressor genes such as TP53 and CDKN2A, are mutated [18]. In addition to constitutive activation of oncogenes or constitutive suppression of tumor suppressor genes, there is inter dependencies of the proteins in these pathways. However, in a recent study it is shown that Ras, PI3K, p53, and cell cycle pathways consists of mutually exclusive pairs where one alteration is sufficient to functionally alter the other pathways [321]. Furthermore, these data suggest that additional pathways remain activated in the presence of the Raf,

MEK, or PI3K inhibition that can continue to repress CD24 expression. For example, as depicted in figure 4.11, both p21 protein (Cdc42/Rac)-activated kinase (PAK) and protein kinase C (PKC) can positively regulate the Raf/MEK/ERK pathway at multiple levels to bypass Raf or MEK inhibition [181, 322, 323].

These inhibitor experiments, as well as our observation that there is a reduction in CD24 cell surface protein expression but not mRNA expression in RasV12G37 cells, strongly suggest that the downregulation of CD24 mRNA and surface expression are not mediated by the same mechanisms. Moreover, CD24 has substantial post-translational modifications, including protein cleavage, addition of the GPI-anchor, and major O- and N-linked glycosylations, that occur prior to surface expression [150]. Thus, the Ras/Raf or the Ras/Ral pathways may also regulate post-translational modification or trafficking. The interaction of Raf-1 with the actin cytoskeleton has been shown to be necessary for efficient activation of MEK/ERK [324], but no Raf-mediated MEK-independent regulation of protein trafficking has been reported. On the other hand, Ral is well known to regulate vesicle trafficking [180]. While Ral can be activated in a Ras-independent manner [325], it is not known if Ral can be activated in a Raf-dependent manner. Alternatively, alteration of GPI-anchor biosynthesis by Ras, as previously identified in *Saccharomyces cerevisiae* [326], may be responsible for altering CD24 surface expression. Therefore, future work will be necessary to unravel the precise mechanism that regulates CD24 surface protein expression by the Ras/Raf pathway.

CD24 expression is dynamically regulated throughout the development of B and T lymphocytes, dendritic cells, neurons, and adipocytes [272, 281, 327]. Moreover, CD24

expression in some normal cell types is associated with proliferation or differentiation [272, 328], while in others it is associated with apoptosis [329]. Therefore, transformation of a particular cell type at a particular cell stage may dictate if CD24 promotes or inhibits proliferation. Previously, it was found that overexpression of oncogenic H-Ras as the last part of the sequential transformation of primary human mammary epithelial cells or in immortalized MCF10A cells resulted in an epithelial to mesenchymal transition (EMT) concomitant with the downregulation of CD24 surface expression [85]. Here, I have found that the expression of oncogenic Ras in mouse embryonic fibroblasts and BC cells, which are already mesenchymal, represses CD24 mRNA and protein expression, and promoter activity. Therefore, it may be the mesenchymal phenotype that predisposes a cell to lose CD24 expression in response to Ras transformation while other cell types will gain or retain CD24 expression dependent on their epithelial vs. mesenchymal status.

Here, I have targeted both Raf/MEK and PI3K/Akt pathways to relieve the CD24 suppression caused by Ras activation. Unlike RasV12 cells, cancer cells find an alternative to downregulate CD24 surface protein expression, even after inhibiting Raf with sorafenib. This suggests that cancer cells can alter the signaling pathways which are favorable for their survival and proliferation. Moreover, this indicates suppression of CD24 expression is important for cancer cells to survive from sorafenib treatment. In the future, a more detailed understanding of CD24 regulation by oncogenic Ras is required in order to increase CD24 protein expression and manipulate the size of the BCSC population to improve therapeutic response of breast cancer patients. This strategy would decrease the percentage of BCSC in the tumor and therefore reduce the ability of the

tumor to be radiation-resistant or initiate secondary tumor formation. These data clearly demonstrate that the oncogenic Ras-mediated suppression of CD24 expression is regulated at multiple levels.

Chapter 5. The effect of extrinsic factors on breast cancer progression

Several 2D co-culture studies have shown that adipocytes or medium from adipocyte co-cultures enhances BC progression, invasion and migration [61, 132, 208, 235]. However, the laminin-rich ECM modeled by matrigel can provide additional insight into the microenvironment of the normal mammary gland [17, 18]. Adipocytes can induce the expression of mesenchymal markers and promote invasion of BC cells in a Transwell culture system, suggesting an increase in EMT [12]. However, the role of adipocytes in colonization or induction of epithelial phenotype in mesenchymal cells is unexplored. Here, I investigated the effects of adipocytes on TNBC progression using a novel 3-dimensional (3D) co-culture system, which better mimics the tumor microenvironment and models both EMT and MET more accurately than 2D culture systems [135, 330].

5.1 Adipocytes cause mesenchymal BC cells grown in 3D to adopt more epithelial type structures with little effect on epithelial BC cells.

I first determined if co-culturing adipocytes with the mesenchymal or partly mesenchymal cells, MDA-MB-231, Hs578t and SUM159 cells or epithelial MCF7 cells grown in 3D cultures affected the structure of the BC cell lines. I found that adipocytes significantly increased the number of grape-like, and round/mass-like structures formed by MDA-MB-231 and Hs578t cells (Fig 5.1A-B). SUM159 cells have a stellate morphology in 2D culture [331] that changes to a mixed morphology in 3D culture with more round/grape like structures, as compared to MDA-MB-231 and Hs578t cells for

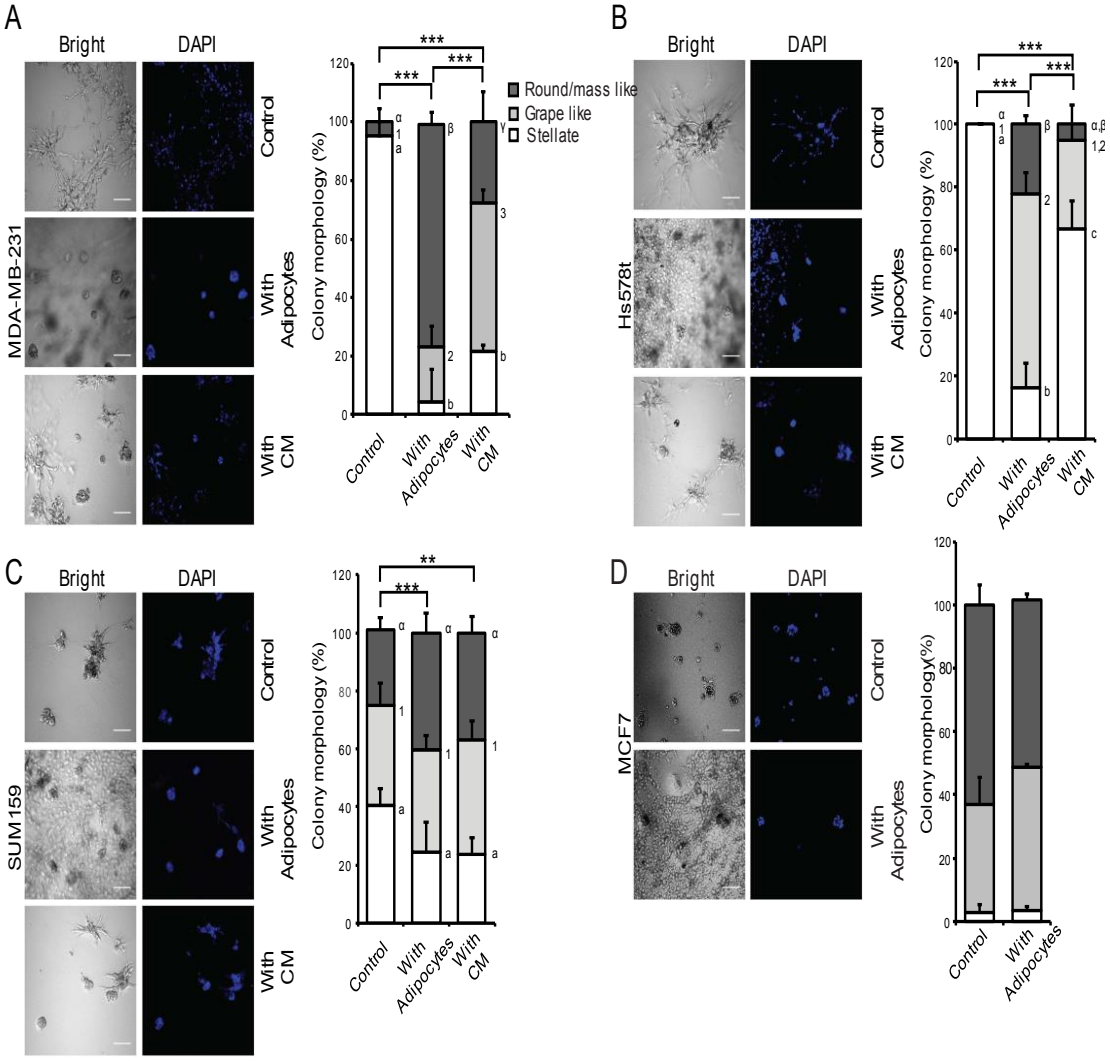
A
Bright
DAPI
Control
With Adipocytes
With CM
MDA-MB-231
Colony morphology (%)
Round/mass like
Grape like
Stellate
Control
With Adipocytes
With CM
B
Hs578t
C
SUM159
D
MCF7

Figure 5.1: Adipocytes alter the characteristic morphology of mesenchymal but not epithelial BC cell lines grown in 3D. Representative images of (A) MDA-MB-231 cells, (B) Hs578t cells, (C) SUM159 cells, and (D) MCF7 cells grown in the 3D co-culture system without adipocytes, with adipocytes, or with adipocyte conditioned medium (CM). To the right of each image, the total percentage of structure shapes is shown as mean ± SD calculated from 3 biological replicates. Overall significance of the proportion of colony shapes between the treatments was determined by χ^2 analysis, **P<0.01, ***P<0.001. If significant by χ^2, differences between the conditions for each shape was determined using one-way ANOVA with Tukey HSD post hoc analysis. Different letters or symbols represent statistically different groups ^{a,b,c}P<0.05 for stellate, ^{1,2,3}P<0.05 for grape-like, and $^{\alpha,\beta,Y,\theta}$P<0.01 for round/mass-like.

example. This mixed morphology was minimally affected by co-culture with adipocytes (Fig 5.1C). MCF7 cells form a cobblestone-like morphology in 2D culture that changes to round/mass-like morphology in 3D culture [332]. I found that adipocytes had no significant effect on the morphology of MCF7 cells in the co-culture system (Fig 5.1D).

I next analyzed if these morphological changes are induced by a secretory mediator released by adipocytes cultured with ECM or via a physical interaction with the adipocytes. I focused only on cell lines where an adipocyte-induced effect was seen. I found that adipocyte CM induced the loss of stellate and the gain of grape-like structures in MDA-MB-231 and Hs578t cultures, along with an intermediate and non-significant increase in round/mass-like structures (Fig. 5.1A, B). Similar to adipocytes, CM had no substantial effect on the specific colony morphology of SUM159 cells in 3D cultures (Fig. 5.1C).

5.2 Adipocytes have a partial effect on expression of mesenchymal to epithelial transition markers in MDA-MB-231 and Hs578t cells

I next assessed the use of IF to specifically detect the expression of EMT protein markers in the 3D co-cultures. I examined expression of Claudin-7, ZO-1, and E-cadherin, which are epithelial markers, and vimentin, a mesenchymal marker in the presence and absence of adipocyte co-culture [202].

As expected, the MDA-MB-231 and Hs578t cells grown in the absence of adipocytes had high vimentin and low E-cadherin, ZO-1 and Claudin-7 expression. MCF7 cells had high expression of epithelial markers and low expression of vimentin,

whereas, SUM159 cells had high E-cadherin, ZO-1, Claudin-7 and vimentin expression (Fig 5.2). I observed that adipocytes induced a significant gain in the expression of both E-cadherin and Claudin-7 in MDA-MB-231 and Hs578t cells (Fig 5.2A-D). In addition, Hs578t showed a significant reduction in vimentin expression (Fig. 5.2C-D). Significant changes to ZO-1 were not observed in any of the cell lines when co-cultured with adipocytes. EMT markers were not significantly altered in either SUM159 or MCF7 cells (Fig 5.2E-H). When cultured with adipocyte CM, no significant changes in EMT biomarker expression were observed in any of the cells (Fig 5.2). Together, these data suggest that mature adipocytes promote a partial MET in mesenchymal MDA-MB-231 and Hs578t cells that is not fully recapitulated by secretory mediator.

5.3 Adipocytes have a partial effect on BC stem cell biomarkers but no effect on proliferation markers

Similarly, I analyzed the effect of adipocytes on the presence of BC stem cells (BCSCs) as indicated by $CD44^{high}/CD24^{low}$ expression, biomarkers known to correlate with the abundance of BCSCs in cell culture [18]. I found that adipocytes and adipocyte CM increased CD24 levels in MDA-MB-231 cells with no change observed in any of the other cell lines (Fig 5.3). Thus, mature adipocytes induce the gain of CD24 but this is not likely to be associated with the BCSC phenotype. Moreover, the CM-induced increase of CD24 expression indicates that a secretory factor promotes this increase.

I next analyzed the effect of adipocytes on expression of the Ki67 proliferation marker. I found that there was no significant change in Ki67 expression levels in any of

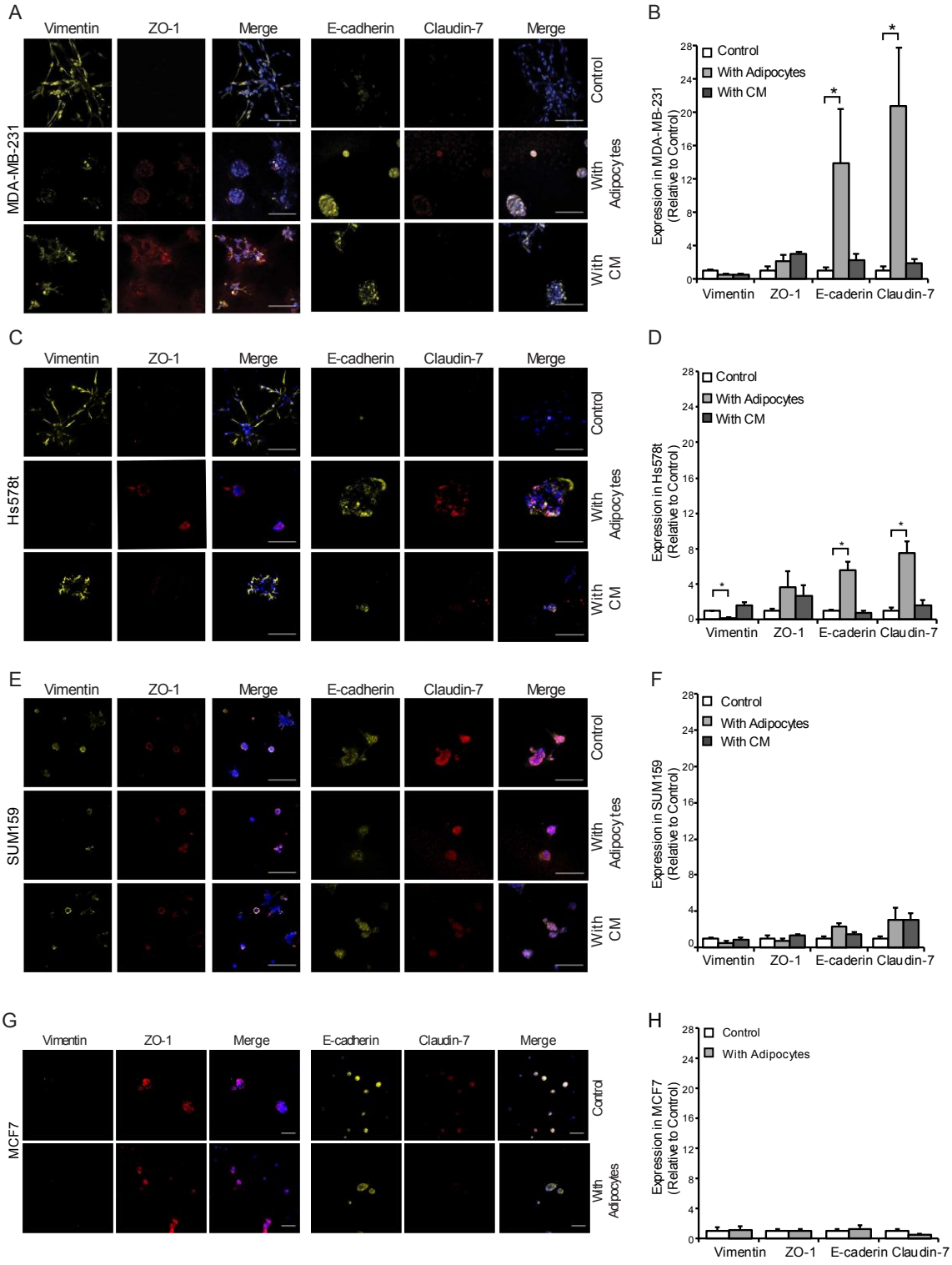
A
Vimentin
ZO-1
Merge
E-cadherin
Claudin-7
Merge
MDA-MB-231
Control
With Adipocytes
With CM
B
Control
With Adipocytes
With CM
Expression in MDA-MB-231 (Relative to Control)
Vimentin
ZO-1
E-caderin
Claudin-7
C
Hs578t
D
Expression in Hs578t (Relative to Control)
E
SUM159
F
Expression in SUM159 (Relative to Control)
G
MCF7
H
Expression in MCF7 (Relative to Control)

Figure 5.2: Adipocytes partially enhance MET of mesenchymal BC cells in 3D culture with little to no effect on epithelial BC cells. Representative images of (A) MDA-MB-231 cells, (C) Hs578t cells, (E) SUM159 cells and (G) MCF7 cells cultured with or without adipocytes or CM and co-stained with anti-vimentin, anti-ZO-1, and DAPI (left panel), or with anti-E-cadherin, anti-Claudin-7 and DAPI (right panel) (scale bar=50μm). The average protein expression in (B) MDA-MB-231 cells, (D) Hs578t cells, (F) SUM159 cells and (H) MCF7 from 5 images per replicate from different fields of view for the BC cells was normalized to DAPI and analyzed relative to control cultures. Significance was determined using Kruskal-Wallis test on ranks compared to control. *$P<0.05$, mean ± SD are shown from n=3.

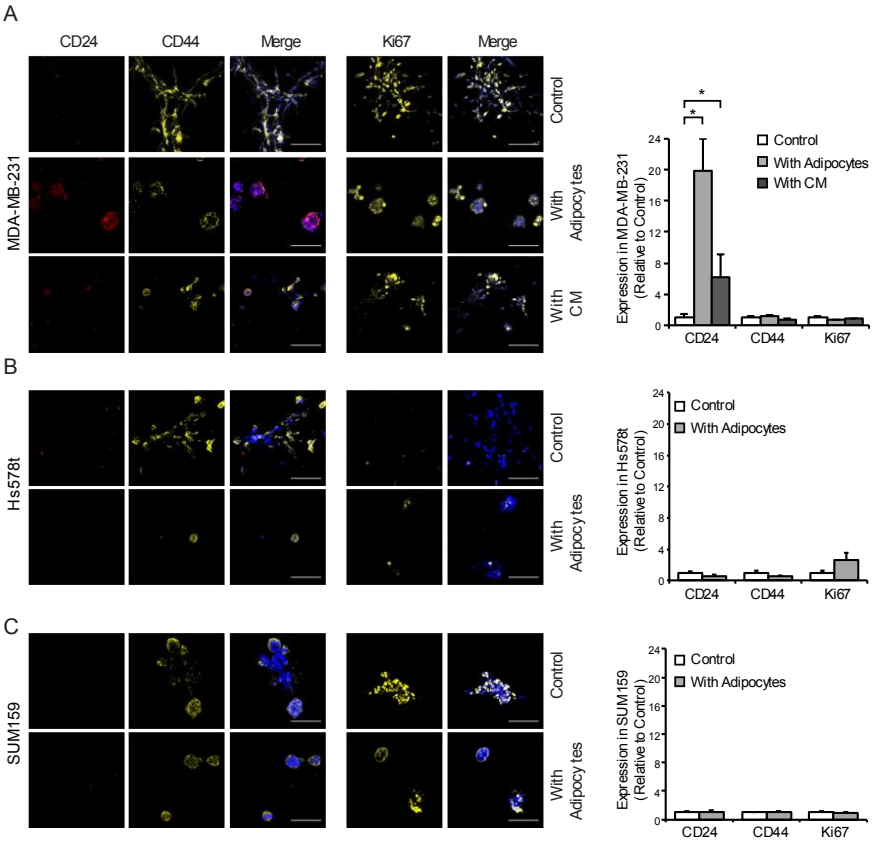

Figure 5.3: Adipocytes increase CD24 in MDA-MB-21 cells with no effect on CD44 or the Ki67 proliferation marker in any cell line. Representative images of (A) MDA-MB-231 cells, (B) Hs578t cells and (C) SUM159 cells in the presence or absence of adipocytes and conditioned medium co-stained with anti-CD24, anti-CD44, and DAPI (left panel), or co-stained with anti-Ki67 and DAPI (right panel) (scale bar=50µm). To the right of each image, the average protein expression of 5 images per replicate from different fields of view for the BC cells was normalized to DAPI and analyzed relative to control cultures. Significance was determined using Kruskal-Wallis test on ranks compared to control. *P<0.05, n=3.

the co-culture conditions tested (Fig 5.3).

5.4 The change in morphology or MET of mesenchymal BC cells is specific to mature adipocytes

To determine if I could apply this model to differentiate the effects caused by other cell types on the BC cell lines, I examined the effect of undifferentiated pre-adipocytes co-cultured with BC cell lines, focusing on cell lines that were affected by adipocytes. I found that incubation with undifferentiated pre-adipocytes had a partial effect on the morphology of the cell lines that was much less dramatic than seen with mature adipocytes (Fig 5.4). Similarly, I analyzed EMT markers expression in the BC cell lines in the presence of pre-adipocytes and found no effect on any of the cell lines (Fig. 5.5). Since MDA-MB-231 were the only cells with changes to CD24, we analyzed the effect of pre-adipocytes on this line only for stemness and proliferation makers and found that pre-adipocytes caused no significant change in CD24, CD44 or Ki67 expression (Fig 5.5G, H).

5.5 LD size is decreased in 3D co-cultures

To determine if I was able to analyze the adipocytes, which are located beneath the Matrigel layer, I stained adipocyte LD with the fluorescent lipophilic dye BODIPY 493/503. Using confocal microscopy, I was clearly able to image and analyze both the size and number of LDs. I observed that the number of LDs did not significantly change in the presence of any of BC cell line (MDA-MB-231: P=0.142, Hs578t: P=0.429, SUM159: P=0.999, MCF7: P=0.052) (Fig 5.6B). However, adipocytes displayed an

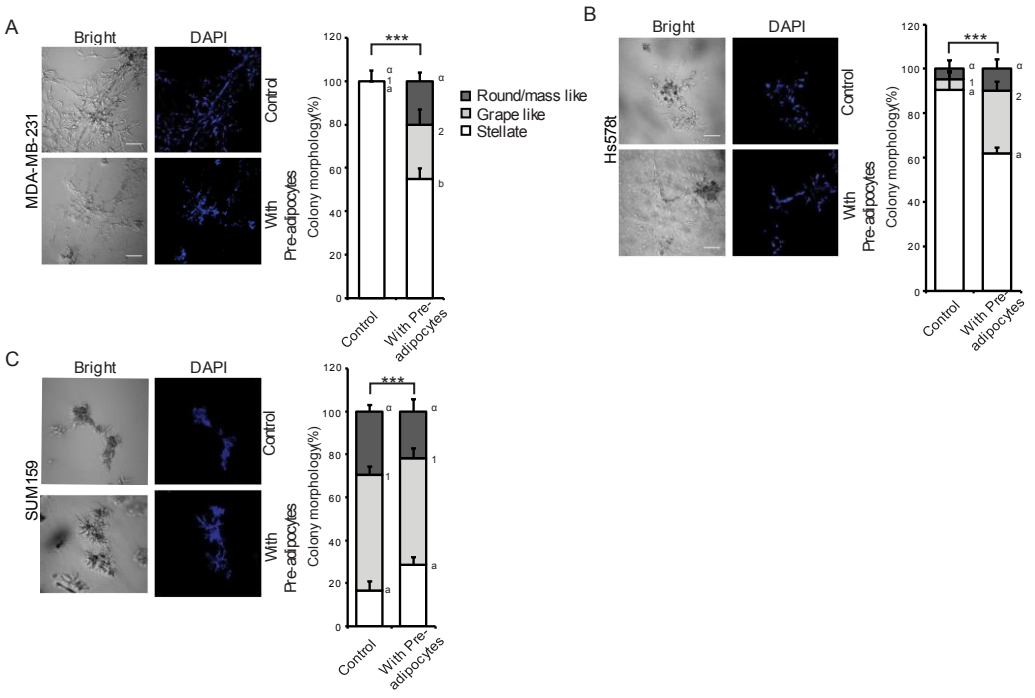

Figure 5.4: Pre-adipocytes have a partial effect on morphology of BC cells.

Representative images of (A) MDA-MB-231 cells, (B) Hs578t cells and (C) SUM159 cells grown in the 3D co-culture system in the presence or absence of pre-adipocytes (Scale bar=100μm). To the right of each image, the total percentage of structure shapes as mean ± SD are shown from 3 biological replicates. Overall significance of the proportion of colony shapes between the treatments was determined by χ^2 analysis, **P<0.01, ***P<0.001. If significant by χ^2, differences between the conditions for each shape was determined using one-way ANOVA with Tukey HSD post hoc analysis. Different letters or symbols represent statistically different groups ^{a,b,c}P<0.05 for stellate, ^{1,2,3}P<0.05 for grape-like, and $^{\alpha,\beta,Y,\theta}$P<0.01 for round/mass-like.

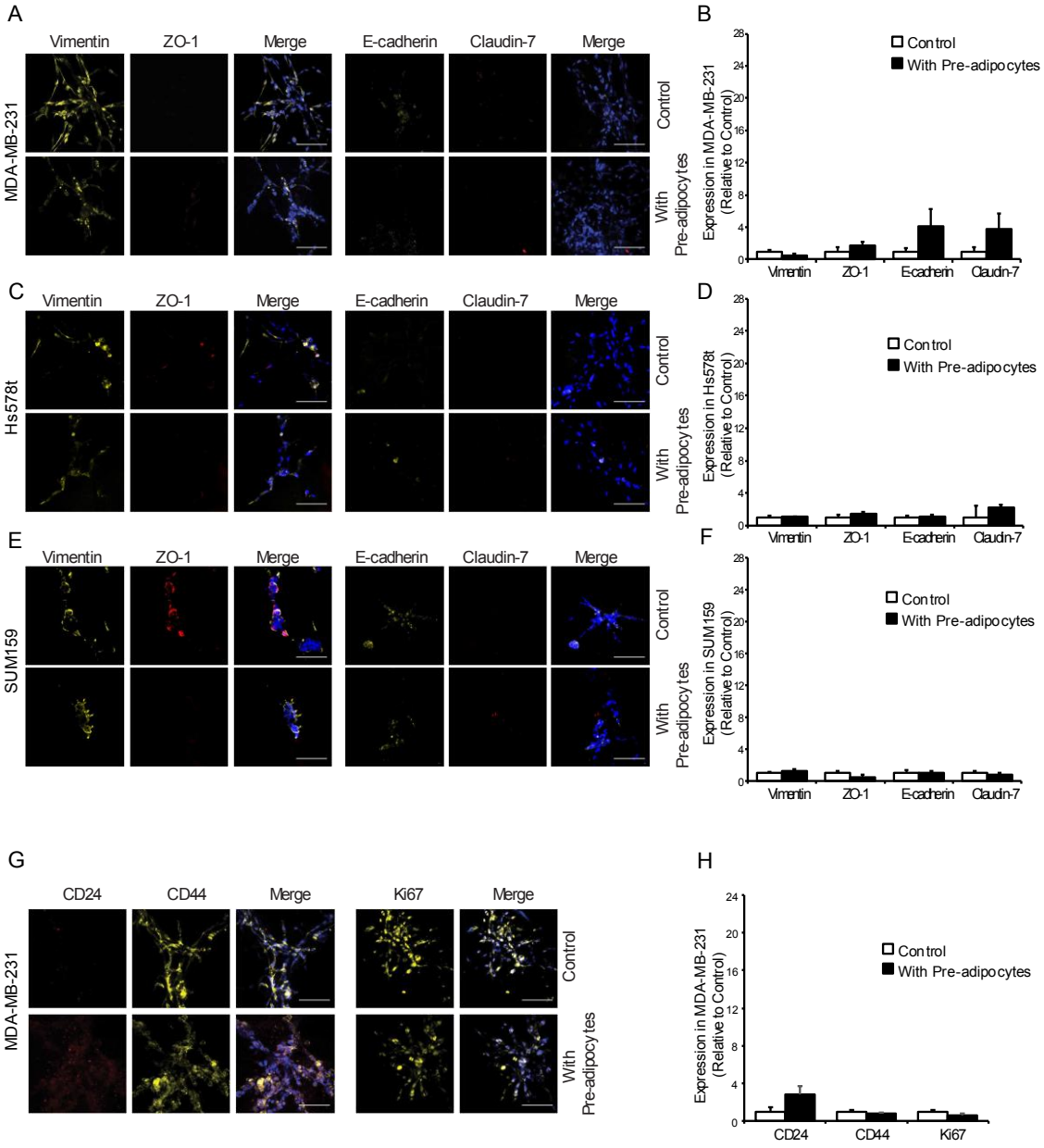
A
Vimentin
ZO-1
Merge
E-cadherin
Claudin-7
Merge
MDA-MB-231
Control
With Pre-adipocytes
B
Control
With Pre-adipocytes
Expression in MDA-MB-231 (Relative to Control)
Vimentin
ZO-1
E-cadherin
Claudin-7
C
Hs578t
D
Expression in Hs578t (Relative to Control)
E
SUM159
F
Expression in SUM159 (Relative to Control)
G
CD24
CD44
Ki67
H

Figure 5.5: Pre-adipocytes have no effect on MET or on stemness markers of BC cells. Representative images of (A) MDA-MB-231 cells, (C) Hs578t cells and (E) SUM159 cells cultured with or without pre-adipocytes, and co-stained with anti-vimentin, anti-ZO-1, and DAPI (left panel), or co-stained with anti-E-cadherin, anti-Claudin-7 and DAPI (right panel). (B, D, F, H) The average protein expression of 5 images per replicate from different fields of view for the TNBC cells was normalized to DAPI and analyzed relative to control cultures. Significance was determined using Kruskal-Wallis test on ranks compared to control. n=3. Representative images of (G) MDA-MB-231 cells, grown in 3D culture in the absence or presence of pre-adipocytes, and then co-stained with anti-CD24, anti-CD44, and DAPI (left panel), or co-stained with anti-Ki67 and DAPI (right panel), (scale bar=50μm).

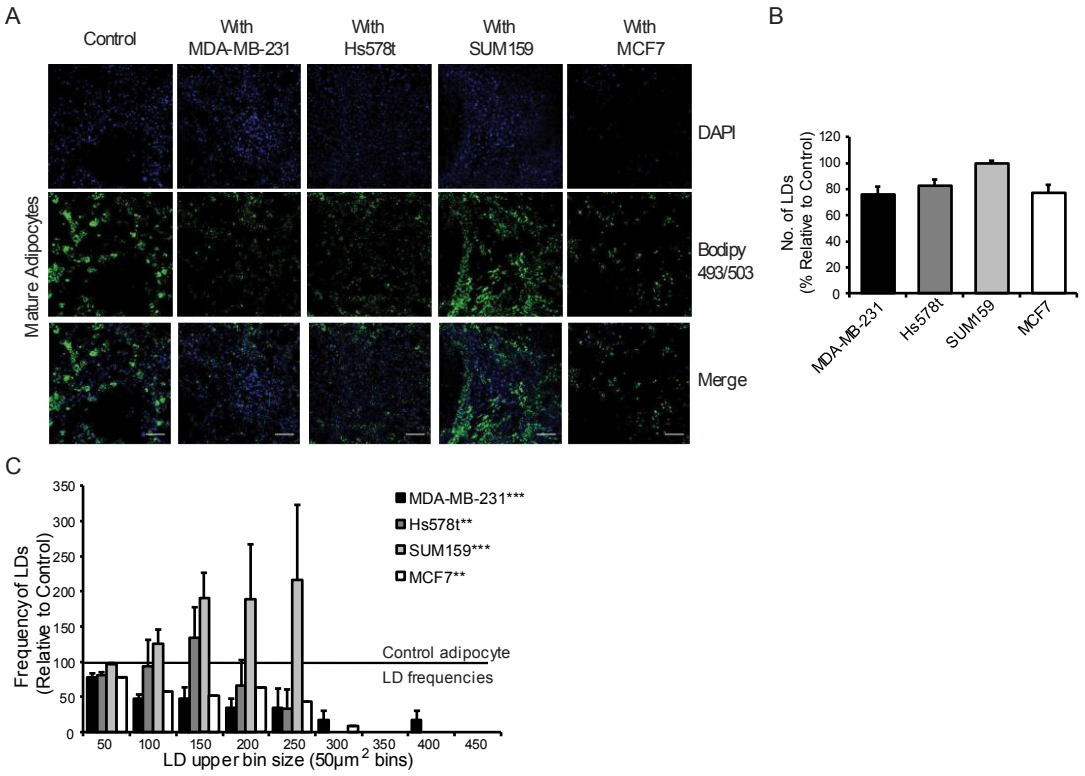

Figure 5.6: Co-culture with BC cells decreases the size but not number of LD present in mature adipocytes. (A) Representative images of adipocyte LDs co-stained with Bodipy 493/503 and DAPI in the presence and absence of BC cells in the 3D co-culture system. (scale bar = 100μm), n=3. (B) Number of LDs analyzed from 5 random fields of view per replicate shown as mean ± SD. Significant differences were determined using Students t-test, n=3. (C) Distributions of areas binned by 50μm^2. Significance was determined using Kolmogorov-Smirnov test, n=3, **P<0.01, ***P<0.001, mean ± SD are shown from n=3. Note: error bars for MCF7 are too small to be visible.

altered distribution of LDs sizes in response to co-culture with any of the BC cell lines (MDA-MB-231: P<0.0001, Hs578t: P=0.00812, SUM159: P<0.0001, MCF7: P<0.0001) (Fig. 5.6C). MDA-MB-231 cells caused a decrease in the number of LD in all bins 100 μm^2 or greater. Hs578t cells had a less dramatic effect with a reduction in LD of 250 μm^2 or greater. Even MCF7 cells, that were themselves not affected by adipocyte co-culture, caused a reduction in LDs 100 μm^2 and greater. In contrast, we observed an increase in the frequency of LDs greater than 150 μm^2 with SUM159 co-culture.

5.6 Discussion

Here, I report on the development and use of a 3D co-culture system to allow the evaluation of interactions between two different cell types where both cell types are in contact with the ECM. The system I describe does not require custom equipment, scaffolding, or other techniques inaccessible to modern cellular biology labs. The system has the noted benefit of allowing assessment of epithelial and mesenchymal states that are particularly vulnerable to differences in the 2D vs. 3D environment [135].

I developed this novel 3D co-culture system to enable the analysis of proteins or lipid of interest by IF staining and confocal imaging. Here, I focused on analysis of the EMT status of BC cell lines using human specific antibodies. I have used adipocytes and laminin-rich ECM in this study, however, this method could easily be modified to analyse interaction with other types of ECM, stromal cells, or primary cells from mouse or human at different stages of cancer progression, and in the presence of drugs or other biological activators or inhibitors. Similarly, this 3D co-culture system could be easily

modified to allow paraffin embedded IHC staining or electron microscopic imaging [333]. It has been shown that BC cells isolated from 3D culture can maintain their characteristics for up to 8 weeks, thus, allowing for further assessment of changes to the migration and invasion ability induced by co-culture [334, 335].

It is important to note that the major technical limitation for imaging the 3D co-cultures is obtaining high resolution images due to the thickness of the sample, which limits the ability to obtain well focused images, particularly at higher magnification objectives with limited focal length. It is possible that this limitation could be overcome by formalin fixed, paraffin embedded - immunofluorescence or immunohistochemistry (FFPE-IF/IHC) techniques, which would create thinner physical slices. However, the additional processing and need for compatible antibodies adds a different set of caveats. [333].

To demonstrate the utility of this method, we analyzed the effect of adipocytes on the 3D morphology of BC cell lines with different proportions of mesenchymal or epithelial colonies. Interestingly, and in contrast to a previous report [43], we found that adipocytes promoted a partial MET in mesenchymal BC cells, as evidenced by the changes to colony morphology and changes in expression of Claudin-7 and E-cadherin in MDA-MB-231 and Hs578t cells and vimentin in Hs578t cells. In contrast, SUM159 cells, which are more epithelial in 3D-culture, did not show any significant changes to specific colony morphologies or EMT marker expression. Surprisingly, MCF7 cells also showed no change in their EMT status in the presence of adipocytes even though these changes

were seen in Transwell culture studies [43]. This suggests that physical interactions of BC cells and adipocytes with the ECM has an essential role in the biology of EMT and MET of BC cells.

Because either physical interactions and secretory factors could be responsible for inducing these changes in mesenchymal BC cells, I determined if CM could recapitulate the adipocyte-induced effects. I found that CM was sufficient to change the morphology of MDA-MB-231 and Hs578t cells to an epithelial-like colony shape but did not induce similar MET-like changes in biomarker expression. It must be noted that the CM was diluted by 50% at each medium change to ensure replenishment of nutrients for cell survival. Thus, the reduced concentration of secretory factors may have caused this partial effect. Alternatively, constant exposure of a mediator or the physical presence of mature adipocytes may be necessary to surpass a signaling threshold in the BC cells. A partial change that was even less dramatic was observed in the presence of pre-adipocytes suggesting that the mediator is more abundant or effective when originating from adipocytes.

During EMT *in vivo*, an increase in BCSC can further enhance invasion and migration of the tumor and this change can be suppressed during MET [336]. I found that CD24 levels were increased in MDA-MB-231 cells by adipocyte and CM co-culture, but not in the other cell lines, with no change in CD44 expression in any cell line. This suggests there is no change in the proportion of BCSC in the culture, although future investigation is necessary to fully determine this. Since CD24 is an epithelial marker that

was found to be increased in metastatic sites [337], the observed increase in CD24 could instead be reflective of the observed increase in the epithelial phenotype. Moreover, this increase in CD24 might be regulated by suppression of Ras pathway genes by adipocytes.

The most common sites for secondary tumor formation in TNBC or ER/PR+ tumors are bone and lungs [338]. Increased adiposity in the bone marrow has been shown to lead to metastasis from ovarian and prostate cancers [113, 339]. However, it is not known whether the composition and/or mechanical properties of the ECM at sites of metastasis, such as the bone marrow, are similar to that used in the present study. Future work will be required to elucidate the precise mechanism(s) contributed by adipocytes to BC metastasis at specific sites and the role of the ECM in these processes.

Differences in LD size suggests that lipid in the adipocytes could be mobilized by MDA-MB-231, Hs578t cells, or MCF7, which may provide energy in the form of free fatty acids taken up by BC cells to fuel cellular processes. Increased lipolysis by adipocytes in the BC microenvironment and increased expression of fatty acid binding proteins in ovarian cancer, combined with studies showing high levels of oxidative phosphorylation in BC cells, supports this possibility [206, 340]. Alternatively, adipocytes can affect BC cells via the increased secretion of leptin, IL-6, TNF, and VEGF, as observed in obese patients [104]. In SUM159 cells, there was no decrease in LD size which may also explain the lack of change to the phenotype of these cells, however it remains to be determined why the MCF7 cell phenotype is unaffected by

adipocytes yet LD size is decreased. This suggests the LD might be used only as source of energy by these BC cells and might not involved in the phenotypic changes of BC cells

Breast is a fatty tissue where occurrence of tumor has influential interactions with adipocytes [341]. Adipokines such as adiponectin and leptin have opposite effects on BC progression. However, leptin secreted by BC cells into microenvironment can bind the leptin receptors on the adipocytes activating lipolysis [342, 343]. This could be one of the possibilities of decrease of lipid content in adipocytes when co-cultured with BC cells. The free fatty acids released might have a reciprocal effect on MET of BC cells. This can be explained by blocking leptin and analyzing the effect on BC cells in 3D co-culture. Another possibility for the decrease in lipid content could be the presence of fibroblast-like cells that can be generated by de-differentiation of adipocytes, also called as adipocyte derived fibroblasts (ADFs). Cancer associated fibroblasts are a significant part of the stromal cell population that contributes to BC progression and metastasis [344]. The Wnt/β-catenin pathway is re-activated in ADFs via Wnt3a in the presence of cancer cells [345], indicating generation of ADFs. Both de-lipidation and de-differentiation increases the free fatty acids, and inflammatory cytokines that leads to aggressive breast cancer formation gaining invasive, and migration properties [346].

Here, I demonstrate the use of a novel, straightforward, and accessible 3D co-culture method to show that adipocytes can promote a MET-like change in mesenchymal TNBC cells. This work provides more insight into relationship between high adiposity and metastasis to bone or other sites with adipocyte abundance. Future work, using this

and other models, to identify the mechanism(s) underlying this process may enable identification of better therapeutic targets for metastatic BC.

Chapter 6. Discussion

Overall, BC progression and metastasis depends on intrinsic factors such as the genetic and epigenetic instability of genes involved in cell growth, proliferation and differentiation. It is essential to determine the structure, function, and regulation of these genes in order to target and regulate the tumor progression. In addition, BC progression and metastasis are further influenced by extrinsic factors such as the stromal cells and ECM surrounding cancer cells (Fig 6.1). These extrinsic and intrinsic factors can be influenced by other conditions of the patient, such as heredity, aging, or lifestyle issues such as obesity, alcohol consumption, or smoking. All of the factors mentioned above can interact to enhance BC progression and metastasis. Thus, the goal of this thesis is to investigate some aspects of the above-mentioned factors that affect the tumorigenesis, progression and metastasis of BC.

The root cause of tumor initiation is genetic or epigenetic alterations of genes involved in cell cycle regulation [347]. Accumulation of mutations in cells decides the outcome of tumor progression. Irrespective of the number of mutations, it is mutations in driver genes such as RTKs, Ras, PI3K, and ERK, that drives cell proliferation [348]. In addition, resistance to cell death, metabolic changes, increased angiogenesis, and invasive properties are acquired that further promote tumor progression [349]. Moreover, inter-dependencies between signaling pathways co-operate with each other in order to achieve cancer growth, survival, and progression [321].

A

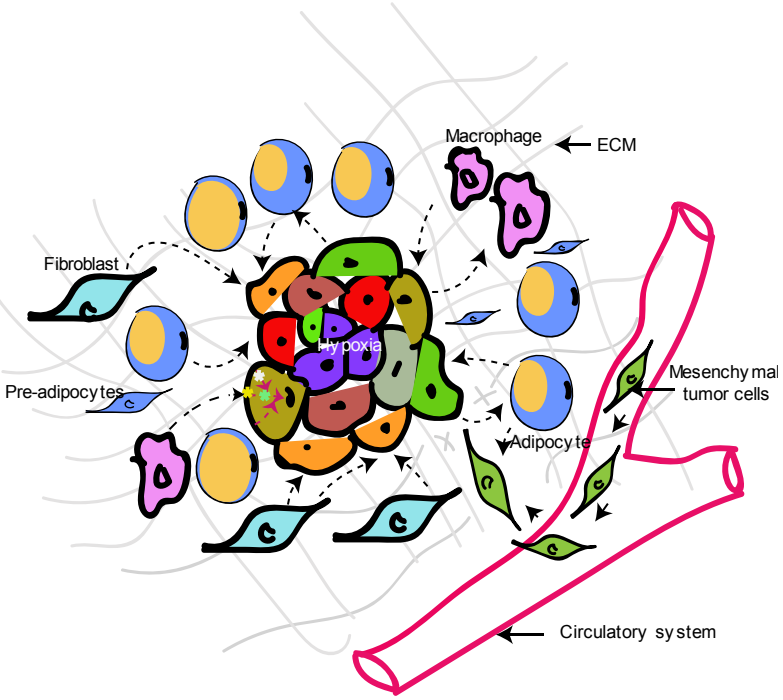
Macrophage
ECM
Fibroblast
Hypoxia
Pre-adipocytes
Mesenchymal
tumor cells
Adipocyte
Circulatory system

B

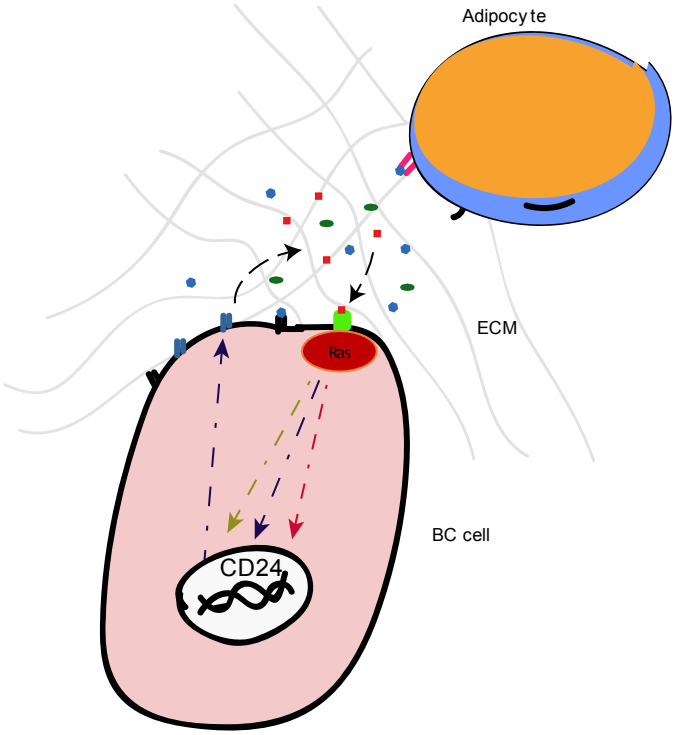
Adipocyte
ECM
Ras
BC cell
CD24

Figure 6.1: Schematic illustration of the tumor microenvironment showing the interaction between the tumor cells and the surrounding ECM and non-cancerous cells at secondary site. (A)The tumor consists of a heterogeneous population of cells with varied mutation burden between cells. The colored * indicates complexity of cross-talk between different signaling pathways when cells have multiple mutations. The lipid engorged adipocytes are shown interacting with mesenchymal cells, which aid in the denaturation of the ECM and subsequent MET of cancer cells at the site of colonization. Dashed lines with arrows indicate the interaction within or between cells. Different colors of cells within the tumor indicates tumor heterogeneity due to diverse mutations. (B) An overview of the extrinsic factors such as adipocytes interacting with BC cells and activating signalling cascade such as Ras in the presence of ECM.

Similarly, proteins such as CD24 are downregulated, especially in BCSC in order to maintain the stem-like properties of the cells. Here, I have analyzed the structure and evolution of the CD24 gene, which plays an important role as a biomarker for BCSCs. Analysis of the CD24 gene structure and evolution revealed the importance of glycosylation sites that have been conserved over 200 million years. I have shown that the CD24 gene structure is dynamic and varies among species. However, the conserved glycosylation sites suggests their importance in the CD24 protein function. The role of glycosylation in CD24 function among BC cells has not been reported. Comparison of glycosylation patterns between neuroblastoma, lymphoblastoma and astrocytoma suggests different patterns between these cell types [147]. These conserved regions can be considered in the design of potential drugs against the CD24 protein to inhibit or stabilize its activity. Moreover, in TNBC patients, differential drug treatment switches the $CD24^{+}$ to $CD24^{low/-}$ phenotype and *vice versa*, which has been suggested to be a potential cause of drug resistance in these patients [350]. Thus, targeting CD24 function may reduce drug resistance in TNBC patients. In addition, inhibition of CD24 signaling or adhesion might be a potential targeted therapy for the cancers where high CD24 expression leads to cancer progression [82]. In the future, identifying the glycosylation patterns among different BC subtypes could help to explain the dynamic role of CD24 signaling between these cancer cells.

Understanding the regulation of CD24 can contribute to understanding the regulation of BCSC and TNBC progression. Thus, I targeted multiple downstream proteins of Ras to understand the regulation of CD24 protein expression by the Ras

pathway. However, I found that complex cross-talk downstream of Ras triggers multiple pathways to downregulate CD24 at promoter, mRNA, and protein levels. This suggests that it is important for BC cells to downregulate CD24 surface protein expression, which might involve in inhibition of signaling that inhibits tumorigenesis and proliferation. Moreover, I have shown that Ras downregulates CD24 mRNA and protein independently via the Raf/MEK or the PI3K/Akt pathway. Identifying the regulatory pathways of CD24 that regulate the BCSC phenotype may allow for the identification of strategies to reduce drug resistance and progression in TNBC patients. BCSC can be identified by the absence of CD24 on cell surface, this suppression might be regulated by oncogenic Ras pathway. Targeting the proteins involved in protein trafficking downstream of Ras to promote CD24 expression on cell surface or inhibition of microRNA to increase the stability of CD24 mRNA or identifying the TF that repress CD24 promoter regions to increase CD24 transcription in RasV12 cells and BC cells are the potential future strategies to understand the downregulation of CD24 by oncogenic Ras at multiple levels.

In addition to the internal regulation of cancer cells, driver mutations can trigger activation of signaling networks to allow interactions with non-cancerous cells and the ECM in the microenvironment that is favorable for tumor progression. The breast TME consists of a heterogenic population of cells, including proliferating host cells, cancer stem cells, and stromal cells such as immune cells, endothelial cells, and adipocytes. Autocrine and paracrine signaling among these cells via growth factors and chemokines causes changes in metabolism, oxidative stress, and hypoxia that contribute to cancer cell growth, dissemination, and metastasis (Fig 6.1). Therefore, I have studied the

contribution of the ECM and adipocytes to BC progression through the use of a newly developed *in vitro* 3D co-culture system.

The ECM is the soul of the microenvironment, providing biophysical and mechanical support to the tumor. *In vitro* 3D cell culture studies have revealed the invasive properties and metastatic efficiencies of cancer cells in ECM [351]. Secretion of MMPs by stromal cells changes the dynamics of the microenvironment to allow morphological dissemination of cancer cells away from the solid tumor. In addition, adipocytes can also secrete ECM proteins, especially collagen type I and fibronectin, that stiffens the breast tumor microenvironment, leading to hypoxic or acidic conditions that allow cancer cells to survive over normal cells [352]. Moreover, in addition to systemic changes caused by obesity, the effect of adipocytes on cancer progression is worsened, resulting in poor disease outcome in cancer patients. Adiposity causes increased inflammatory cytokines, free fatty acids, and IGF1, contributing to changes in metabolic activity to allow the cancer cells to survive. There is increased drug resistance in obese patients due to the increased stiffness of the ECM, which further changes the dynamics of the vasculature that can restrict the delivery of chemotherapy. Here, I have developed an *in vitro* 3D co-culture system that can potentially aid in finding new therapeutic targets present in microenvironment that enhance BC progression. Therapeutic targeting of the tumor microenvironment in any condition, in addition to targeting the specific gene expression, will have more profound effect when compared to general chemotherapy. In the future, identifying the soluble mediator that is involved in this partial MET can

provide a new strategy to treat metastasis in BC patients. This effect of soluble mediator on MET of BC cells can be validated using human adipocytes.

Overall, for the very first time I have identified the presence of CD24 in the tree of evolution since the divergence from reptiles. Moreover, CD24 functional regions are evolutionarily conserved. I also found that oncogenic Ras downregulates both CD24 mRNA and protein expression by multiple mechanisms. Downregulation of CD24 surface protein can be relieved by supressing Raf activity only when Ras is mutated and this can not be achieved in BC cells where additional mutations are present (Fig 6.1B). This suggests that inhibition of Raf is not sufficient to increases $CD24^{+}$ population in BC cells. Finally, I developed a novel 3D co-culture system, where two different cell lines can be studied in the presence of ECM. Moreover, I found that adipocytes promote partial MET, suggesting its role in colonization of BC cells at secondary site during micro or macro-metastasis. Cancer metastasis is the leading cause for death from cancer. Tumor heterogeneity, the presence of cancer stem cells, and TME, all contribute to resistance to therapy. To overcome the drug resistance, heterogeneity, and aggressiveness of the TNBC progression, targeting intrinsic factors is not sufficient. In order to achieve effective drug treatment, it is important to consider the extrinsic factors present in the microenvironment that contribute to TNBC progression. Over the last decade, personalized medicine, where combination drugs targeting the genetic changes specific to the patient, has been found to improve treatment response in patients with cancer [353]. Overall, considering both intrinsic and extrinsic factors in combination drug treatment

that can target different aspects of the tumor such as microenvironment and intrinsic factors including function and regulation of genes, is the future of the TNBC treatment.

References

1. Canadian Cancer Statistics 2017. (2017) Canadian Cancer Society's Advisory Committee on Cancer Statistics. Can Cancer Soc 2017

2. Seely JM, Alhassan T (2018) Screening for breast cancer in 2018-what should we be doing today? Curr Oncol 25:S115–S124 . doi: 10.3747/co.25.3770

3. Wong Eric CS and RM (2012) Breast cancer | Oncology

4. Abdelmessieh P (2016) Breast Cancer Histology: Overview, Ductal Carcinoma In Situ, Lobular Carcinoma In Situ. In: Medcape

5. Malhotra GK, Zhao X, Band H, Band V (2010) Histological, molecular and functional subtypes of breast cancers. Cancer Biol Ther 10:955–60 . doi: 10.4161/CBT.10.10.13879

6. Makki J (2015) Diversity of Breast Carcinoma: Histological Subtypes and Clinical Relevance. Clin Med Insights Pathol 8:23–31 . doi: 10.4137/CPath.S31563

7. Kagara N, Huynh KT, Kuo C, et al (2012) Epigenetic regulation of cancer stem cell genes in triple-negative breast cancer. Am J Pathol 181:257–267 . doi: 10.1016/j.ajpath.2012.03.019;

8. Alkabban FM, Ferguson T (2018) Cancer, Breast. StatPearls

9. Subik K, Lee J-FF, Baxter L, et al (2010) The Expression Patterns of ER, PR, HER2, CK5/6, EGFR, Ki-67 and AR by Immunohistochemical Analysis in Breast

Cancer Cell Lines. Breast cancer 4:35–41

10. Onitilo AA, Engel JM, Greenlee RT, Mukesh BN (2009) Breast cancer subtypes based on ER/PR and Her2 expression: Comparison of clinicopathologic features and survival. Clin Med Res 7:4–13 . doi: 10.3121/cmr.2009.825

11. Cadoo KA, Fornier MN, Morris PG (2013) Biological subtypes of breast cancer: current concepts and implications for recurrence patterns. Q J Nucl Med Mol imaging 57:312–321

12. Feeley LP, Mulligan AM, Pinnaduwage D, et al (2014) Distinguishing luminal breast cancer subtypes by Ki67, progesterone receptor or TP53 status provides prognostic information. Mod Pathol 27:554–561 . doi: 10.1038/modpathol.2013.153

13. Hubalek M, Czech T, Müller H (2017) Biological Subtypes of Triple-Negative Breast Cancer. Breast care 12:8–14 . doi: 10.1159/000455820

14. Pareja F, Geyer FC, Marchiò C, et al (2016) Triple-negative breast cancer: the importance of molecular and histologic subtyping, and recognition of low-grade variants. Breast Cancer 2:16036 . doi: 10.1038/npjbcancer.2016.36

15. Dent R, Trudeau M, Pritchard KI, et al (2007) Triple-Negative Breast Cancer: Clinical Features and Patterns of Recurrence. Clin Cancer Res 13:4429–4434 . doi: 10.1158/1078-0432.CCR-06-3045

16. Neophytou C, Boutsikos P, Papageorgis P (2018) Molecular Mechanisms and

Emerging Therapeutic Targets of Triple-Negative Breast Cancer Metastasis. Front Oncol 8:31 . doi: 10.3389/fonc.2018.00031

17. Kreike B, van Kouwenhove M, Horlings H, et al (2007) Gene expression profiling and histopathological characterization of triple-negative/basal-like breast carcinomas. Breast Cancer Res 9:R65 . doi: 10.1186/bcr1771

18. Lehmann BD, Bauer JA, Chen X, et al (2011) Identification of human triple-negative breast cancer subtypes and preclinical models for selection of targeted therapies. J Clin Invest 121:2750–2767 . doi: 10.1172/JCI45014

19. Lehmann BD, Jovanović B, Chen X, et al (2016) Refinement of Triple-Negative Breast Cancer Molecular Subtypes: Implications for Neoadjuvant Chemotherapy Selection. PLoS One 11:e0157368 . doi: 10.1371/journal.pone.0157368

20. Denkert C, Liedtke C, Tutt A, von Minckwitz G (2017) Molecular alterations in triple-negative breast cancer—the road to new treatment strategies. Lancet 389:2430–2442 . doi: 10.1016/S0140-6736(16)32454-0

21. Lehmann BD, Pietenpol JA (2014) Identification and use of biomarkers in treatment strategies for triple-negative breast cancer subtypes. J Pathol 232:142–150 . doi: 10.1002/path.4280

22. Ma CX, Luo J, Ellis MJ (2010) Molecular profiling of triple negative breast cancer. Breast Dis 32:73–84 . doi: 10.3233/BD-2010-0309

23. Burstein MD, Tsimelzon A, Poage GM, et al (2015) Comprehensive Genomic

Analysis Identifies Novel Subtypes and Targets of Triple-Negative Breast Cancer. Clin Cancer Res 21:1688–1698 . doi: 10.1158/1078-0432.CCR-14-0432

24. Ahn SG, Kim SJ, Kim C, Jeong J (2016) Molecular Classification of Triple-Negative Breast Cancer. J Breast Cancer 19:223–230 . doi: 10.4048/jbc.2016.19.3.223

25. Gucalp A, Tolaney S, Isakoff SJ, et al (2013) Phase II Trial of Bicalutamide in Patients with Androgen Receptor-Positive, Estrogen Receptor-Negative Metastatic Breast Cancer. Clin Cancer Res 19:5505–5512 . doi: 10.1158/1078-0432.CCR-12-3327

26. Chaffer CL, Weinberg RA (2011) A perspective on cancer cell metastasis. Science 331:1559–1564 . doi: 10.1126/science.1203543

27. Tseng LM, Hsui CN, Chen SC, et al (2013) Distant metastasis in triple-negative breast cancer. Neoplasma 60:290–294 . doi: 10.4149/neo_2013_038

28. Gjorevski N, Nelson CM (2011) Integrated morphodynamic signalling of the mammary gland. Nat Rev Mol Cell Biol. doi: 10.1038/nrm3168

29. Kalluri R, Weinberg RA (2009) The basics of epithelial-mesenchymal transition. J. Clin. Invest. 119:1420–1428

30. Becker A, Thakur BK, Weiss JM, et al (2016) Extracellular Vesicles in Cancer: Cell-to-Cell Mediators of Metastasis. Cancer Cell 30:836–848 . doi: 10.1016/j.ccell.2016.10.009

31. Seyfried TN, Huysentruyt LC (2013) On the origin of cancer metastasis. Crit Rev Oncog 18:43–73

32. Martin TA, Jiang WG (2009) Loss of tight junction barrier function and its role in cancer metastasis. Biochim Biophys Acta - Biomembr 1788:872–891

33. Lu J, Steeg PS, Price JE, et al (2009) Breast Cancer Metastasis: Challenges and Opportunities. Cancer Res 69:4951–4953 . doi: 10.1158/0008-5472.CAN-09-0099

34. Thiery JP, Acloque H, Huang RYJ, et al (2009) Epithelial-mesenchymal transitions in development and disease. Cell 139:871–890 . doi: 10.1016/j.cell.2009.11.007

35. Craene B De, Berx G (2013) Regulatory networks defining EMT during cancer initiation and progression. Nat Rev Cancer 13:97–110 . doi: 10.1038/nrc3447

36. Gupta GP, Massagué J (2006) Cancer metastasis: building a framework. Cell 127:679–95 . doi: 10.1016/j.cell.2006.11.001

37. Thiery JP, Lim CT (2013) Tumor Dissemination: An EMT Affair. Cancer Cell 23:272–273 . doi: 10.1016/j.ccr.2013.03.004

38. Horak CE, Steeg PS (2005) Metastasis gets site specific. Cancer Cell 8:93–5 . doi: 10.1016/j.ccr.2005.07.013

39. Matei I, Ghajar CM, Lyden D (2011) A TeNaCious foundation for the metastatic niche. Cancer Cell 20:139–41 . doi: 10.1016/j.ccr.2011.08.004

40. Bondow BJ, Faber ML, Wojta KJ, et al (2012) E-cadherin is required for intestinal morphogenesis in the mouse. Dev Biol 371:1–12 . doi: 10.1016/J.YDBIO.2012.06.005

41. Adhikary A, Chakraborty S, Mazumdar M, et al (2014) Inhibition of epithelial to mesenchymal transition by E-cadherin up-regulation via repression of slug transcription and inhibition of E-cadherin degradation: dual role of scaffold/matrix attachment region-binding protein 1 (SMAR1) in breast cancer cells. J Biol Chem 289:25431–44 . doi: 10.1074/jbc.M113.527267

42. Wu Y, Sarkissyan M, Vadgama J (2016) Epithelial-Mesenchymal Transition and Breast Cancer. J Clin Med 5:13 . doi: 10.3390/jcm5020013

43. Lee Y, Jung WH, Koo JS (2015) Adipocytes can induce epithelial-mesenchymal transition in breast cancer cells. Breast Cancer Res Treat 153:323–335 . doi: 10.1007/s10549-015-3550-9

44. Ritter A, Friemel A, Fornoff F, et al (2015) Characterization of adipose-derived stem cells from subcutaneous and visceral adipose tissues and their function in breast cancer cells. Oncotarget 6:34475–93 . doi: 10.18632/oncotarget.5922

45. Ogunwobi OO, Liu C (2011) Hepatocyte growth factor upregulation promotes carcinogenesis and epithelial-mesenchymal transition in hepatocellular carcinoma via Akt and COX-2 pathways. Clin Exp Metastasis 28:721–31 . doi: 10.1007/s10585-011-9404-x

46. Xu J, Lamouille S, Derynck R (2009) TGF-beta-induced epithelial to mesenchymal transition. Cell Res 19:156–72 . doi: 10.1038/cr.2009.5

47. Moreno-Bueno G, Portillo F, Cano A (2008) Transcriptional regulation of cell polarity in EMT and cancer. Oncogene 27:6958–6969 . doi: 10.1038/onc.2008.346

48. Battula VL, Evans KW, Hollier BG, et al (2010) Epithelial-mesenchymal transition-derived cells exhibit multilineage differentiation potential similar to mesenchymal stem cells. Stem Cells 28:1435–1445 . doi: 10.1002/stem.467

49. Mani SA, Guo W, Liao M-JJ, et al (2008) The Epithelial-Mesenchymal Transition Generates Cells with Properties of Stem Cells. Cell 133:704–715 . doi: http://dx.doi.org/10.1016/j.cell.2008.03.027

50. Ota I, Li X-Y, Hu Y, Weiss SJ (2009) Induction of a MT1-MMP and MT2-MMP-dependent basement membrane transmigration program in cancer cells by Snail1. Proc Natl Acad Sci 106:20318–20323 . doi: 10.1073/pnas.0910962106

51. Tsai JH, Yang J (2013) Epithelial – mesenchymal plasticity in carcinoma metastasis. Genes Dev 27:2192–2206 . doi: 10.1101/gad.225334.113.2192

52. Drake JM, Strohbehn G, Bair TB, et al (2009) ZEB1 enhances transendothelial migration and represses the epithelial phenotype of prostate cancer cells. Mol Biol Cell 20:2207–17 . doi: 10.1091/mbc.E08-10-1076

53. Gupta GP, Nguyen DX, Chiang AC, et al (2007) Mediators of vascular remodelling co-opted for sequential steps in lung metastasis. Nature 446:765–770 .

doi: 10.1038/nature05760

54. Yu M, Bardia A, Wittner BS, et al (2013) Circulating breast tumor cells exhibit dynamic changes in epithelial and mesenchymal composition. Science (80-) 339:580–584 . doi: 10.1126/science.1228522

55. Hüsemann Y, Geigl JB, Schubert F, et al (2008) Systemic Spread Is an Early Step in Breast Cancer. Cancer Cell 13:58–68 . doi: 10.1016/j.ccr.2007.12.003

56. Lambert AW, Pattabiraman DR, Weinberg RA (2017) Emerging Biological Principles of Metastasis. Cell 168:670–691 . doi: 10.1016/j.cell.2016.11.037

57. Labelle M, Begum S, Hynes RO (2011) Direct Signaling between Platelets and Cancer Cells Induces an Epithelial-Mesenchymal-Like Transition and Promotes Metastasis. Cancer Cell 20:576–590 . doi: 10.1016/j.ccr.2011.09.009

58. Shibue T, Brooks MW, Fatih Inan M, et al (2012) The outgrowth of micrometastases is enabled by the formation of filopodium-like protrusions. Cancer Discov 2:706–721 . doi: 10.1158/2159-8290.CD-11-0239

59. Labelle M, Hynes RO (2012) The initial hours of metastasis: The importance of cooperative host-tumor cell interactions during hematogenous dissemination. Cancer Discov. 2:1091–1099

60. Yao D, Dai C, Peng S (2011) Mechanism of the Mesenchymal-Epithelial Transition and Its Relationship with Metastatic Tumor Formation. Mol Cancer Res 9:1608–1620 . doi: 10.1158/1541-7786.MCR-10-0568

61. Yates CC, Shepard CR, Stolz DB, Wells A (2007) Co-culturing human prostate carcinoma cells with hepatocytes leads to increased expression of E-cadherin. Br J Cancer 96:1246–1252 . doi: 10.1038/sj.bjc.6603700

62. Chao YL, Shepard CR, Wells A (2010) Breast carcinoma cells re-express E-cadherin during mesenchymal to epithelial reverting transition. Mol Cancer 9: . doi: 10.1186/1476-4598-9-179

63. Aokage K, Ishii G, Ohtaki Y, et al (2011) Dynamic molecular changes associated with epithelial-mesenchymal transition and subsequent mesenchymal-epithelial transition in the early phase of metastatic tumor formation. Int J Cancer 128:1585–1595 . doi: 10.1002/ijc.25500

64. Xie H, Liao N, Lan F, et al (2017) 3D-cultured adipose tissue-derived stem cells inhibit liver cancer cell migration and invasion through suppressing epithelial-mesenchymal transition. Int J Mol Med 41:1385–1396 . doi: 10.3892/ijmm.2017.3336

65. Jie X-X, Zhang X-Y, Xu C-J, et al (2017) Epithelial-to-mesenchymal transition, circulating tumor cells and cancer metastasis: Mechanisms and clinical applications. Oncotarget 8:81558–81571 . doi: 10.18632/oncotarget.18277

66. Zhou XD, Agazie YM (2008) Inhibition of SHP2 leads to mesenchymal to epithelial transition in breast cancer cells. Cell Death Differ 15:988–996 . doi: 10.1038/cdd.2008.54

67. Tsuji T, Ibaragi S, Hu GF (2009) Epithelial-mesenchymal transition and cell cooperativity in metastasis. Cancer Res. 69:7135–7139

68. Wells A, Yates C, Shepard CR (2008) E-cadherin as an indicator of mesenchymal to epithelial reverting transitions during the metastatic seeding of disseminated carcinomas. Clin Exp Metastasis 25:621–628 . doi: 10.1007/s10585-008-9167-1

69. Al-Hajj MM (2003) From the Cover: Prospective identification of tumorigenic breast cancer cells. Proc Natl Acad Sci - PNAS 100:3983–3988;

70. Reya T, Morrison SJ, Clarke MF, Weissman IL (2001) Stem Cells, Cancer, and Cancer Stem Cells. Nature 414:105–111 . doi: 10.1007/978-1-60327-933-8

71. Williams C, Helguero L, Edvardsson K, et al (2009) Gene expression in murine mammary epithelial stem cell-like cells shows similarities to human breast cancer gene expression. Breast Cancer Res 11:R26 . doi: 10.1186/bcr2256

72. Ginestier C, Hur MH, Charafe-Jauffret E, et al (2007) ALDH1 Is a Marker of Normal and Malignant Human Mammary Stem Cells and a Predictor of Poor Clinical Outcome. Cell Stem Cell 1:555–567 . doi: 10.1016/j.stem.2007.08.014

73. Li W, Ma H, Zhang J, et al (2017) Unraveling the roles of CD44/CD24 and ALDH1 as cancer stem cell markers in tumorigenesis and metastasis. Sci Rep 7:13856 . doi: 10.1038/s41598-017-14364-2

74. Meyer MJ, Fleming JM, Ali MA, et al (2009) Dynamic regulation of CD24 and the invasive, CD44posCD24neg phenotype in breast cancer cell lines. Breast

Cancer Res 11:R82 . doi: 10.1186/bcr2449;

75. McDermott SP, Wicha MS (2010) Targeting breast cancer stem cells. Mol Oncol 4:404–419 . doi: 10.1016/j.molonc.2010.06.005

76. Lawson DA, Bhakta NR, Kessenbrock K, et al (2015) Single-cell analysis reveals a stem-cell program in human metastatic breast cancer cells. Nature 526:131–135 . doi: 10.1038/nature15260

77. Owens TW, Naylor MJ (2013) Breast cancer stem cells. Front Physiol 4:225 . doi: 10.3389/fphys.2013.00225;

78. Charafe-Jauffret E, Ginestier C, Iovino F, et al (2009) Breast Cancer Cell Lines Contain Functional Cancer Stem Cells with Metastatic Capacity and a Distinct Molecular Signature. Cancer Res 69:1302–1313 . doi: 10.1158/0008-5472.CAN-08-2741

79. Sheridan CC, Kishimoto H, Fuchs RK, et al (2006) CD44+/CD24- breast cancer cells exhibit enhanced invasive properties: an early step necessary for metastasis. Breast Cancer Res 8:R59 . doi: 10.1186/bcr1610

80. Phillips TTM, McBride WH, Pajonk F (2006) The Response of CD24-/low/CD44 Breast Cancer-Initiating Cells to Radiation. J Natl Cancer Inst 98:1777–1785; . doi: 10.1093/jnci/djj495

81. Chuthapisith S, Eremin J, El-Sheemey M, Eremin O (2010) Breast cancer chemoresistance: Emerging importance of cancer stem cells. Surg. Oncol. 19:27–

82. Kristiansen GG, Sammar M, Altevogt P (2004) Tumour Biological Aspects of CD24, A Mucin-Like Adhesion Molecule. J Mol Histol 35:255–262;

83. Yan W, Chen Y, Yao Y, et al (2013) Increased invasion and tumorigenicity capacity of CD44+/CD24- breast cancer MCF7 cells in vitro and in nude mice. Cancer Cell Int 13:62 . doi: 10.1186/1475-2867-13-62;

84. Wang H, Wang L, Song Y, et al (2017) CD44+/CD24‐ phenotype predicts a poor prognosis in triple‐negative breast cancer. Oncol Lett 14:5890–5898 . doi: 10.3892/ol.2017.6959

85. Morel A-P Thomas C, Hinkal G, Ansieau S, et al. LM, Morel AP, Lievre M, et al (2008) Generation of Breast Cancer Stem Cells through Epithelial-Mesenchymal Transition. PLoS ONE. PLoS One 3(8): e288:e2888 . doi: 10.1371/journal.pone.0002888; 10.1371/journal.pone.0002888

86. Zhang C, Gao H, Li C, et al (2018) TGFβ1 Promotes Breast Cancer Local Invasion and Liver Metastasis by Increasing the CD44 ^{high} /CD24 $^{-}$ Subpopulation. Technol Cancer Res Treat 17:153303381876449 . doi: 10.1177/1533033818764497

87. Guo W, Keckesova Z, Donaher JL, et al (2012) Slug and Sox9 Cooperatively Determine the Mammary Stem Cell State. Cell 148:1015–1028 . doi: 10.1016/j.cell.2012.02.008

88. Aktas B, Tewes M, Fehm T, et al (2009) Stem cell and epithelial-mesenchymal transition markers are frequently overexpressed in circulating tumor cells of metastatic breast cancer patients. Breast Cancer Res 11:R46 . doi: 10.1186/bcr2333

89. Ouyang G, Wang Z, Fang X, et al (2010) Molecular signaling of the epithelial to mesenchymal transition in generating and maintaining cancer stem cells. Cell. Mol. Life Sci. 67:2605–2618

90. Wellner U, Schubert J, Burk UC, et al (2009) The EMT-activator ZEB1 promotes tumorigenicity by repressing stemness-inhibiting microRNAs. Nat Cell Biol 11:1487–1495 . doi: 10.1038/ncb1998

91. Korpal M, Lee ES, Hu G, Kang Y (2008) The miR-200 Family Inhibits Epithelial-Mesenchymal Transition and Cancer Cell Migration by Direct Targeting of E-cadherin Transcriptional Repressors *ZEB1* and *ZEB2*. J Biol Chem 283:14910–14914 . doi: 10.1074/jbc.C800074200

92. Eaton CL, Colombel M, van der Pluijm G, et al (2010) Evaluation of the frequency of putative prostate cancer stem cells in primary and metastatic prostate cancer. Prostate 70:875–82 . doi: 10.1002/pros.21121

93. WHO (2016) Obesity and overweight. World Heal Organ Fact sheet:

94. Finkelstein EA, Khavjou OA, Thompson H, et al (2012) Obesity and severe obesity forecasts through 2030. Am J Prev Med 42:563–570 . doi:

10.1016/j.amepre.2011.10.026

95. Smith KB, Smith MS (2016) Obesity Statistics. Prim. Care 43:121–135

96. Calle EE, Thun MJ (2004) Obesity and cancer. Oncogene 23:6365–6378

97. Wolin KY, Carson K, Colditz GA (2010) Obesity and Cancer. Oncologist 15:556–565 . doi: 10.1634/theoncologist.2009-0285

98. Ramos Chaves M, Boléo-Tomé C, Monteiro-Grillo I, et al (2010) The diversity of nutritional status in cancer: new insights. Oncologist 15:523–30 . doi: 10.1634/theoncologist.2009-0283

99. Gioulbasanis I, Martin L, Baracos VE, et al (2015) Nutritional assessment in overweight and obese patients with metastatic cancer: does it make sense? Ann Oncol 26:217–221 . doi: 10.1093/annonc/mdu501

100. Protani M, Coory M, Martin JH (2010) Effect of obesity on survival of women with breast cancer: systematic review and meta-analysis. Breast Cancer Res Treat 123:627–635 . doi: 10.1007/s10549-010-0990-0

101. Chan DS, Norat T (2015) Obesity and breast cancer: not only a risk factor of the disease. Curr Treat Options Oncol 16:22-015-0341-9 . doi: 10.1007/s11864-015-0341-9

102. Ewertz M, Jensen M-B, Gunnarsdóttir KÁ, et al (2011) Effect of obesity on prognosis after early-stage breast cancer. J Clin Oncol 29:25–31 . doi:

10.1200/JCO.2010.29.7614

103. James FR, Wootton S, Jackson A, et al (2015) Obesity in breast cancer--what is the risk factor? Eur J Cancer 51:705–720 . doi: 10.1016/j.ejca.2015.01.057

104. Pierobon M, Frankenfeld CL (2013) Obesity as a risk factor for triple-negative breast cancers: a systematic review and meta-analysis. Breast Cancer Res Treat 137:307–314 . doi: 10.1007/s10549-012-2339-3

105. Sidossis L, Kajimura S (2015) Brown and beige fat in humans: Thermogenic adipocytes that control energy and glucose homeostasis. J. Clin. Invest. 125:478–486

106. Vandeweyer E, Hertens D (2002) Quantification of glands and fat in breast tissue: An experimental determination. Ann Anat 184:181–184 . doi: 10.1016/S0940-9602(02)80016-4

107. Choi J, Cha YJ, Koo JS (2018) Adipocyte biology in breast cancer: From silent bystander to active facilitator. Prog. Lipid Res. 69:11–20

108. Ambrosi TH, Scialdone A, Graja A, et al (2017) Adipocyte Accumulation in the Bone Marrow during Obesity and Aging Impairs Stem Cell-Based Hematopoietic and Bone Regeneration. Cell Stem Cell 20:771–784.e6 . doi: 10.1016/j.stem.2017.02.009

109. Donohoe CL, Doyle SL, Reynolds J V. (2011) Visceral adiposity, insulin resistance and cancer risk. Diabetol. Metab. Syndr.

110. Schapira D V., Clark RA, Wolff PA, et al (1994) Visceral obesity and breast cancer risk. Cancer 74:632–639 . doi: 10.1002/1097-0142(19940715)74:2<632::AID-CNCR2820740215>3.0.CO;2-T

111. Osman M, Hennessy B (2015) Obesity Correlation With Metastases Development and Response to First-Line Metastatic Chemotherapy in Breast Cancer. Clin Med Insights Oncol 105 . doi: 10.4137/CMO.S32812

112. Morris E V, Edwards CM (2016) The role of bone marrow adipocytes in bone metastasis. J bone Oncol 5:121–123 . doi: 10.1016/j.jbo.2016.03.006

113. Chkourko Gusky H, Diedrich J, MacDougald OA, Podgorski I (2016) Omentum and bone marrow: how adipocyte-rich organs create tumour microenvironments conducive for metastatic progression. Obes Rev 17:1015–1029 . doi: 10.1111/obr.12450

114. Sundaram S, Johnson AR, Makowski L (2013) Obesity, metabolism and the microenvironment: Links to cancer. J Carcinog 12:19 . doi: 10.4103/1477-3163.119606

115. Seo BR, Bhardwaj P, Choi S, et al (2015) Obesity-dependent changes in interstitial ECM mechanics promote breast tumorigenesis. Sci Transl Med 7:301ra130 . doi: 10.1126/scitranslmed.3010467

116. Place AE, Jin Huh S, Polyak K (2011) The microenvironment in breast cancer progression: biology and implications for treatment. Breast Cancer Res 13:227 .

doi: 10.1186/bcr2912

117. Muschler J, Streuli CH (2010) Cell-matrix interactions in mammary gland development and breast cancer. Cold Spring Harb Perspect Biol 2:a003202 . doi: 10.1101/cshperspect.a003202

118. Streuli CH, Schmidhauser C, Bailey N, et al (1995) Laminin mediates tissue-specific gene expression in mammary epithelia. J Cell Biol 129:591–603

119. Humphrey JD, Dufresne ER, Schwartz MA (2014) Mechanotransduction and extracellular matrix homeostasis. Nat Rev Mol Cell Biol 15:802–812 . doi: 10.1038/nrm3896

120. Ha HY, Moon HB, Nam MS, et al (2001) Overexpression of membrane-type matrix metalloproteinase-1 gene induces mammary gland abnormalities and adenocarcinoma in transgenic mice. Cancer Res 61:984–90

121. Sternlicht MD, Lochter A, Sympson CJ, et al (1999) The stromal proteinase MMP3/stromelysin-1 promotes mammary carcinogenesis. Cell 98:137–46

122. Gudjonsson T, Rønnov-Jessen L, Villadsen R, et al (2002) Normal and tumor-derived myoepithelial cells differ in their ability to interact with luminal breast epithelial cells for polarity and basement membrane deposition. J Cell Sci 115:39–50

123. Shen Y, Shen R, Ge L, et al (2012) Fibrillar type I collagen matrices enhance metastasis/invasion of ovarian epithelial cancer via beta1 integrin and PTEN

signals. Int J Gynecol Cancer 22:1316–1324 . doi: 10.1097/IGC.0b013e318263ef34 [doi]

124. Graham JS, Vomund AN, Phillips CL, Grandbois M (2004) Structural changes in human type I collagen fibrils investigated by force spectroscopy. Exp Cell Res 299:335–342

125. Levental KR, Yu H, Kass L, et al (2009) Matrix Crosslinking Forces Tumor Progression by Enhancing Integrin Signaling. Cell 139:891–906 . doi: 10.1016/j.cell.2009.10.027

126. Oskarsson T, Hynes RO, Muschler J, et al (2013) Extracellular matrix components in breast cancer progression and metastasis. The Breast 22:S66--S72 . doi: 10.1016/j.breast.2013.07.012

127. Howlett AR, Bissell MJ (1993) The influence of tissue microenvironment (stroma and extracellular matrix) on the development and function of mammary epithelium. Epithelial Cell Biol 2:79–89

128. Chaudhuri O, Koshy ST, Branco da Cunha C, et al (2014) Extracellular matrix stiffness and composition jointly regulate the induction of malignant phenotypes in mammary epithelium. Nat Mater 13:970–978 . doi: 10.1038/nmat4009

129. Pellegrinelli V, Heuvingh J, du Roure O, et al (2014) Human adipocyte function is impacted by mechanical cues. J Pathol 233:183–195 . doi: 10.1002/path.4347

130. Chanmee T, Ontong P, Konno K, Itano N (2014) Tumor-associated macrophages

as major players in the tumor microenvironment. Cancers (Basel). 6:1670–1690

131. Arendt LM, Kuperwasser C (2015) Working stiff: how obesity boosts cancer risk. Sci Transl Med 7:301fs34 . doi: 10.1126/scitranslmed.aac9446

132. Tyan S-W, Kuo W-H, Huang C-K, et al (2011) Breast Cancer Cells Induce Cancer-Associated Fibroblasts to Secrete Hepatocyte Growth Factor to Enhance Breast Tumorigenesis. PLoS One 6:e15313 . doi: 10.1371/journal.pone.0015313

133. Duong MN, Geneste A, Fallone F, et al (2017) The fat and the bad: Mature adipocytes, key actors in tumor progression and resistance. Oncotarget 8:57622–57641 . doi: 10.18632/oncotarget.18038

134. Duval K, Grover H, Han L-H, et al (2017) Modeling Physiological Events in 2D vs. 3D Cell Culture. Physiology (Bethesda) 32:266–277 . doi: 10.1152/physiol.00036.2016

135. Kenny PA, Lee GY, Myers CA, et al (2007) The morphologies of breast cancer cell lines in three-dimensional assays correlate with their profiles of gene expression. Mol Oncol 1:84–96 . doi: 10.1016/j.molonc.2007.02.004

136. Ravi M, Paramesh V, Kaviya SR, et al (2015) 3D Cell Culture Systems: Advantages and Applications. J Cell Physiol 230:16–26 . doi: 10.1002/jcp.24683

137. Baker BM, Chen CS (2012) Deconstructing the third dimension: how 3D culture microenvironments alter cellular cues. J Cell Sci 125:3015–24 . doi: 10.1242/jcs.079509

138. Luca AC, Mersch S, Deenen R, et al (2013) Impact of the 3D Microenvironment on Phenotype, Gene Expression, and EGFR Inhibition of Colorectal Cancer Cell Lines. PLoS One 8:e59689 . doi: 10.1371/journal.pone.0059689

139. Aljitawi OS, Li D, Xiao Y, et al (2014) A novel three-dimensional stromal-based model for in vitro chemotherapy sensitivity testing of leukemia cells. Leuk Lymphoma 55:378–391 . doi: 10.3109/10428194.2013.793323

140. Fang Y, Eglen RM (2017) Three-Dimensional Cell Cultures in Drug Discovery and Development. SLAS Discov 22:456–472 . doi: 10.1177/1087057117696795

141. Bidarra SJ, Oliveira P, Rocha S, et al (2016) A 3D in vitro model to explore the inter-conversion between epithelial and mesenchymal states during EMT and its reversion. Sci Rep 6:27072 . doi: 10.1038/srep27072

142. Salameh TS, Le TT, Nichols MB, et al (2013) An ex vivo co-culture model system to evaluate stromal-epithelial interactions in breast cancer. Int J Cancer 132:288–296 . doi: 10.1002/ijc.27672

143. Herroon MK, Diedrich JD, Podgorski I (2016) New 3D-Culture Approaches to Study Interactions of Bone Marrow Adipocytes with Metastatic Prostate Cancer Cells. Front Endocrinol (Lausanne) 7:84 . doi: 10.3389/fendo.2016.00084

144. Kay R, Rosten PM, Humphries RK (1991) CD24, a signal transducer modulating B cell activation responses, is a very short peptide with a glycosyl phosphatidylinositol membrane anchor. J Immunol 147:1412–1416

145. Springer T, Galfrè G, Secher DS, Milstein C (1978) Monoclonal xenogeneic antibodies to murine cell surface antigens: identification of novel leukocyte differentiation antigens. Eur J Immunol 8:539–551 . doi: 10.1002/eji.1830080802

146. Motari E, Zheng X, Su X, et al (2009) Analysis of Recombinant CD24 Glycans by MALDI-TOF-MS Reveals Prevalence of Sialyl-T Antigen. Am J Biomed Sci 1:1–11 . doi: 10.5099/aj090100001

147. Ohl C, Albach C, Altevogt P, Schmitz B (2003) N-glycosylation patterns of HSA/CD24 from different cell lines and brain homogenates: a comparison. Biochimie 85:565–73

148. Pruitt KD, Brown GR, Hiatt SM, et al (2014) RefSeq: an update on mammalian reference sequences. Nucleic Acids Res 42:D756–D763 . doi: 10.1093/nar/gkt1114

149. Hough MR, Rosten PM, Sexton TL, et al (1994) Mapping of CD24 and homologous sequences to multiple chromosomal loci. Genomics 22:154–61 . doi: 10.1006/geno.1994.1356

150. Fang X, Zheng P, Tang J, Liu Y (2010) CD24: from A to Z. Cell Mol Immunol 7:100–103 . doi: 10.1038/cmi.2009.119;

151. Ju JH, Jang K, Lee KM, et al (2011) CD24 enhances DNA damage-induced apoptosis by modulating NF-kappaB signaling in CD44-expressing breast cancer cells. Carcinogenesis 32:1474–1483 . doi: 10.1093/carcin/bgr173;

152. Ibrahim SA, Hassan H, Vilardo L, et al (2013) Syndecan-1 (CD138) Modulates Triple-Negative Breast Cancer Stem Cell Properties via Regulation of LRP-6 and IL-6-Mediated STAT3 Signaling. PLoS One 8:e85737 . doi: 10.1371/journal.pone.0085737

153. McGowan PM, Simedrea C, Ribot EJ, et al (2011) Notch1 inhibition alters the CD44hi/CD24lo population and reduces the formation of brain metastases from breast cancer. Mol Cancer Res 9:834–44 . doi: 10.1158/1541-7786.MCR-10-0457

154. Vazquez-Martin A, Oliveras-Ferraros C, Cufí S, et al (2011) The anti-diabetic drug metformin suppresses the metastasis-associated protein CD24 in MDA-MB-468 triple-negative breast cancer cells. Oncol Rep 25:135–40

155. Vazquez-Martin A, Oliveras-Ferraros C, Cufí S, et al (2010) Metformin regulates breast cancer stem cell ontogeny by transcriptional regulation of the epithelial-mesenchymal transition (EMT) status. Cell Cycle 9:3807–14

156. Li X, Zhou N, Wang J, et al (2018) Quercetin suppresses breast cancer stem cells (CD44 + /CD24 −) by inhibiting the PI3K/Akt/mTOR-signaling pathway. Life Sci 196:56–62 . doi: 10.1016/j.lfs.2018.01.014

157. Wang L, Liu R, Li D, et al (2012) A hypermorphic SP1-binding CD24 variant associates with risk and progression of multiple sclerosis. Am J Transl Res 4:347–356

158. Berga-Bolaños R, Drews-Elger K, Aramburu J, López-Rodríguez C (2010)

NFAT5 Regulates T Lymphocyte Homeostasis and CD24-Dependent T Cell Expansion under Pathologic Hypernatremia. J Immunol 185:6624–6635 . doi: 10.4049/jimmunol.1001232

159. Vesuna F, Lisok A, Kimble B, Raman V (2009) Twist modulates breast cancer stem cells by transcriptional regulation of CD24 expression. Neoplasia 11:1318–1328

160. Liu AY, Cai Y, Mao Y, et al (2014) Twist2 promotes self-renewal of liver cancer stem-like cells by regulating CD24. Carcinogenesis 35:537–545 . doi: 10.1093/carcin/bgt364

161. Shulewitz M, Soloviev I, Wu T, et al (2006) Repressor roles for TCF-4 and Sfrp1 in Wnt signaling in breast cancer. Oncogene 25:4361–9 . doi: 10.1038/sj.onc.1209470

162. Pass MK, Quintini G, Zarn JA, et al (1998) The 5'-flanking region of human CD24 gene has cell-type-specific promoter activity in small-cell lung cancer. Int J cancerJournal Int du cancer 78:496–502

163. Kent WJ, Sugnet CW, Furey TS, et al (2002) The Human Genome Browser at UCSC. Genome Res 12:996–1006 . doi: 10.1101/gr.229102

164. Fukushima T, Tezuka T, Shimomura T, et al (2007) Silencing of insulin-like growth factor-binding protein-2 in human glioblastoma cells reduces both invasiveness and expression of progression-associated gene CD24. J Biol Chem

282:18634–18644 . doi: 10.1074/jbc.M609567200

165. Riau AK, Wong TT, Lan W, et al (2011) Aberrant DNA methylation of matrix remodeling and cell adhesion related genes in pterygium. PLoS One 6:e14687 . doi: 10.1371/journal.pone.0014687;

166. Zhou Q, Guo Y, Liu Y (1998) Regulation of the stability of heat-stable antigen mRNA by interplay between two novel cis elements in the 3' untranslated region. Mol Cell Biol 18:815–26

167. Wang L, Lin S, Rammohan KW, et al (2007) A dinucleotide deletion in CD24 confers protection against autoimmune diseases. PLoS Genet 3:e49 . doi: 10.1371/journal.pgen.0030049

168. Muppala S, Mudduluru G, Leupold JH, et al (2013) CD24 induces expression of the oncomir miR-21 via Src, and CD24 and Src are both post-transcriptionally downregulated by the tumor suppressor miR-34a. PLoS One 8:e59563 . doi: 10.1371/journal.pone.0059563;

169. Kaipparettu BA, Malik S, Konduri SD, et al (2008) Estrogen-mediated downregulation of CD24 in breast cancer cells. Int J cancerJournal Int du cancer 123:66–72 . doi: 10.1002/ijc.23480;

170. Overdevest JB, Knubel KH, Duex JE, et al (2012) CD24 expression is important in male urothelial tumorigenesis and metastasis in mice and is androgen regulated. Proc Natl Acad Sci U S A 109:E3588-96 . doi: 10.1073/pnas.1113960109;

171. Liu W, Vadgama J V (2000) Identification and characterization of amino acid starvation-induced CD24 gene in MCF-7 human breast cancer cells. Int J Oncol 16:1049–54

172. Hira SK, Manna PP (2012) Down regulation of CD24 and HER-2/neu in breast carcinoma cells by activated human dendritic cell. Role of STAT3. Cell Immunol 275:69–79 . doi: 10.1016/j.cellimm.2012.02.015

173. Zheng J, Liu Q, Li Y, et al (2010) NDRG2 expression regulates CD24 and metastatic potential of breast cancer cells. Asian Pac J Cancer Prev 11:1817–21

174. Cao X, Geradts J, Dewhirst MW, Lo H-WW (2012) Upregulation of VEGF-A and CD24 gene expression by the tGLI1 transcription factor contributes to the aggressive behavior of breast cancer cells. Oncogene 31:104–115 . doi: 10.1038/onc.2011.219;

175. Thomas S, Harding MA, Smith SC, et al (2012) CD24 is an effector of HIF-1-driven primary tumor growth and metastasis. Cancer Res 72:5600–5612 . doi: 10.1158/0008-5472.CAN-11-3666;

176. Schubbert S, Shannon K, Bollag G (2007) Hyperactive Ras in developmental disorders and cancer. Nat Rev 7:295–308 . doi: 10.1038/nrc2109

177. Foulkes WD, Smith IE, Reis-Filho JS (2010) Triple-Negative Breast Cancer. N Engl J Med 363:1938–1948 . doi: 10.1056/NEJMra1001389

178. McLaughlin SK, Olsen SN, Dake B, et al (2013) The RasGAP gene, RASAL2, is a

tumor and metastasis suppressor. Cancer Cell 24:365–78 . doi: 10.1016/j.ccr.2013.08.004

179. McCubrey JA, Steelman LS, Chappell WH, et al (2012) Ras/Raf/MEK/ERK and PI3K/PTEN/Akt/mTOR cascade inhibitors: how mutations can result in therapy resistance and how to overcome resistance. Oncotarget 3:1068–1111

180. Feig LA (2003) Ral-GTPases: approaching their 15 minutes of fame. Trends Cell Biol 13:419–425 . doi: http://dx.doi.org/10.1016/S0962-8924(03)00152-1

181. Aksamitiene E, Kiyatkin A, Kholodenko BN (2012) Cross-talk between mitogenic Ras/MAPK and survival PI3K/Akt pathways: a fine balance. Biochem Soc Trans 40:139–146 . doi: 10.1042/BST20110609;

182. Pylayeva-Gupta Y, Grabocka E, Bar-Sagi D (2011) RAS oncogenes: weaving a tumorigenic web. Nat Rev 11:761–774 . doi: 10.1038/nrc3106;

183. Giehl K (2005) Oncogenic Ras in tumour progression and metastasis. Biol Chem 386:193–205 . doi: 10.1515/BC.2005.025

184. Brabletz T, Kalluri R, Nieto MA, Weinberg RA (2018) EMT in cancer. Nat Rev Cancer 18:128–134 . doi: 10.1038/nrc.2017.118

185. Vleminckx K, Vakaet L, Mareel M, et al (1991) Genetic manipulation of E-cadherin expression by epithelial tumor cells reveals an invasion suppressor role. Cell 66:107–19

186. Mahler-Araujo B, Savage K, Parry S, Reis-Filho JS (2008) Reduction of E-cadherin expression is associated with non-lobular breast carcinomas of basal-like and triple negative phenotype. J Clin Pathol 61:615–620 . doi: 10.1136/jcp.2007.053991

187. Gravdal K, Halvorsen OJ, Haukaas SA, Akslen LA (2007) A Switch from E-Cadherin to N-Cadherin Expression Indicates Epithelial to Mesenchymal Transition and Is of Strong and Independent Importance for the Progress of Prostate Cancer. Clin Cancer Res 13:7003–7011 . doi: 10.1158/1078-0432.CCR-07-1263

188. Prat A, Parker JS, Karginova O, et al (2010) Phenotypic and molecular characterization of the claudin-low intrinsic subtype of breast cancer. Breast Cancer Res 12:R68 . doi: 10.1186/bcr2635

189. Kominsky SL, Argani P, Korz D, et al (2003) Loss of the tight junction protein claudin-7 correlates with histological grade in both ductal carcinoma in situ and invasive ductal carcinoma of the breast. Oncogene 22:2021–2033 . doi: 10.1038/sj.onc.1206199

190. Osanai M, Murata M, Nishikiori N, et al (2007) Occludin-mediated premature senescence is a fail-safe mechanism against tumorigenesis in breast carcinoma cells. Cancer Sci 98:1027–1034 . doi: 10.1111/j.1349-7006.2007.00494.x

191. Martin TA, Watkins G, Mansel RE, Jiang WG (2004) Loss of tight junction plaque

molecules in breast cancer tissues is associated with a poor prognosis in patients with breast cancer. Eur J Cancer 40:2717–2725 . doi: 10.1016/J.EJCA.2004.08.008

192. Brown RL, Reinke LM, Damerow MS, et al (2011) CD44 splice isoform switching in human and mouse epithelium is essential for epithelial-mesenchymal transition and breast cancer progression. J Clin Invest 121:1064–1074 . doi: 10.1172/JCI44540

193. Liu C-Y, Lin H-H, Tang M-J, Wang Y-K (2015) Vimentin contributes to epithelial-mesenchymal transition cancer cell mechanics by mediating cytoskeletal organization and focal adhesion maturation. Oncotarget 6:15966–83 . doi: 10.18632/oncotarget.3862

194. Yamashita N, Tokunaga E, Kitao H, et al (2013) Vimentin as a poor prognostic factor for triple-negative breast cancer. J Cancer Res Clin Oncol 139:739–746 . doi: 10.1007/s00432-013-1376-6

195. McInroy L, Määttä A (2007) Down-regulation of vimentin expression inhibits carcinoma cell migration and adhesion. Biochem Biophys Res Commun 360:109–14 . doi: 10.1016/j.bbrc.2007.06.036

196. Mendez MG, Kojima S-I, Goldman RD (2010) Vimentin induces changes in cell shape, motility, and adhesion during the epithelial to mesenchymal transition. FASEB J 24:1838–51 . doi: 10.1096/fj.09-151639

197. Sun BO, Fang Y, Li Z, et al (2015) Role of cellular cytoskeleton in epithelial-

mesenchymal transition process during cancer progression. Biomed reports 3:603–610 . doi: 10.3892/br.2015.494

198. Shankar J, Nabi IR (2015) Actin cytoskeleton regulation of epithelial mesenchymal transition in metastatic cancer cells. PLoS One 10:e0119954 . doi: 10.1371/journal.pone.0119954

199. Bienz M (2005) beta-Catenin: a pivot between cell adhesion and Wnt signalling. Curr Biol 15:R64-7 . doi: 10.1016/j.cub.2004.12.058

200. Liu F, Gu L-N, Shan B-E, et al (2016) Biomarkers for EMT and MET in breast cancer: An update. Oncol Lett 12:4869–4876 . doi: 10.3892/ol.2016.5369

201. Puisieux A, Brabletz T, Caramel J (2014) Oncogenic roles of EMT-inducing transcription factors. Nat Cell Biol 16:488–494 . doi: 10.1038/ncb2976

202. Lamouille S, Xu J, Derynck R (2014) Molecular mechanisms of epithelial-mesenchymal transition. Nat Rev Mol Cell Biol 15:178–96 . doi: 10.1038/nrm3758

203. Nieman KM, Romero IL, Van Houten B, Lengyel E (2013) Adipose tissue and adipocytes support tumorigenesis and metastasis. Biochim Biophys Acta - Mol Cell Biol Lipids 1831:1533–1541 . doi: 10.1016/j.bbalip.2013.02.010

204. Divella R, De Luca R, Abbate I, et al (2016) Obesity and cancer: the role of adipose tissue and adipo-cytokines-induced chronic inflammation. J Cancer 7:2346–2359 . doi: 10.7150/jca.16884

205. Ribeiro RJT, Monteiro CPD, Cunha VFPM, et al (2012) Tumor Cell-educated Periprostatic Adipose Tissue Acquires an Aggressive Cancer-promoting Secretory Profile. Cell Physiol Biochem 29:233–240 . doi: 10.1159/000337604

206. Nieman KM, Kenny HA, Penicka C V, et al (2011) Adipocytes promote ovarian cancer metastasis and provide energy for rapid tumor growth. Nat Med 17:1498–1503 . doi: 10.1038/nm.2492

207. Abramczyk H, Surmacki J, Kopeć M, et al (2015) The role of lipid droplets and adipocytes in cancer. Raman imaging of cell cultures: MCF10A, MCF7, and MDA-MB-231 compared to adipocytes in cancerous human breast tissue. Analyst 140:2224–2235 . doi: 10.1039/c4an01875c

208. Zoico E, Darra E, Rizzatti V, et al (2018) Role of adipose tissue in melanoma cancer microenvironment and progression. Int J Obes 42:344–352 . doi: 10.1038/ijo.2017.218

209. Peinado JR, Pardo M, de la Rosa O, Malagón MM (2012) Proteomic characterization of adipose tissue constituents, a necessary step for understanding adipose tissue complexity. Proteomics 12:607–620 . doi: 10.1002/pmic.201100355

210. Iikuni N, Lam QLK, Lu L, et al (2008) Leptin and Inflammation. Curr Immunol Rev 4:70–79 . doi: 10.2174/157339508784325046

211. Ray A, Nkhata KJ, Cleary MP (2007) Effects of leptin on human breast cancer cell lines in relationship to estrogen receptor and HER2 status. Int J Oncol 30:1499–

1509

212. Jardé T, Caldefie-Chézet F, Damez M, et al (2008) Leptin and leptin receptor involvement in cancer development: A study on human primary breast carcinoma. Oncol Rep 19:905–911

213. Mullen M, Gonzalez-Perez RR (2016) Leptin-Induced JAK/STAT Signaling and Cancer Growth. Vaccines 4:26 . doi: 10.3390/vaccines4030026

214. Nepal S, Kim MJ, Hong JT, et al (2015) Autophagy induction by leptin contributes to suppression of apoptosis in cancer cells and xenograft model: involvement of p53/FoxO3A axis. Oncotarget 6:7166–81 . doi: 10.18632/oncotarget.3347

215. Zheng Q, Banaszak L, Fracci S, et al (2013) Leptin receptor maintains cancer stem-like properties in triple negative breast cancer cells. Endocr Relat Cancer 20:797–808 . doi: 10.1530/ERC-13-0329

216. Kwon H, Pessin JE (2013) Adipokines mediate inflammation and insulin resistance. Front Endocrinol (Lausanne) 4:71 . doi: 10.3389/fendo.2013.00071

217. Shehzad A, Iqbal W, Shehzad O, Lee YS (2012) Adiponectin: regulation of its production and its role in human diseases. Horm 11:8–20

218. Sultana R, Kataki AC, Borthakur BB, et al (2017) Imbalance in leptin-adiponectin levels and leptin receptor expression as chief contributors to triple negative breast cancer progression in Northeast India. Gene 621:51–58 . doi: 10.1016/j.gene.2017.04.021

219. Gyamfi J, Eom M, Koo J-S, Choi J (2018) Multifaceted Roles of Interleukin-6 in Adipocyte–Breast Cancer Cell Interaction. Transl Oncol 11:275–285 . doi: 10.1016/J.TRANON.2017.12.009

220. Esquivel-Velázquez M, Ostoa-Saloma P, Palacios-Arreola MI, et al (2015) The role of cytokines in breast cancer development and progression. J Interferon Cytokine Res 35:1–16 . doi: 10.1089/jir.2014.0026

221. Pileczki V, Braicu C, Gherman C, Berindan-Neagoe I (2012) TNF-α Gene Knockout in Triple Negative Breast Cancer Cell Line Induces Apoptosis. Int J Mol Sci 14:411–420 . doi: 10.3390/ijms14010411

222. Li J, Han X (2018) Adipocytokines and breast cancer. Curr Probl Cancer 0: . doi: 10.1016/j.currproblcancer.2018.01.004

223. Christopoulos PF, Msaouel P, Koutsilieris M, et al (2015) The role of the insulin-like growth factor-1 system in breast cancer. Mol Cancer 14:43 . doi: 10.1186/s12943-015-0291-7

224. Creighton CJ, Casa A, Lazard Z, et al (2008) Insulin-Like Growth Factor-I Activates Gene Transcription Programs Strongly Associated With Poor Breast Cancer Prognosis. J Clin Oncol 26:4078–4085 . doi: 10.1200/JCO.2007.13.4429

225. Pollak M (2008) Insulin and insulin-like growth factor signalling in neoplasia. Nat Rev Cancer 8:915–928 . doi: 10.1038/nrc2536

226. Edakuni G, Sasatomi E, Satoh T, et al (2001) Expression of the hepatocyte growth

factor/c-Met pathway is increased at the cancer front in breast carcinoma. Pathol Int 51:172–8

227. Bell LN, Ward JL, Degawa-Yamauchi M, et al (2006) Adipose tissue production of hepatocyte growth factor contributes to elevated serum HGF in obesity. Am J Physiol Metab 291:E843–E848 . doi: 10.1152/ajpendo.00174.2006

228. Ojima K, Oe M, Nakajima I, et al (2016) Dynamics of protein secretion during adipocyte differentiation. FEBS Open Bio

229. Sun K, Tordjman J, Clément K, Scherer PE (2013) Fibrosis and Adipose Tissue Dysfunction. Cell Metab 18:470–477 . doi: 10.1016/j.cmet.2013.06.016

230. Mariman EC, Wang P (2010) Adipocyte extracellular matrix composition, dynamics and role in obesity. Cel 67:1277–Mo fe S

231. Iyengar P, Espina V, Williams TW, et al (2005) Adipocyte-derived collagen VI affects early mammary tumor progression in vivo, demonstrating a critical interaction in the tumor/stroma microenvironment. J Clin Invest 115:1163–1176 . doi: 10.1172/JCI23424

232. Park J, Scherer PE (2012) Adipocyte-derived endotrophin promotes malignant tumor progression. J Clin Invest 122:4243–4256 . doi: 10.1172/JCI63930

233. Chavey C, Mari B, Monthouel M-N, et al (2003) Matrix Metalloproteinases Are Differentially Expressed in Adipose Tissue during Obesity and Modulate Adipocyte Differentiation. J Biol Chem 278:11888–11896 . doi:

10.1074/jbc.M209196200

234. Jia L, Wang S, Cao J, et al (2007) siRNA targeted against matrix metalloproteinase 11 inhibits the metastatic capability of murine hepatocarcinoma cell Hca-F to lymph nodes. Int J Biochem Cell Biol 39:2049–2062 . doi: 10.1016/j.biocel.2007.05.023

235. Templeton ZS, Lie W-RR, Wang W, et al (2015) Breast Cancer Cell Colonization of the Human Bone Marrow Adipose Tissue Niche. Neoplasia 17:849–861 . doi: 10.1016/j.neo.2015.11.005

236. Ward PS, Thompson CB (2012) Metabolic reprogramming: a cancer hallmark even warburg did not anticipate. Cancer Cell 21:297–308 . doi: 10.1016/j.ccr.2012.02.014

237. Beloribi-Djefaflia S, Vasseur S, Guillaumond F (2016) Lipid metabolic reprogramming in cancer cells. Oncogenesis 5:e189–e189 . doi: 10.1038/oncsis.2015.49

238. Vander Heiden M, Cantley L, Thompson C (2009) Understanding the Warburg effect: The metabolic Requiremetns of cell proliferation. Science (80-) 324:1029–1033 . doi: 10.1126/science.1160809;

239. Pavlides S, Whitaker-Menezes D, Castello-Cros R, et al (2009) The reverse Warburg effect: Aerobic glycolysis in cancer associated fibroblasts and the tumor stroma. Cell Cycle 8:3984–4001 . doi: 10.4161/cc.8.23.10238

240. Martinez-Outschoorn UE, Pestell RG, Howell A, et al (2011) Energy transfer in "parasitic" cancer metabolism: mitochondria are the powerhouse and Achilles' heel of tumor cells. Cell Cycle 10:4208–16 . doi: 10.4161/cc.10.24.18487

241. Fadaka A, Ajiboye B, Ojo O, et al (2017) Biology of glucose metabolization in cancer cells. J Oncol Sci 3:45–51 . doi: 10.1016/J.JONS.2017.06.002

242. Santos CR, Schulze A (2012) Lipid metabolism in cancer. FEBS J 279:2610–2623 . doi: 10.1111/j.1742-4658.2012.08644.x

243. Balaban S, Shearer RF, Lee LS, et al (2017) Adipocyte lipolysis links obesity to breast cancer growth: adipocyte-derived fatty acids drive breast cancer cell proliferation and migration. Cancer Metab 5:1 . doi: 10.1186/s40170-016-0163-7

244. Guaita-Esteruelas S, Gumà J, Masana L, Borràs J (2018) The peritumoural adipose tissue microenvironment and cancer. The roles of fatty acid binding protein 4 and fatty acid binding protein 5. Mol Cell Endocrinol 462:107–118 . doi: 10.1016/J.MCE.2017.02.002

245. Fagone P, Jackowski S (2009) Membrane phospholipid synthesis and endoplasmic reticulum function. J Lipid Res 50 Suppl:S311-6 . doi: 10.1194/jlr.R800049-JLR200

246. Pascual G, Avgustinova A, Mejetta S, et al (2017) Targeting metastasis-initiating cells through the fatty acid receptor CD36. Nature 541:41–45 . doi:

10.1038/nature20791

247. Lazar I, Clement E, Dauvillier S, et al (2016) Adipocyte Exosomes Promote Melanoma Aggressiveness through Fatty Acid Oxidation: A Novel Mechanism Linking Obesity and Cancer. Cancer Res 76:4051–4057 . doi: 10.1158/0008-5472.CAN-16-0651 [doi]

248. Cunningham F, Amode MR, Barrell D, et al (2015) Ensembl 2015. Nucleic Acids Res. doi: 10.1093/nar/gku1010

249. Hall TATA (1999) BioEdit: a user-friendly biological sequence alignment editor and analysis program for Windows 95/98/NT. Nucleic Acid Symp Ser 41:95 . doi: citeulike-article-id:691774

250. Felsenstein J (1981) Evolutionary trees from DNA sequences: a maximum likelihood approach. J Mol Evol. doi: 10.1007/BF01734359

251. Kimura M (1980) A simple method for estimating evolutionary rates of base substitutions through comparative studies of nucleotide sequences. J Mol Evol. doi: 10.1007/BF01731581

252. Tamura K, Stecher G, Peterson D, et al (2013) MEGA6: Molecular Evolutionary Genetics Analysis version 6.0. Mol Biol Evol. doi: 10.1093/molbev/mst197

253. Felsenstein J (1985) Confidence limits on phylogenies: an approach using the bootstrap. Evolution (N Y). doi: 10.2307/2408678

254. Warren WC, Hillier LDW, Marshall Graves JA, et al (2008) Genome analysis of the platypus reveals unique signatures of evolution. Nature 453:175–183 . doi: 10.1038/nature06936

255. Mikkelsen TS, Wakefield MJ, Aken B, et al (2007) Genome of the marsupial Monodelphis domestica reveals innovation in non-coding sequences. Nature 447:167–177 . doi: 10.1038/nature05805

256. Murchison EP, Schulz-Trieglaff OB, Ning Z, et al (2012) Genome sequencing and analysis of the Tasmanian devil and its transmissible cancer. Cell 148:780–791 . doi: 10.1016/j.cell.2011.11.065

257. Renfree MB, Papenfuss AT, Deakin JE, et al (2011) Genome sequence of an Australian kangaroo, Macropus eugenii, provides insight into the evolution of mammalian reproduction and development. Genome Biol 12:R81 . doi: 10.1186/gb-2011-12-8-r81

258. Crooks GE, Hon G, Chandonia JM, Brenner SE (2004) WebLogo: A sequence logo generator. Genome Res 14:1188–1190 . doi: 10.1101/gr.849004

259. Yang J, Zhang Y (2015) I-TASSER server: New development for protein structure and function predictions. Nucleic Acids Res 43:W174–W181 . doi: 10.1093/nar/gkv342

260. Zhang T, Faraggi E, Xue B, et al (2012) Spine-d: Accurate prediction of short and long disordered regions by a single neural-network based method. J Biomol Struct

Dyn 29:799–813 . doi: 10.1080/073911012010525022

261. Edgar R, Domrachev M, Lash AE (2002) Gene Expression Omnibus: NCBI gene expression and hybridization array data repository. Nucleic Acids Res 30:207–210

262. Carvalho B, Bengtsson H, Speed TP, Irizarry RA (2007) Exploration, normalization, and genotype calls of high-density oligonucleotide SNP array data. Biostatistics 8:485–499 . doi: 10.1093/biostatistics/kxl042

263. Team RC, R Core Team (2014) R: A Language and Environment for Statistical Computing. R Found Stat Comput Vienna, Austria 2014 . doi: 10.1017/CBO9781107415324.004

264. Sturn A, Quackenbush J, Trajanoski Z (2002) Genesis: cluster analysis of microarray data. Bioinformatics 18:207–208

265. Girardini JE, Napoli M, Piazza S, et al (2011) A Pin1/Mutant p53 Axis Promotes Aggressiveness in Breast Cancer. Cancer Cell 20:79–91 . doi: http://dx.doi.org/10.1016/j.ccr.2011.06.004

266. Liu S, Cong Y, Wang D, et al (2014) Breast cancer stem cells transition between epithelial and mesenchymal states reflective of their normal counterparts. Stem cell reports 2:78–91 . doi: 10.1016/j.stemcr.2013.11.009

267. Madak-Erdogan Z, Lupien M, Stossi F, et al (2011) Genomic Collaboration of Estrogen Receptor a and Extracellular Signal-Regulated Kinase 2 in Regulating Gene and Proliferation Programs. Mol Cell Biol 31:226–236 . doi:

10.1128/MCB.00821-10

268. Huang Y, Fernandez S V, Goodwin S, et al (2007) Epithelial to Mesenchymal Transition in Human Breast Epithelial Cells Transformed by 17ß-Estradiol. Cancer Res 67:11147–11157 . doi: 10.1158/0008-5472.CAN-07-1371

269. Battcock SM, Collier TW, Zu D, Hirasawa K (2006) Negative Regulation of the Alpha Interferon-Induced Antiviral Response by the Ras/Raf/MEK Pathway. J Virol 80:4422–4430 . doi: 10.1128/JVI.80.9.4422-4430.2006

270. Davies SP, Reddy H, Caivano M, Cohen P (2000) Specificity and mechanism of action of some commonly used protein kinase inhibitors. Biochem J 351:95–105

271. Xue L, Gyles SL, Barrow A, Pettipher R (2007) Inhibition of PI3K and calcineurin suppresses chemoattractant receptor-homologous molecule expressed on Th2 cells (CRTH2)-dependent responses of Th2 lymphocytes to prostaglandin D(2). Biochem Pharmacol 73:843–853 . doi: 10.1016/j.bcp.2006.11.021

272. Smith NC, Fairbridge NA, Pallegar NK, Christian SL (2014) Dynamic upregulation of CD24 in pre-adipocytes promotes adipogenesis. Adipocyte 4:89–100 . doi: 10.4161/21623945.2014.985015

273. Lemma S, Avnet S, Salerno M, et al (2016) Identification and Validation of Housekeeping Genes for Gene Expression Analysis of Cancer Stem Cells. PLoS One 11:e0149481 . doi: 10.1371/journal.pone.0149481

274. Livak KJ, Schmittgen TD (2001) Analysis of relative gene expression data using

real-time quantitative PCR and the 2(-Delta Delta C(T)) Method. Methods 25:402–408 . doi: 10.1006/meth.2001.1262

275. Team RC (2015) R: A Language and Environment for Statistical Computing. R Foundation for Statistical Computing, Vienna, Austria

276. RStudio Team (2015) RStudio: Integrated Development for R. RStudio, Inc., Boston, MA

277. Debnath J, Muthuswamy SK, Brugge JS (2003) Morphogenesis and oncogenesis of MCF-10A mammary epithelial acini grown in three-dimensional basement membrane cultures. Methods 30:256–68

278. Simpson KJ, Dugan AS, Mercurio AM (2004) Functional Analysis of the Contribution of RhoA and RhoC GTPases to Invasive Breast Carcinoma. Cancer Res 64:8694–8701 . doi: 10.1158/0008-5472.CAN-04-2247

279. Schneider CA, Rasband WS, Eliceiri KW (2012) NIH Image to ImageJ: 25 years of image analysis. Nat Methods 9:671–675

280. Grishagin I V (2015) Automatic cell counting with ImageJ

281. Tan Y, Zhao M, Xiang B, et al (2015) CD24: from a Hematopoietic Differentiation Antigen to a Genetic Risk Factor for Multiple Autoimmune Diseases. Clin Rev Allergy Immunol 1–14 . doi: 10.1007/s12016-015-8470-2

282. Shirasawa T, Akashi T, Sakamoto K, et al (1993) Gene expression of CD24 core

peptide molecule in developing brain and developing non-neural tissues. Dev. Dyn.,. Dev Dyn 198: 1–13.:1–13 . doi: 10.1002/aja.1001980102

283. Medzihradszky KF (2008) Characterization of Site-specific N-Glycosylation. In: Post-translational Modifi cations of Proteins. Humana Press, Totowa, NJ, pp 293–316

284. Hitsumoto Y, Nakano A, Ohnishi H, et al (1992) Purification of the murine heat-stable antigen from erythrocytes. Biochem Biophys Res Commun 187:773–777 . doi: 10.1016/0006-291X(92)91262-O

285. Finn RD, Bateman A, Clements J, et al (2014) Pfam: the protein families database. Nucleic Acids Res 42:D222–D230 . doi: 10.1093/nar/gkt1223

286. Chen G-Y, Chen X, King S, et al (2011) Amelioration of sepsis by inhibiting sialidase-mediated disruption of the CD24-SiglecG interaction. Nat Biotechnol 29:428–435 . doi: 10.1038/nbt.1846

287. Kay R, Rosten PM, Humphries RK (1991) CD24, a signal transducer modulating B cell activation responses, is a very short peptide with a glycosyl phosphatidylinositol membrane anchor. J Immunol 147:1412–1416

288. Lieberoth A, Splittstoesser F, Katagihallimath N, et al (2009) Lewis(x) and alpha2,3-sialyl glycans and their receptors TAG-1, Contactin, and L1 mediate CD24-dependent neurite outgrowth. J Neurosci 29:6677–90 . doi: 10.1523/JNEUROSCI.4361-08.2009

289. EVANS SE (2003) At the feet of the dinosaurs: the early history and radiation of lizards. Biol Rev 78:S1464793103006134 . doi: 10.1017/S1464793103006134

290. Nagy B, Berkes E, Rigó B, et al (2008) Under-Expression of CD24 in Pre-Eclamptic Placental Tissues Determined by Quantitative Real-Time RT-PCR. Fetal Diagn Ther 23:263–266 . doi: 10.1159/000123612

291. Keller S, Rupp C, Stoeck A, et al (2007) CD24 is a marker of exosomes secreted into urine and amniotic fluid. Kidney Int 72:1095–1102 . doi: 10.1038/sj.ki.5002486

292. Dunker AK, Lawson JD, Brown CJ, et al (2001) Intrinsically disordered protein. J Mol Graph Model 19:26–59

293. Perez RB, Tischer A, Auton M, Whitten ST (2014) Alanine and proline content modulate global sensitivity to discrete perturbations in disordered proteins. Proteins Struct Funct Bioinforma 82:3373–3384 . doi: 10.1002/prot.24692

294. Jentoft N (1990) Why are proteins O-glycosylated? Trends Biochem Sci 15:291–4

295. Ayre DC, Pallegar NK, Fairbridge NA, et al (2016) Analysis of the structure, evolution, and expression of CD24, an important regulator of cell fate. Gene. doi: 10.1016/j.gene.2016.05.038

296. Komatsu Y, Hirasawa K, Christian SL (2015) Global gene analysis identifying genes commonly regulated by the Ras/Raf/MEK and type I IFN pathways. Genomics data 4:84–7 . doi: 10.1016/j.gdata.2015.03.012

297. Christian SL, Collier TW, Zu D, et al (2009) Activated Ras/MEK inhibits the antiviral response of alpha interferon by reducing STAT2 levels. J Virol 83:6717–6726 . doi: 10.1128/JVI.02213-08;

298. Dürr I, Numberger M, Berberich C, Witzemann V (1994) Characterization of the functional role of E-box elements for the transcriptional activity of rat acetylcholine receptor epsilon-subunit and gamma-subunit gene promoters in primary muscle cell cultures. Eur J Biochem 224:353–64

299. Mathelier A, Zhao X, Zhang AW, et al (2014) JASPAR 2014: an extensively expanded and updated open-access database of transcription factor binding profiles. Nucleic Acids Res 42:D142–D147 . doi: 10.1093/nar/gkt997

300. Hamad NM, Elconin JH, Karnoub AE, et al (2002) Distinct requirements for Ras oncogenesis in human versus mouse cells. Genes Dev 16:2045–2057 . doi: 10.1101/gad.993902

301. Khosravi-Far R, White MA, Westwick JK, et al (1996) Oncogenic Ras activation of Raf/mitogen-activated protein kinase-independent pathways is sufficient to cause tumorigenic transformation. Mol Cell Biol 16:3923–3933

302. Webb CP, Van Aelst L, Wigler MH, Vande Woude GF (1998) Signaling pathways in Ras-mediated tumorigenicity and metastasis. Proc Natl Acad Sci U S A 95:8773–8778

303. White MA, Nicolette C, Minden A, et al (1995) Multiple ras functions can

contribute to mammalian cell transformation. Cell 80:533–541 . doi: http://dx.doi.org/10.1016/0092-8674(95)90507-3

304. Mao C, Ray-Gallet D, Tavitian A, Moreau-Gachelin F (1996) Differential phosphorylations of Spi-B and Spi-1 transcription factors. Oncogene 12:863–73

305. Ray-Gallet D, Moreau-Gachelin F (1999) Phosphorylation of the Spi-B transcription factor reduces its intrinsic stability. FEBS Lett 464:164–8

306. Halacli SO, Dogan AL (2015) FOXP1 regulation via the PI3K/Akt/p70S6K signaling pathway in breast cancer cells. Oncol Lett 9:1482–1488 . doi: 10.3892/ol.2015.2885

307. Santo EE, Stroeken P, Sluis P V, et al (2013) FOXO3a is a major target of inactivation by PI3K/AKT signaling in aggressive neuroblastoma. Cancer Res 73:2189–98 . doi: 10.1158/0008-5472.CAN-12-3767

308. Gollob JA, Wilhelm S, Carter C, Kelley SL (2006) Role of Raf kinase in cancer: therapeutic potential of targeting the Raf/MEK/ERK signal transduction pathway. Semin Oncol 33:392–406 . doi: 10.1053/j.seminoncol.2006.04.002

309. Wilhelm SM, Carter C, Tang L, et al (2004) BAY 43-9006 exhibits broad spectrum oral antitumor activity and targets the RAF/MEK/ERK pathway and receptor tyrosine kinases involved in tumor progression and angiogenesis. Cancer Res 64:7099–7109 . doi: 64/19/7099 [pii]

310. Adnane L, Trail PA, Taylor I, Wilhelm SM (2006) Sorafenib (BAY 43-9006,

Nexavar), a dual-action inhibitor that targets RAF/MEK/ERK pathway in tumor cells and tyrosine kinases VEGFR/PDGFR in tumor vasculature. Methods Enzymol 407:597–612 . doi: S0076-6879(05)07047-3 [pii]

311. Litzenburger BC, Creighton CJ, Tsimelzon A, et al (2011) High IGF-IR Activity in Triple-Negative Breast Cancer Cell Lines and Tumorgrafts Correlates with Sensitivity to Anti–IGF-IR Therapy. Clin Cancer Res 17:2314–2327 . doi: 10.1158/1078-0432.CCR-10-1903

312. Grigoriadis A, Mackay A, Noel E, et al (2012) Molecular characterisation of cell line models for triple-negative breast cancers. BMC Genomics 13:619–2164 . doi: 10.1186/1471-2164-13-619;

313. Wulf GMG, Ryo A, Wulf GMG, et al (2001) Pin1 is overexpressed in breast cancer and cooperates with Ras signaling in increasing the transcriptional activity of c-Jun towards cyclin D1. EMBO J 20:3459–3472 . doi: 10.1093/emboj/20.13.3459

314. Hollestelle A, Elstrodt F, Nagel JHA, et al (2007) Phosphatidylinositol-3-OH kinase or RAS pathway mutations in human breast cancer cell lines. Mol Cancer Res 5:195–201 . doi: 10.1158/1541-7786.MCR-06-0263

315. Kozma SC, Bogaard ME, Buser K, et al (1987) The human c-Kirsten ras gene is activated by a novel mutation in codon 13 in the breast carcinoma cell line MDA-MB231. Nucleic Acids Res 15:5963–5971

316. Chavez KJ, Garimella S V, Lipkowitz S (2010) Triple Negative Breast Cancer Cell Lines: One Tool in the Search for Better Treatment of Triple Negative Breast Cancer. Breast Dis 32:35–48 . doi: 10.3233/BD-2010-0307

317. Tsai EM, Wang SC, Lee JN, Hung MC (2001) Akt activation by estrogen in estrogen receptor-negative breast cancer cells. Cancer Res 61:8390–2

318. Yndestad S, Austreid E, Svanberg IR, et al (2017) Activation of Akt characterizes estrogen receptor positive human breast cancers which respond to anthracyclines. Oncotarget 8:41227–41241 . doi: 10.18632/oncotarget.17167

319. Smith SC, Oxford G, Wu Z, et al (2006) The Metastasis-Associated Gene CD24 Is Regulated by Ral GTPase and Is a Mediator of Cell Proliferation and Survival in Human Cancer. Cancer Res 66:1917–1922 . doi: 10.1158/0008-5472.CAN-05-3855

320. Murohashi M, Hinohara K, Kuroda M, et al (2010) Gene set enrichment analysis provides insight into novel signalling pathways in breast cancer stem cells. Br J Cancer 102:206–212 . doi: 10.1038/sj.bjc.6605468;

321. Sanchez-Vega F, Mina M, Armenia J, et al (2018) Oncogenic Signaling Pathways in The Cancer Genome Atlas. Cell 173:321–337.e10 . doi: 10.1016/j.cell.2018.03.035

322. Jimenez C, Portela RA, Mellado M, et al (2000) Role of the PI3K regulatory subunit in the control of actin organization and cell migration. J Cell Biol

151:249–262

323. Kaga S, Ragg S, Rogers KA, Ochi A (1998) Activation of p21-CDC42/Rac-activated kinases by CD28 signaling: p21-activated kinase (PAK) and MEK kinase 1 (MEKK1) may mediate the interplay between CD3 and CD28 signals. J Immunol (Baltimore, Md 1950) 160:4182–4189

324. Wang R, Mercaitis OP, Jia L, et al (2013) Raf-1, Actin Dynamics, and Abelson Tyrosine Kinase in Human Airway Smooth Muscle Cells. Am J Respir Cell Mol Biol 48:172–178 . doi: 2012-0315OC [pii]

325. Linnemann T, Kiel C, Herter P, Herrmann C (2002) The activation of RalGDS can be achieved independently of its Ras binding domain. Implications of an activation mechanism in Ras effector specificity and signal distribution. J Biol Chem 277:7831–7837 . doi: 10.1074/jbc.M110800200 [doi]

326. Sobering AK, Watanabe R, Romeo MJ, et al (2004) Yeast Ras regulates the complex that catalyzes the first step in GPI-anchor biosynthesis at the ER. Cell 117:637–648 . doi: 10.1016/j.cell.2004.05.003 [doi]

327. Nathan DM, Singer DE, Godine JE, et al (1986) Retinopathy in older type II diabetics. Association with glucose control. Diabetes 35:797–801

328. Li O, Zheng P, Liu Y (2004) CD24 expression on T cells is required for optimal T cell proliferation in lymphopenic host. J Exp Med 200:1083–1089 . doi: 10.1084/jem.20040779

329. Suzuki T, Kiyokawa N, Taguchi T, et al (2001) CD24 Induces Apoptosis in Human B Cells Via the Glycolipid-Enriched Membrane Domains/Rafts-Mediated Signaling System. J Immunol 166:5567–5577 . doi: 10.4049/jimmunol.166.9.5567

330. Zietarska M, Maugard CM, Filali-Mouhim A, et al (2007) Molecular description of a 3D in vitro model for the study of epithelial ovarian cancer (EOC). Mol Carcinog 46:872–885 . doi: 10.1002/mc.20315

331. Barnabas N, Cohen D (2013) Phenotypic and Molecular Characterization of MCF10DCIS and SUM Breast Cancer Cell Lines. Int J Breast Cancer 2013:1–16 . doi: 10.1155/2013/872743

332. Lee GY, Kenny PA, Lee EH, Bissell MJ (2007) Three-dimensional culture models of normal and malignant breast epithelial cells. Nat Methods 4:359–365 . doi: 10.1038/nmeth1015

333. Sawant S, Dongre H, Singh AK, et al (2016) Establishment of 3D Co-Culture Models from Different Stages of Human Tongue Tumorigenesis: Utility in Understanding Neoplastic Progression. PLoS One 11:e0160615 . doi: 10.1371/journal.pone.0160615

334. Xu K, Buchsbaum RJ (2012) Isolation of Mammary Epithelial Cells from Three-dimensional Mixed-cell Spheroid Co-culture. J Vis Exp. doi: 10.3791/3760

335. Xu K, Tian X, Oh SY, et al (2016) The fibroblast Tiam1-osteopontin pathway modulates breast cancer invasion and metastasis. Breast Cancer Res 18:14 . doi:

10.1186/s13058-016-0674-8

336. Luo M, Brooks M, Wicha MS (2015) Epithelial-mesenchymal plasticity of breast cancer stem cells: implications for metastasis and therapeutic resistance. Curr Pharm Des 21:1301–10

337. Shipitsin MM (2007) Molecular Definition of Breast Tumor Heterogeneity. Cancer Cell 11:259; 259-273; 273

338. Wang H, Zhang C, Zhang J, et al (2017) The prognosis analysis of different metastasis pattern in patients with different breast cancer subtypes: a SEER based study. Oncotarget 8:26368–26379 . doi: 10.18632/oncotarget.14300

339. Hardaway AL, Herroon MK, Rajagurubandara E, Podgorski I (2014) Bone marrow fat: linking adipocyte-induced inflammation with skeletal metastases. Cancer Metastasis Rev 33:527–43 . doi: 10.1007/s10555-013-9484-y

340. Hilvo M, Orešič M (2012) Regulation of lipid metabolism in breast cancer provides diagnostic and therapeutic opportunities. Clin Lipidol 7:177–188 . doi: 10.2217/clp.12.10

341. Picon-Ruiz M, Pan C, Drews-Elger K, et al (2016) Interactions between Adipocytes and Breast Cancer Cells Stimulate Cytokine Production and Drive Src/Sox2/miR-302b-Mediated Malignant Progression. Cancer Res 76:491–504 . doi: 10.1158/0008-5472.CAN-15-0927

342. Stern JH, Rutkowski JM, Scherer PE (2016) Adiponectin, Leptin, and Fatty Acids

in the Maintenance of Metabolic Homeostasis through Adipose Tissue Crosstalk. Cell Metab 23:770–784 . doi: 10.1016/j.cmet.2016.04.011

343. Deng T, Lyon CJ, Bergin S, et al (2016) Obesity, Inflammation, and Cancer. Annu Rev Pathol 11:421–449 . doi: 10.1146/annurev-pathol-012615-044359 [doi]

344. Tao L, Huang G, Song H, et al (2017) Cancer associated fibroblasts: An essential role in the tumor microenvironment. Oncol Lett 14:2611–2620 . doi: 10.3892/ol.2017.6497

345. Bochet L, Lehuede C, Dauvillier S, et al (2013) Adipocyte-Derived Fibroblasts Promote Tumor Progression and Contribute to the Desmoplastic Reaction in Breast Cancer. Cancer Res 73:5657–5668 . doi: 10.1158/0008-5472.CAN-13-0530

346. Blücher C, Stadler SC (2017) Obesity and Breast Cancer: Current Insights on the Role of Fatty Acids and Lipid Metabolism in Promoting Breast Cancer Growth and Progression. Front Endocrinol (Lausanne) 8:293 . doi: 10.3389/fendo.2017.00293

347. Casimiro MC, Crosariol M, Loro E, et al (2012) Cyclins and cell cycle control in cancer and disease. Genes Cancer. doi: 10.1177/1947601913479022

348. Vogelstein B, Kinzler KW (2004) Cancer genes and the pathways they control. Nat Med 10:789–799 . doi: 10.1038/nm1087

349. Pickup MW, Mouw JK, Weaver VM (2014) The extracellular matrix modulates the hallmarks of cancer. EMBO Rep 15:1243–53 . doi: 10.15252/embr.201439246

350. Deng X, Apple S, Zhao H, et al (2017) CD24 Expression and differential resistance to chemotherapy in triple-negative breast cancer. Oncotarget 8:38294–38308 . doi: 10.18632/oncotarget.16203

351. Lv D, Hu Z, Lu L, et al (2017) Three-dimensional cell culture: A powerful tool in tumor research and drug discovery. Oncol Lett 14:6999–7010 . doi: 10.3892/ol.2017.7134

352. Seager RJ, Hajal C, Spill F, et al (2017) Dynamic interplay between tumour, stroma and immune system can drive or prevent tumour progression. Converg Sci Phys Oncol 3:034002 . doi: 10.1088/2057-1739/aa7e86

353. Wu M, Sirota M, Butte AJ, Chen B (2015) Characteristics of drug combination therapy in oncology by analyzing clinical trial data on ClinicalTrials.gov. Pacific Symp Biocomput 68–79

Appendix I:

Accession numbers for nucleotide sequences for 106 *CD24* genes from 56 different species

Refseq accession numbers
NM_001291737.1_Human_v2
NM_001291738.1_Human_v3
NM_009846.2_House mouse
NM_012752.3_Norway rat
XM_002690126.3_Cow
XM_010968193.1_Bactrian camel
XM_010621816.1_Damaraland mole rat
XM_010707543.1_Turkey
XM_010573395.1_Bald eagle
XM_009093196.1_Common canary
XM_008120756.1_Green anole
XM_008007449.1_Green monkey_v1
XM_008576828.1_Lemur
XM_008007450.1_Green monkey_v2
XM_007940836.1_Ant bear
XM_006982756.1_Prairie deer mouse
XM_003940810.2_Black capped-squirrel monkey
XM_003902737.2_Olive baboon

NM_013230.3_Human_v1
XM_003496974.2_Chinese hamster
XM_009242120.1_Sumatran orangutan_v3
XM_008994848.1_Marmoset_v1
XM_008994849.1_Marmoset_v2
XM_008994850.1_Marmoset_v3
ENSVPAT00000011368_Alpaca
ENSCAFT00000011592_Dog
ENSLAFT00000007742_Elephant
ENSMPUT00000009749_Ferret
ENSNLET00000023931_Gibbon
ENSGGOT00000004639_Gorilla
ENSCPOT00000006426_Guinea pig
ENSECAT00000003157_Horse
ENSETET00000010513_Lesser Hedgehog
ENSMMUT00000022072_Rhesus monkey
ENSPVAT00000004436_Mega bat
ENSSSCT00000036499_Pig
ENSOCUT00000008424_Rabbit
ENSOART00000012053_Sheep
ENSCHOT00000001451_Sloth
XM_004478726.1_Armadillo_L1
XM_004481863.1_Armadillo_L2

XM_005898197.1_Wild yak_L1
XM_003919300.2_Olive baboon_L1
XM_008847580.1_Blind mole rat_L1
XM_005377835.1_Chinchilla
XM_004638116.1_Degu1
XM_004627458.1_Degu2
XM_004641652.1_Degu3
XM_004627999.1_Degu4
XM_004637468.1_Degu5
XM_004623618.1_Degu6
XM_006987801.1_Prairie deer mouse_L1
XM_004328888.1_Commonn bottle nosed dolphin_L1
XM_004313735.1_Commonn bottle nosed dolphin_L2
XM_004315594.1_Commonn bottle nosed dolphin_L3
XM_005086648.1_Golden hamster
XM_003784394.1_Galagos_L1
XM_003794749.1_Galagos_L2
XM_003266872.2_Gibbon_L1
XM_003274235.2_Gibbon_L2
XM_004837180.1_Naked mole rat_L1
XM_004836422.1_Naked mole rat_L2
XM_004855435.1_Naked mole rat_L3
XM_004874111.1_Naked mole rat_L4

XM_004854271.1_Naked mole rat_L5
XM_004904554.1_Naked mole rat_L6
XM_004846605.1_Naked mole rat_L7
XM_004711196.1_Lesser hedgehog_L1
XM_004713801.1_Lesser hedgehog_L2
XM_004703339.1_Lesser hedgehog_L3
XM_004663354.1_Lesser egyptian Jerboa_L1
XM_004649227.1_Lesser egyptian Jerboa_L2
XM_004580347.1_American pika_L1
XM_005363586.1_Prairie vole_L1
XM_004422395.1_White rhinoceros_L1
XM_004436349.1_White rhinoceros_L2
XM_004422175.1_White rhinoceros_L3
XM_010369128.1_Golden snub nosed monkey_L1
XM_005339711.1_Thirteen-lined squirrel monkey_L1
XM_005335884.1_Thirteen-lined squirrel monkey_L3
XM_006159537.1_Chinese tree shrew_L1
XM_006141239.1_Chinese tree shrew_L4
XM_006141355.1_Chinese tree shrew_L5
XM_006146472.1_Chinese tree shrew_L6
XM_006143224.1_Chinese tree shrew_L7
XM_006142132.1_Chinese tree shrew_L10
XM_006168651.1_Chinese tree shrew_L12

XM_006165654.1_Chinese tree shrew_L13
XM_006168455.1_Chinese tree shrew_L15
XM_006165703.1_Chinese tree shrew_L16
XM_004411181.1_Pacific walrus_L1
XM_004412424.1_Pacific walrus_L2
XM_004391983.1_Pacific walrus_L3
XM_004407337.1_Pacific walrus_L4
XM_004406937.1_Pacific walrus_L5
XM_004397896.1_Pacific walrus_L6
XM_004065199.1_Western gorilla_L1
XM_004056236.1_Western gorilla_L2
XM_004278400.1_Killer whale_L1
XM_004283237.1_Killer whale_L2
XM_004278507.1_Killer whale_L3
XM_004271919.1_Killer whale_L4
XM_004274529.1_Killer whale_L5
XM_004284471.1_Killer whale_L6
XM_004264763.1_Killer whale_L7
XM_004281528.1_Killer whale_L8
XM_006181997.1_Wild camel_L1

Appendix II:

R-script for one way ANOVA analysis

```
setwd() #select the folder as working directory

getwd() #confirm the folder

vectorname<-read.csv("filename.csv", header=T) #reads the contents of the file

summary(vectorname) #lays out the summary of the file contents

colnames(vectorname) #lays out the column names in the file

ShapeAOV<-
aov(vectorname$Colname1(parameter1)~vectorname$colname2(parameter2)) #call 1-
way anova, order is important, vectorname$Colname

summary(ShapeAOV) #results of anova, if significant proceed with Tukey

TukeyHSD(ShapeAOV) #post-hoc test
```